The role of class I *TCP* genes in determining leaf shape and size

Vera Arianne Matser

Doctor of Philosophy

University of York

Biology

May 2014

Abstract

Leaf shape is an important feature of plant development and is known to be controlled by genetic, hormonal and environmental factors. Leaves are the plants photosynthetic organs and provide the plant with the energy to grow. Leaf size and shape, and especially the alteration of leaf size and shape, in mutants can provide us with valuable insight into the genetic basis of leaf development. Alterations in the regulatory control of early leaf development can be visualised by analysing the mature leaf. However, the human eye is not made to identify subtle differences between shapes and we have therefore used automated quantitative imaging technology to quantify differences in shape. In this thesis we employ landmark-based geometric morphometrics to analyse *Arabidopsis* leaf size and shape. We have quantified the natural leaf size and shape variation in *Arabidopsis* and built a Leaf Size and Shape Library using *Arabidopsis* accessions.

The *Arabidopsis* leaf shape library has been applied to the leaf size and shape characterization of a sub-clade of plant specific class I *TCP* transcription factors (*TCP8, TCP14, TCP15, TCP22* and *TCP23*) in an attempt to better understand their role in leaf development. Functional characterization of class I *TCP* genes has been hampered by a high degree of redundancy between its family members. We have discovered that *TCP14* and *TCP15* repress cell proliferation in leaves and thereby modulate leaf shape, combined with work from Kieffer et al., 2011 it constitutes proof that class I *TCP* genes can activate or repress transcription in a tissue dependent manner. *TCP8, TCP22* and *TCP23* have a yet to be determined role in modulating leaf shape that may work separately from *TCP14/TCP15*. *TCP8* and *TCP23* appear to have a regulatory role that is not limited to leaves.

Table of contents

Abstract 3

Table of contents 4

Acknowledgements 11

Author's declaration 12

Chapter 1 13

Introduction 13

1.1 Leaf development 14

1.1.1 The Shoot Apical Meristem 15

1.1.2 Organ initiation 16

1.1.3 Organ boundary domain 17

1.1.4 Establishment of axis of asymmetry 18

1.1.4.1 Adaxial-abaxial axis 18

1.1.4.2 Proximal-distal axis 20

1.1.5 Leaf lamina development 21

1.2 Plant-specific *TCP* gene family 22

1.2.1 Discovery of a new gene family 22

1.2.2 Sequence and biochemical characterization 23

1.2.3 Evolution of *TCP* family 25

1.2.4 Role of *TCP* genes during development 26

1.2.5 Interaction between *TCP*s and organ boundary genes 27

1.2.5.1 The role of the *CUC* genes in leaf development 27

1.2.5.2 Cross talk between *CUC* genes and *TCP* factors 28

1.3 Geometric morphometrics 29

1.3.1 Landmark-based geometric morphometrics 31

1.3.2 Connecting shape to underlying gene expression and function 33
1.4 Aims 33
Chapter 2 35
Methods & Material 35
2.1 Plant material 35
2.2 Plant growing conditions 35
2.3 In vitro culture 36
2.3.1 Sterilizing *Arabidopsis thaliana* seeds 36
2.3.2 Growth media 37
2.3.2.1 Composition of ATS (*Arabidopsis thaliana* salts) 37
2.3.2.2 Composition of LB medium 37
2.3.3 List of antibiotics 38
2.3.4 Bacterial culture 38
2.4 DNA extraction from plants 38
2.4.1 For use in plant genotyping 38
2.4.2 For use in molecular cloning 39
2.5 RNA extraction 40
2.6 cDNA synthesis 40
2.7 Plasmid DNA extraction 41
2.8 DNA Analysis 41
2.8.1 Restriction enzyme digestion 41
2.8.2 Polymerase Chain Reaction (PCR) 42
2.8.2.1 Standard PCR 42
2.8.2.2 Error-free PCR* 43
2.8.2.3 Reducing non-specific amplification 44
2.8.3 PCR Primers 45

2.8.4 Gel electrophoresis 45
2.8.5 Sequencing & alignments 46
2.9 Cloning from PCR products 46
2.10 Creation of transgenic organisms 47
2.10.1 *Escherichia coli* transformation 47
2.10.2 *Agrobacterium tumefaciens* transformation 48
2.10.3 *Arabidopsis thaliana* transformation 49
2.11 GUS: Histochemical Staining with X-Gluc 50
2.12 Leaf size and shape analysis 51
2.12.1 LeafAnalyser 51
2.12.2 LeafPredictor 52
2.13 Epidermal cell analysis 54
2.14 Root Growth Assay 54
2.15 Statistics 54
2.16 Graphs 55
Chapter 3 56
The *Arabidopsis* Leaf Shape Library 56
3.1 Introduction 56
3.2 Building the library and the development over time 57
3.2.1 Version 1.0 58
3.2.2 Version 1.1 60
3.2.3 Version 1.2 62
3.3 Establishing a stable reference set 64
3.4 Leaf shape and size analysis for the *Arabidopsis* reference set 67
3.5 Discussion 71
Chapter 4 74
Exploring the *Arabidopsis* Leaf Shape Library 74

4.1 Exploring the *Arabidopsis* Leaf Shape Library 74
4.1.1 Identifying outliers in the dataset 74
4.1.2 Comparing wild-type lines from different research groups ... 75
4.1.3 Healthy versus diseased plant populations 76
4.1.4 Tracking a seed line across multiple seasons 77
4.2 Exploring natural *Arabidopsis* PC space 77
4.3 Case Studies 82
4.3.1 *MORE AXILLARY GROWTH (MAX)* 82
4.3.2 *CUP-SHAPED COTYLEDON (CUC)* 85
4.3.3 *YABBY* Gene family 89
4.3.3.1 *CRABS CLAW (CRC)* 89
4.3.3.2 YABBY 3 (YAB3) 91
4.3.4 *KANADI (KAN)* & *ERECTA (ER)* 93
4.4 Discussion 95
4.4.1 Limitations of the LeafAnalyser tool and experimental method 95
4.4.2 Case studies 99
Chapter 5 102
Phenotypic analysis of class I *TCP* genes 102
5.1 Investigating the role of *TCP14* and *TCP15* 102
5.1.1 Applying the *Arabidopsis* reference library to *TCP* lines 104
5.1.2 *TCP14* and *TCP15* specify leaf shape 106
5.1.3 Discussion 106
5.2 Isolation of homozygous mutants for *TCP8*, *TCP22* and *TCP23* 108
5.2.1 TCP14 and TCP15 are closely related to TCP8, TCP22 and TCP23 108
5.2.2 Isolation of T-DNA insertion mutants 109
5.2.2.1 Identification of suitable T-DNA insertion mutants 109

5.2.2.2 Identifying insertion points for T-DNA insertion lines 110

5.2.2.3 Determining T-DNA insertion point for *tcp8-1* 112

5.2.2.4 Determining T-DNA insertion point for *tcp8-2* 113

5.2.2.5 Determining T-DNA insertion point for *tcp22* 113

5.2.2.6 Determining the T-DNA insertion point for *tcp23* 114

5.2.3 Creating multiple mutants 114

5.2.4 Expression levels 124

5.2.5 Discussion 125

5.2.5.1 T-DNA insertion lines 125

5.2.5.2 Isolating homozygous mutants 126

5.2.5.3 Further work 127

5.3 Leaf size and shape analysis for *TCP8*, *TCP22* and *TCP23* 128

5.3.1 Quantitative analysis of modification to leaf shape in putative *TCP* mutants 129

5.3.2 Discussion 132

5.3.2.1 Biological function of *TCP8*, *TCP22* and *TCP23* 132

5.3.2.2 Do *TCP8*, *TCP22* and *TCP23* act antagonistically with *TCP14* and *TCP15*? 133

5.4 Phenotypic characterization of *TCP8*, *TCP22* and *TCP23* 134

5.4.1 Analysing the expression patterns of TCP8, TCP22 and TCP23 135

5.4.1.1 Construction of *pTCP8:TCP8:GUS* and *pTCP22:TCP22:GUS* 135

5.4.1.2 Construction of pTCP23:TCP23:GUS 136

5.4.2 Spatial and temporal patterns of cell division 137

5.4.3 Epidermal cell analysis 139

5.4.3.1 Adaxial epidermal cell morphology 140

5.4.3.2 Abaxial epidermal cell morphology 143

5.4.4 Preliminary root growth assays 146
5.4.5 Discussion 148
Chapter 6. 151
General discussion 151
6.1 Quantifying leaf shape 151
6.1.1 The *Arabidopsis* leaf shape library 151
6.1.2 Establishing an experimental method 152
6.1.3 Procrustes superimposition 154
6.1.4 LeafAnalyser as a method to distinguish subtle phenotypes 155
6.2 The functional role of class I *TCP* genes 157
6.2.1 *TCP14* and *TCP15* repress cell proliferation in leaves 157
6.2.2 Investigation of functional redundancy of class I *TCP* genes 158
6.2.3 New advances in the understanding of the functionality of class I *TCP* genes 160
6.2.4 Final remarks and future work 164
Appendix 167
Appendix A1 167
Appendix A2 171
Appendix 2.1: T-DNA Insertion line *TCP8* (N817775) 171
Appendix 2.2: T-DNA Insertion line *TCP8* (N803036) 172
Appendix 2.3: T-DNA Insertion line *TCP22* 173
Appendix 2.4: T-DNA Insertion line *TCP23* 174
Appendix 3 176
Appendix 3.1: Sequence Alignment of the *pTCP8* entry vector (pENTR™/D-TOPO®). 176
Appendix 3.2: Sequence Alignment of the *pTCP22* entry vector (pENTR™/D-TOPO®) 180

Appendix A4 185
Appendix A5 187
References 188

Acknowledgements

I would like to thank my supervisor, Richard Waites, for all his help and guidance along the way and for allowing me to start this project in the first place. To the University of York and the Biology Department for their continued support when life was temporarily very difficult. My training committee, Ottoline Leyser and Calvin Dytham, and co-supervisor Brendan Davies for their scientific input and helping to prioritise the ever expanding work load. A very big thank you goes to the Leyser lab in general for adopting me and being so free with their advice. I would like to especially thank Gosia Domalgalska for sharing her expertise in molecular cloning. My fellow PhD students for tea drinking, boardgames, and gossiping.

My thesis mentors Joanna Hepworth and Patrick Gordon for all their encouragement and support, Alastair and Hannah Droop for providing a sense of perspective and a welcome anchor to York. EMBL-EBI and Dominic Clark for helping me rediscover my love of science and providing a quiet place to work.

Last but not least my husband Adam Faulconbridge and my beautiful baby girl Abigail for helping me find the motivation to finish writing this thesis and for being the light of my life; without a shadow of a doubt the best two "things" to have come out of my PhD.

Author's declaration

Except where otherwise stated, the work presented in this thesis is my own.

Caitlin Potter worked alongside me in the lab for 2 weeks on a summer studentship and assisted in the PCR screening of insertion mutants.

Joe Vaughan shared his R script to visualise PCs.

The *Arabidopsis* reference set presented in chapter 3 and the *TCP14/TCP15* analysis in chapter 5 have previously been published in Kieffer et al., 2011.

Chapter 1

Introduction

"Anyone who thinks fallen leaves are dead has never watched them dancing on a windy day."

Shira Tamir

Leaves are the photosynthetic organs of the plant converting light energy, carbon dioxide and water into sugar and oxygen, thereby providing the plant with the energy sources to grow. The chloroplasts in the leaves are used to store starch, the primary way plants store carbohydrates (Grennan, 2006). Plants have developed specific epidermal features to optimise gas exchange. Stomata open or close to facilitate the exchange of carbon dioxide, oxygen, and water vapour with the atmosphere (transpiration) (Yeats and Rose, 2013).

Plants have an incredible potential for regeneration and high level of plasticity compared to animals, partly attributed to their sessile nature. Due to the inability to move plants are more resilient to damage and will grow their way out of suboptimal conditions. Leaf shape is an important feature of plant development and is known to be controlled by genetic, hormonal and environmental factors (Chitwood et al., 2014; Yano and Terashima, 2001). Evergreens have evolved needle-like shapes to reduce water loss, plants endemic to low light regions have increased the surface area of the leaf to capture more light energy. Plants reduce the number of leaves, and change the shape of their leaves when moving from a vegetative to a flowering state to channel energy into the production of flowers.

Most leaves have distinctive features that differentiate the upper from the lower side of the leaf (adaxial and abaxial sides); though some plants have developed isobilateral leaves such as *Eucalyptus*. For almost every distinct plant feature we can name a number of exceptions have evolved, most plants have developed leaves with flat thin blades oriented towards the light to maximise the surface area directly exposed to light and thereby promote photosynthetic activity; succulent leaves and needles have chosen a different strategy to minimize water loss. Often the resulting leaf shape is presumed to be a trade-off between different factors, such as sacrificing optimal light-absorption efficiency to protect from herbivores, wind, or desiccation (Nicotra et al., 2011).

Morphology of shape is historically one of the cornerstones of the taxonomic classification of organisms, and our understanding of the diversity of biological life. However, our eyes are ill equipped at distinguishing changes in shape and we turn to automated computational methods to quantify differences in shape. In this work we discuss one method to define and quantify leaf shape and a group of plant-specific genes to determine whether they have a role in determining leaf shape in plants. By doing so we hope to contribute one piece of the puzzle in understanding what underlying genetic mechanisms define leaf shape.

1.1 Leaf development

As all multicellular organisms plants start life as a unicellular zygote and develop into an embryo. The bipolar *Arabidopsis* embryo is characterised by 2 meristematic regions, a root meristem which will give rise to the root system and a shoot apical meristem (SAM) giving rise to all the aerial parts of the plant. Meristems are tightly controlled domains of undifferentiated, pluripotent cells. The SAM produces repeating developmental modules called phytomers, consisting of a leaf, a stem section or internode, and an

axillary or secondary shoot meristem (McSteen and Leyser, 2005). In this manuscript we will only discuss the SAM unless otherwise specified.

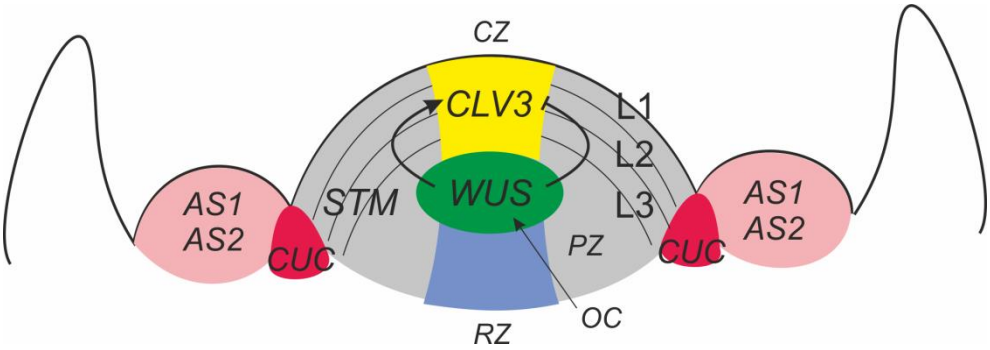

Figure 1.1: The shoot apical meristem in Arabidopsis. Yellow = central zone, Green = organising centre, Blue = rib zone (RZ), Grey = meristem (CZ and peripheral zone (PZ)), Red = organ boundary domain, Pink = developing primordia. The expression domains of some of the key regulatory genes are labelled; *WUSCHEL* (*WUS*), *CLAVATA3* (*CLV3*), *SHOOTMERISTEMLESS* (*STM*), *CUP-SHAPED COTYLEDON* (*CUC*), *ASYMMETRIC LEAF 1/2* (*AS1*, *AS2*) (adapted from Besnard et al., 2011).

1.1.1 The Shoot Apical Meristem

The dome-shaped SAM is characterised by layers of structural and functional organization (figure 1.1). Based on the orientation of the cell division meristem can be divided into three clonally distinct cell layers. The first two layers divide perpendicular to the surface (anticlinally), the L1 layer will maintain this orientation throughout plant development but the L2 layer will lose the anticlinal division pattern at the leaf initiation sites. The L3 layer divides both peri- and anticlinally. The L1 will give rise to the plant's epidermal layer, while the L2 and L3 layer contribute to the organ body (reviewed by Besnard et al., 2011; Braybrook et al., 2010).

A functional organisation is superimposed over the layered structure. The central zone (CZ) contains a group of slowly dividing pluripotent stem cells which are responsible for the maintenance of the meristem. Stem cells continuously divide to produce daughter cells which are eventually pushed into the peripheral zone (PZ). The ring-shaped PZ surrounds the central

zone, where founder cells will develop into organ primordia through the process of organogenesis. Only a number of cells become founder cells, thereby limiting the number of developing primordia. The zone between the meristem and the primordium is the organ boundary domain which is characterized by a lower growth rate and established the boundary between the developing organ and the meristem. Located under the CZ is the rib zone (RZ) which develops the stem tissues (Besnard et al., 2011).

The pluripotency of the cells in the CZ is controlled by an intricate regulatory feedback loop between the homeobox transcription factor (TF) *WUSCHEL* (*WUS*) and the signal peptide *CLAVATA3 (CLV3). WUS* is expressed in a domain of cells termed the organizing centre (OC) located below the CZ, and promotes stem cell identity in the CZ. WUS proteins migrate into the CZ and transcriptionally activate *CLV3,* which in turn restricts the expression of *WUS* to the OC (Katsir et al., 2011; Yadav et al., 2011). Though the *CLV3*-*WUS* feedback loop is at the core of meristem maintenance a complex regulatory network including hormone signalling, nutrient availability, transcription regulation and chromatin remodelling is involved (Besnard et al., 2011). In the meristem gibberellins (GA) promote cell elongation and cell differentiation and cytokinin (CK) promotes cell proliferation, low levels of GA and high levels of CK are therefore required to maintain the indeterminate state of the SAM. Auxin and *WUS* regulate high CK levels by negative regulation of CK repressors (Moon et al., 2011; Durbak et al., 2012). The class I *KNOTTED1-LIKE HOMEOBOX (KNOX)* gene *SHOOTMERISTEMLESS (STM)* is expressed throughout the CZ and PZ and is necessary to maintain the pluripotency of the stem cells in the CZ. *STM* activates CK signalling and represses GA biosynthesis, but also represses genes required for organ initiation (Byrne, 2012).

1.1.2 Organ initiation

Organ initiation in the peripheral zone of the meristem is not random but follows a predictable phyllotaxis. In *Arabidopsis* wild-type plants display a

spiral phyllotaxis with new organs emerging at a predictable angle of 137.5º. It is assumed that the inhibitory field produced by existing organs will determine the placement of new initiation sites. New organs will form where the sum of the inhibitory effects is the lowest. The initiation site is determined by local auxin maxima, established by polar localization of the auxin efflux carrier PIN-FORMED1 (PIN1) (Braybrook et al., 2010). The inhibitory field around the organ is formed by auxin depletion around the organ; a secondary inhibitory field is believed to be generated through the action of a cytokinin signalling inhibitor and acts as a stabilizing force on the phyllotaxis (Besnard et al., 2014). The hormone inhibitory fields are fundamental to establishing the organ initiation site but additional factors such as light signalling, mechanical stress and a network of transcriptional regulators are additionally required. (Byrne et al., 2012; Besnard et al., 2011). Auxin down regulates *KNOX* genes in the organ primordium signalling the transition from high CK and low GA levels in the meristem, to low CK and high GA levels in the organ primordium necessary to promote the switch from an indeterminate to a determinate state (Moon et al., 2011; Byrne 2012).

Arabidopsis has four class I *KNOX* genes: *STM*, *BREVIPEDICELLUS (BP)*, *Kn1-like in Arabidopsis thaliana 2 (KNAT2)* and *KNAT6. KNOX* regulation is complex, besides down regulation by auxin, KNOX proteins interact with the BEL1-like homeodomain TF family (BELL) and work antagonistically with ARP genes, named after *ASYMMETRIC LEAF1 (AS1)* from *Arabidopsis*, *rough sheath2 (rs2)* from *Maize* and *phantastica (phan)* from *Antirrhinum*. *ARP* genes are expressed in the developing primordia and repress *KNOX* genes in the meristem (Hay and Tsiantis, 2010; Moon et al., 2011).

1.1.3 Organ boundary domain

Genes expressed in the organ boundary domain are essential for proper organ separation, *CUP-SHAPED COTYLEDON (CUC)* genes *CUC1*,

CUC2, and *CUC3* are members of the NAC transcription factor family and are specifically expressed in the organ boundary. In concert with STM the partially redundant *CUC* genes are essential in the formation and maintenance of the shoot meristem and the specification of the organ boundary domain (Aida et al., 1999; Aida et al., 2006; Vroemen et al., 2003).

1.1.4 Establishment of axis of asymmetry

1.1.4.1 Adaxial-abaxial axis

As the primordium develops three axes of asymmetry will be specified, the adaxial-abaxial (upper/under), medial-lateral (midvein/margin), and proximal-distal axis (base/tip) (figure 1.2). Part of this asymmetry is already established by the meristem, the proximal end of the leaf is attached to the meristem and the side closest to the meristem is the adaxial side.

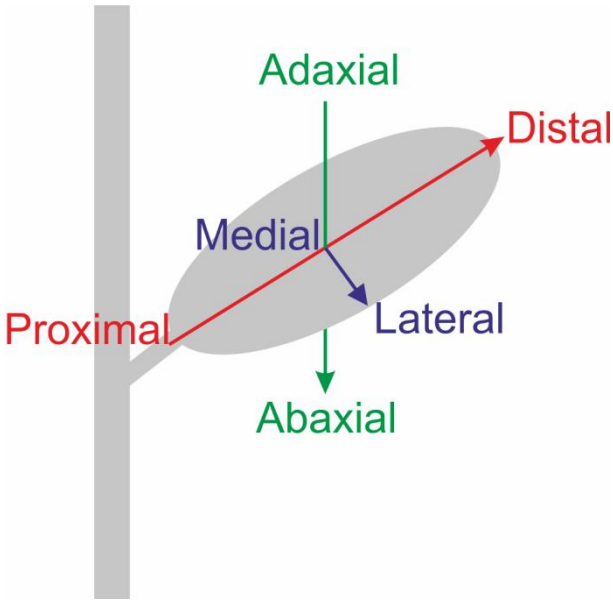

Figure 1.2: Axis of asymmetry in leaves. Adaxial-abaxial axis (Green) from the upper to the lower side of the leaf, proximal-distal axis (Red) from the base to the tip of the leaf, and medial-lateral axis (Blue) from the midvein to the margin of the leaf.

The upper-side or adaxial side of the leaf is enriched in photosynthesizing light harvesting cells, has a thick cuticle and densely packed palisade mesophyll cells, and exhibits high numbers of trichomes. While the bottom- or abaxial side of the leaf is specialised in gas-exchange and characterised by stomata and spongy mesophyll cells (Yamaguchi et al., 2012). The cell types of the vascular bundles are differentially expressed, xylem typically lies on the adaxial side of the cell and phloem on the abaxial side. The adaxial side of the leaf is specified by class III *HOMEO-DOMAIN LEUCINE ZIPPER (HD-ZIPIII)* and the *AS1/AS2* complex, while the abaxial domain is determined by *KANADI (KAN)* and the *AUXIN REPONSE FACTORS ARF3/ARF4* (TFs) (figure 1.3). *HD-ZIPIII* expression is restricted to the adaxial domain by mutual repression with *KAN* and positive regulation by the *AS1/AS2* complex, which also represses *KAN* and *YABBY* expression. The *YABBY* gene family acts downstream of *KAN* and is positively regulated by *KAN* and *ARF3/ARF4.* Two sets of antagonistically working small RNAs miR165/166 and trans-acting short interfering RNAs (tasiRNA) provide an additional level of regulation. miR165/166 is expressed in the abaxial side of the leaf and limits the *HD-ZIPIII* expression to the adaxial domain of the leaf. *ARF3/ARF4* promote abaxialisation and are limited to the abaxial domain by the tasiRNAs by mRNA cleavage and subsequent degradation (reviewed by Baybrook et al., 2010; Moon et al., 2011; Byrne, 2012). The L1 layer of the SAM is required for determination of the adaxial domain of the primordium, as shown by laser ablation and microsurgery experiments (Reinhardt et al., 2005). The antagonistic between *HD-ZIPIII* and *KANADI* also plays a role in the radial patterning of the leaf vasculature (Yamaguchi et al., 2012).

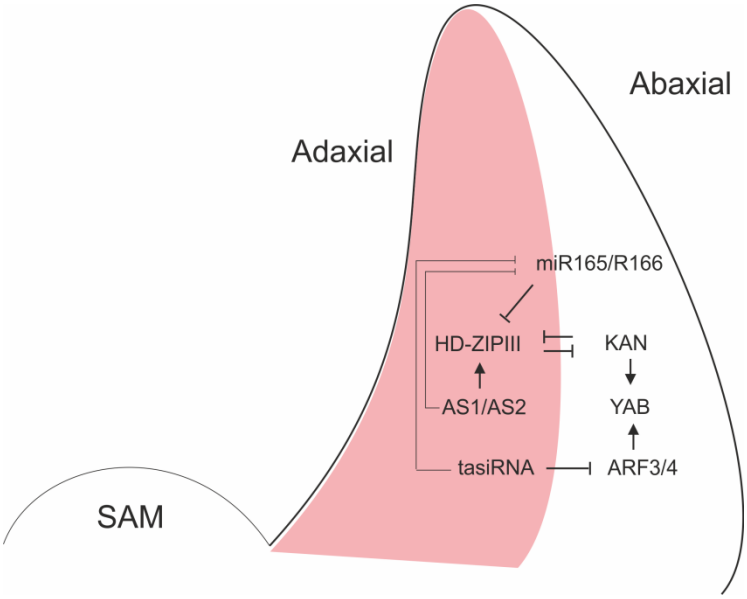

Figure 1.3: Regulatory network responsible for determination of the adaxial-abaxial domains. Adaxial = pink, Abaxial = white (adapted from Moon et al., 2011).

1.1.4.2 Proximal-distal axis

Leaf differentiation occurs basipetally with the cell cycle arrest front starting in the leaf blade and subsequently moving to the proximal region of the leaf as can be observed with the cell cycle reporter construct *Cyc1At::GUS* (Donnelly et al., 1999). An auxin maximum at the tip of the leaf primordium is believed to direct distal leaf growth and auxin derived from the margin is redistributed along the midvein during lamina outgrowth (Yamaguchi et al., 2012). Compared to the adaxial/abaxial axis, the establishment of proximal-distal polarity is not well characterised. Genes implicated along-side auxin are *KNOX* genes, *ULTRACURVATA1 (UCU1),* and *BLADE ON PETIOLE (BOP)* (Ramirez et al., 2009; Pérez- Pérez et al., 2002; Hepworth et al., 2005).

UCU1 encodes an AtSK kinase involved in the interaction between auxin and brassinosteroid signaling pathways, mutation of *UCU1* leads to reduced cell expansion along the proximodistal axis (Pérez- Pérez et al., 2002). Disruption of *BOP1* and *BOP2* result in loss of distinct proximal and distal zones in the leaf (Hepworth et al., 2005). *BOP1* and *BOP2* repress the

KNOX genes *BP*, *KNAT2* and *KNAT6* in the proximal region of the leaf (Hamant et al., 2010).

1.1.5 Leaf lamina development

Development of a flat broad lamina allows maximum light capture and is accomplished by outgrowth along the medial-lateral axis (Yamaguchi et al., 2012, Nakata et al., 2012b). Waites and Hudson theorised that the adaxial/abaxial patterning is required for blade expansion (Waites and Hudson, 1995). Four members of the *YABBY* family, *FILAMENTOUS FLOWER (FIL), YAB2, YAB3* and *YAB5* are expressed in the abaxial leaf domain. Though not required for initial adaxial/abaxial patterning *YABBY* genes are required for abaxial/adaxial juxtaposition-mediated lamina expansion and the maintenance of polarity (Eshed et al., 2004). Nakata et al. (2012a), defined the two middle mesophyll layers and the margin between the adaxial and abaxial sides of the leaf primordia as the "middle domain" which organizes the outgrowth of leaf blades and is determined by the expression of *PRESSED FLOWER (PRS* or *WOX3)* and *WOX1* homeobox transcription factors of the WUSCHEL-RELATED HOMEOBOX (WOX) family. *PRS* and *WOX1* are regulated by the adaxial/abaxial patterning genes, restrict the expression of AS1 and redundantly act in blade outgrowth and margin development by modulating cell proliferation and cell differentiation (Nakata et al., 2012a; Nakata et al., 2012b). *YABBY* genes as well as YUCCA-mediated auxin biosynthesis mediates leaf margin development, *YUC* genes are expressed in response to the adaxial-abaxial juxtaposition, both these gene families provide further context to the involvement of auxin in leaf margin development and subsequent lamina outgrowth (Sarojam et al., 2010; Wang et al., 2011).

1.2 Plant-specific *TCP* gene family

1.2.1 Discovery of a new gene family

The TCP gene family has been named after its founding members, *teosinte branched1* (*tb1*) from maize (*Zea mays*) (Doebley et al., 1997), *CYCLOIDEA* (*CYC*) from snapdragon (*Antirrhinum majus*) (Luo et al., 1996) and the *PROLIFERATING CELL FACTORS 1* and *2* (*PCF1* and *PCF2*) from rice (*Oryza sativa)* (Kosugi and Ohashi 1997). The closely related *PCF1* and *PCF2* specifically bind two *cis*-regulatory elements, designated site IIa and site IIb, in the promoter of *PROLIFERATING CELL NUCLEAR ANTIGEN* (*PCNA*). *PCNA* is a gene involved in the coordination of the cell cycle, DNA replication and DNA repair (Kosugi et al., 1995). Kosugi and Ohashi (1997) speculated *PCF1* and *PCF2* could be part of a novel multigene family that was conserved across monocots and dicots (Kosugi & Ohashi 1997). *CYC*, in concert with a second TCP gene *DICHOTOMA* (*DICH*) is responsible for dorsoventral asymmetry in *Antirrhinum* flowers. Loss of CYC and DICH activity results in radially symmetric or peloric flowers (Luo et al., 1996). TB1 is a modifier of growth, it represses the development of axillary organs and promotes the formation of female inflorescences (ears). The changes in the regulatory control of *TB1* is considered to be one of the elements that contributed to the evolutionary divergence of maize from its wild ancestor teosinte (Doebley et al., 1997). After the cloning of *TB1* it was recognized that the TB1 protein showed homology with CYC and at later stage with PCF1 and PCF2 as well (Doebley et al., 1997, Cubas et al., 1999). Based on the homology of the conserved domain a new family of transcription factors, characterized by the TCP domain, was defined (Cubas et al., 1999).

1.2.2 Sequence and biochemical characterization

TCP genes encode plant specific transcription factors, all its members share a conserved ~60-residue homologous region called the 'TCP' domain, a non-canonical basic-Helix-loop-Helix (bHLH) that is responsible for the DNA binding characteristics and protein-protein interactions (Cubas et al., 1999, Aggarwal et al., 2010). The bHLH motif appears unrelated to the classic or canonical bHLH as seen in MyoD and E12.

The structure and sequence of the TCP domain reveals two major subfamilies or subclasses within the TCP family: class I (or TCP-P) and class II (or TCP-C). Class I contains rice *PCF1* and *PCF2*, and class II *CYC* and *tb1* (Cubas et al., 1999). *Arabidopsis* has a total of 24 TCP genes, 13 class I proteins and 11 class II proteins (Cubas et al., 2002).

The proteins in class I are closely related and the conserved TCP domain has an extended sequence conservation at the C terminus making the total length of the TCP domain 62 residues. The class II TCP domain (58 residues) has a three amino acid insertion in the basic region compared to class I genes (Aggarwal et al., 2010). Sequence alignment of the class II TCP domain show that class II proteins can be further divided into two clades, eight CIN-like proteins named after *CINCINNATA* in *Antirrhinum* and the *CYC*/*tb1* clade containing three genes (figure 1.4) (Cubas et al., 2002).

The class II basic region of TCP domain contains a putative bipartite nuclear localization signal (NLS) (Luo et al. 1996, Doebley et al. 1997, Cubas et al. 1999). A number of TCP proteins (TCP11, TCP15, TCP17, TCP22, TCP23) which do not contain a NLS may be targeted to the chloroplast via putative N-terminal chloroplast transit peptides (cTP) (Wagner & Pfannschmidt 2006; Navaud et al. 2007); this may indicate an involvement of TCPs in the regulation of the transcription of chloroplast genes (Martín-Trillo & Cubas 2010). Additional conserved features are

present in certain members of class II. The R domain, which is an 18-20 residue motif rich in polar residues (arginine, lysine and glutamic acid) is predicted to form a hydrophilic α-helix (Cubas et al. 1999) (Martín-Trillo & Cubas 2010). A glutamic acid stretch (the ECE motif) located between the TCP domain and the R domain is present in the *CYC/tb1* subclade, as with the R domain the ECE motif is of unknown function (Howarth et al., 2005). A subset of the CIN-like genes is regulated by miR319 and therefore contains the microRNA miR319 recognition site (Palatnik et al., 2003). An SP domain has been reported, but only in tb1 in grasses and class I proteins only contain a partial NLS in the basic region (Lukens and Doebley, 2001, Cubas et al., 1999).

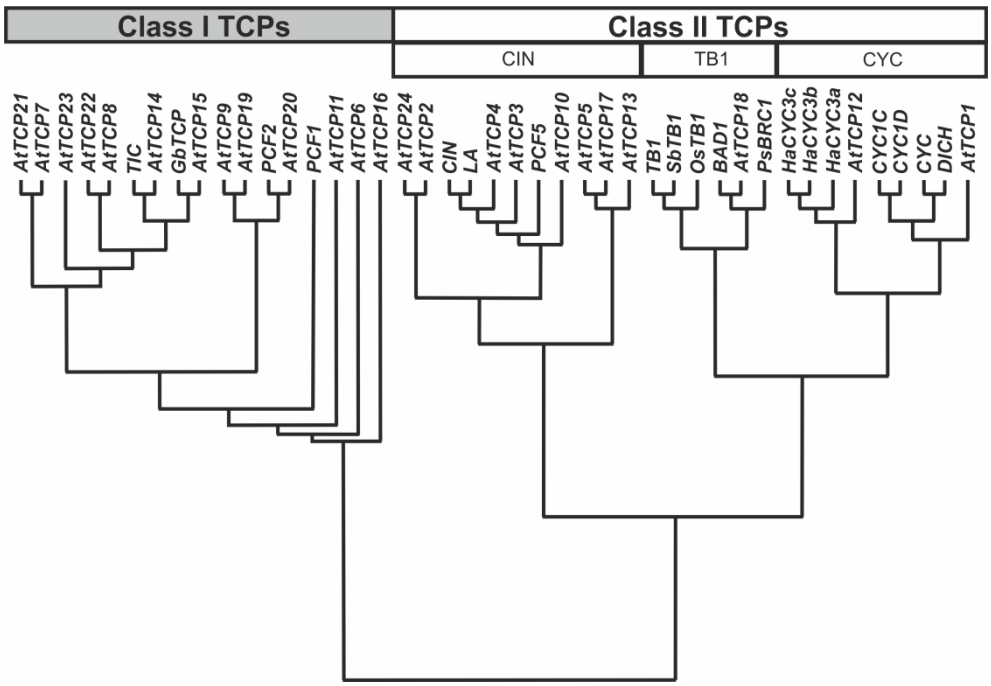

Figure 1.4: Phylogenetic tree of the TCP family showing the different classes and clades mentioned in the text. The 24 *Arabidopsis thaliana TCP* genes have been included, as well as *PCF1, PCF2, PCF5* and *OsTB1* from *Oryza sativa* (rice); *TIC, CIC, DICH* from *Antirrhinum major* (snapdragon); *GbTCP* from *Gossypium barbadense* (seas-island cotton); *LA* from *Solanum lycopersicum* (tomato); *PsBRC1* from *Pisum sativum* (pea), *SbTB1* from *Sorghum bicolor* (sorghum); HaCYC3a, HaCYC3b, HaCYC3c from *Helianthus annuus* (sunflower), and *CYC1C and CYC1D* from *Primulina heterotricha* (African violet) (from Uberti Manassero et al., 2013).

1.2.3 Evolution of TCP *family*

The results described in this thesis do not directly relate to the evolution of the TCP family but a short overview of the current knowledge of the evolution of the TCPs is given due to the importance of the gene family in plants.

TCP transcription factors appear to be ancient and have most likely been part of the ancestral developmental tool kit of land plants and are plant specific (Floyd & Bowman 2007) (Riechmann et al. 2000). *TCP* genes have been found in angiosperms, gymnosperms, in the moss *Physcomitrella patens*, in ferns and in the lycophyte *Selaginella mollendorffii* (clubmoss) as well as in multicellular green algea *Chara* and *Cosmarium* (Floyd & Bowman 2007)(Navaud et al. 2007). *TCP* genes were not found in the early diverged streptophyte lineages (Klebsormidiophyta and Chlorokybophyta) nor in *Scenedesmus* or *Chlamydomonas* both part of the Chlorophyta. Together this indicated the *TCP* genes appeared in the Streptophyta lineage before the divergence of the Zygnemophyta (estimated at 650 and 800 Mya), thus correlating with the emergence of the Phragmoplastophyta (Navaud et al. 2007).

The *Arabidopsis TCP* genes are found across all chromosomes and with the exception of *TCP18*, which has 2 intron, none of the others have introns (Navaud et al. 2007). Current research predicts that the complete TCP families for poplar (*Populus trichocarpa*), rice, *Selaginella* and *Physcomitrella* have been identified. There are 34 *TCP* genes in poplar, 29 in rice, 10 in *Selaginella*, and 6 in *Physcomitrella* genomes. As is the case in *Arabidopsis*, the *TCP* genes in poplar and rice are distributed throughout the genomes, without any clustering on specific chromosomes (Navaud et al. 2007). The *Physcomitrella* genes appear to have been the result of a recent duplication from a single class I and a single class II ancestral gene. It therefore seems likely that the common ancestor of mosses and angiosperms had a single class I and a single class II gene. Previously the R domain was

thought to have originated separately in the subclades of class II genes (Cubas, 2002), however a derivative of the R domain has been identified in *Selaginella* as well as in *Physcomitrella* making it probable that the ancestral class II gene had an R domain (Floyd & Bowman 2007). The R domain appears to have been lost in most angiosperm CIN-like proteins, in *Arabidopsis TCP2* and *TCP24* are the exception (Floyd & Bowman 2007) (Cubas, 2002). The microRNA miR319 recognition sequence was not found in *Selaginella* nor in *Physcomitrella* (Floyd & Bowman 2007), even though miR319 itself was found in *Physcomitrella* (Arazi et al. 2005).

1.2.4 Role of TCP genes during development

The *Antirrhinum* gene *CINCINNATA* (*CIN*) encodes a TCP factor that inhibits growth in the leaf margins but promotes growth in petals. Strong alleles of the *cin* have larger leaves and their leaf margin is wavy due to continuing cell division in this area. In contrast with leaves, petals are smaller in *cin* mutants. In the petals as well as in the leaf margins conical cells are flat (Nath et al., 2003; Palatnik et al., 2003; Crawford et al., 2004). A *cin*-like phenotype is observed in plants that overexpress *miR-JAW*. Several class II TCP factors (*TCP2, TCP3, TCP4, TCP10 and TCP24*) are regulated by miRNAs, encoded by the *JAW*-locus, which are responsible for gene regulation by way of mRNA cleavage (Palatnik et al., 2003).

Recent studies report that TCPs are essential for the morphogenesis of shoot lateral organs. Repressors of *TCP3* lead to the ectopic expression of boundary-specific genes and the production of ectopic shoots, while overexpression of *TCP3* resulted in an inhibition of boundary specific genes and abolishment of shoot production and failure in cotyledon separation. Thus it is believed the *TCP3* regulates the shoot lateral organs by negative regulation of the expression of boundary specific genes, specifically the CUC genes. A range of TCP factors (TCP2, TCP3, TCP4, TCP5, TCP10, TCP13, TCP17, and TCP24) appear to regulate organ boundary-specific genes in similar ways with overlapping but significantly different expression

patterns; these TCPs are grouped together in a subfamily of CIN-like TCPs (Koyama et al., 2007). The grade of redundancy in the TCP family is believed to be much higher in *Arabidopsis* compared to *Antirrhinum;* In *Antirrhinum* mutation in CIN is sufficient to induce a leaf phenotype (Koyama et al., 2007; Nath et al., 2003; Crawford et al., 2004), while multiple CIN-like TCPs need to be disrupted in *Arabidopsis* to yield a phenotype (Koyama et al., 2007). The miR319/*JAW*-dependent TCP transcript cleavage might be essential for the formation of the shoot meristem since TCP activities need to be suppressed in the organ boundary region and the shoot apical meristem (SAM) (Koyama et al., 2007; Palatnik et al., 2003).

TCP14 has recently been linked to the regulation of seed germination. A microarray analysis identified that the upstream regions of genes upregulated during seed germination are unusually enriched with the cis regulatory elements Up1 and Up2. Up1 is virtually identical to the site II motif, which is the predicted TCP target site. *TCP14* showed the highest expression, of all the TCP factors, prior to germination. *TCP14* was primarily expressed in the embryo vasculature and loss-of-function mutants present with an ABA-hypersensitive phenotype (Tatematsu et al., 2008).

1.2.5 Interaction between TCPs and organ boundary genes

1.2.5.1 The role of the *CUC* genes in leaf development

CUP-SHAPED COTYLEDON (CUC) genes, *CUC1*, *CUC2*, and *CUC3* are members of the NAC transcription factor family and are specifically expressed in the organ boundary. In concert with *SHOOT MERISTEMLESS (STM)* the partially redundant *CUC* genes are essential in the formation and maintenance of the shoot meristem and the specification of the organ boundary domain (Aida et al., 1999; Aida et al., 2006; Vroemen et al., 2003). Most single *cuc1* and *cuc2* mutant seedlings look phenotypically normal, but occasionally some seedlings present with fused cotyledons on

one side, called heart-shaped seedlings. Heart-shaped seedlings can be interpreted as a weaker *cuc* phenotype, the extent of the fusion can vary, compared to the stronger cup-shaped cotyledon phenotype. The double mutant *cuc1cuc2* has fused cotyledons shaped like a cup, sepals and stamens and show severe defects in the embryonic and adventitious shoot apical meristems (SAM) (Aida et al., 1997; Aida et al., 1999). *CUC1* and *CUC2* are expressed from the globular stage onwards in the future SAM region and the boundary region of the cotyledon margins. As development progresses the expression of *CUC1* and *CUC2* subsides in the SAM. Expression of *CUC2* is faint in the epidermal layer and *CUC1* is not detected in the epidermis. In general *CUC1* is expressed wider than *CUC2*, and additionally expressed in the boundary of floral organs (Aida et al., 1997; Aida et al., 1999; Hibara et al., 2006; Takada et al., 2001). The expression pattern of *CUC3* overlaps a great deal with the expression patterns of *CUC1* and *CUC2*, however, the differences are that *CUC 3* is expressed from the octant stage onwards and is strongest in the epidermal cell layer. *CUC3*, and to a lesser extend *CUC2* but not *CUC1*, is a regulator of axillary meristem initiation (Hibara *et al.*, 2006).

The regulation of *CUC* genes is complex and involves *STM*, auxin, miRNAs and chromatin remodelling. Auxin is believed to determine the spatial boundaries in which the *CUC* genes are expressed. The accumulation of *CUC1* and *CUC2* mRNA levels is post-transcriptionally regulated by miR164, while *CUC3* levels are not. miR164 is encoded by three separate genes, *miR164A*, *miR164B* and, *miR164C*. Overexpression of miR164 reduces mRNA levels of *CUC1* and *CUC2*. *MiR164* regulation of *CUC1* and *CUC2* helps to define the borders of the boundary domain (Laufs et al., 2004, Aida et al., 1999; Aida et al., 2006).

1.2.5.2 Cross talk between *CUC* genes and TCP factors

In *Antirrhinum* a member of the TCP family, TCP-interacting with *CUP* (*TIC*), has been shown to interact with *CUPULIFORMIS (CUP)*, a NAC-

domain gene, to establish lateral organ boundaries (Weir et al., 2004). In *Arabidopsis* leaf marginal serration is believed to be the result of a 2-step process; the first step determines the pattern of serration and is independent of *CUC2* and miR164 but auxin-dependent. In a second phase the coexpression of *CUC2* and miR164A determines the degree of serration, miR164A mutants have deeper serrations while over expression of miR164 leads to a smooth leaf margin (Nikovics et al., 2006; Barkoulas et al., 2007). TCPs have a role in regulating the expression levels of *CUC2* by controlling, possibly in concert with auxin, the levels of miR164. TCPs are known to act redundantly in negatively regulating the expression levels of *CUC* genes (Nikovics *et al.*, 2006; Barkoulas *et al.*, 2007; Koyama *et al.*, 2007). The exact relationship of auxin, the *CUC* genes, miR164 and TCPs in establishing serration is not well understood (Nikovics *et al*., 2006).

1.3 Geometric morphometrics

Shape is all the geometric information that remains when location, scale, and rotational effects are filtered out from an object.
(Kendall, 1977)

The analysis of shape knows a long history, the painter Albrecht Dürer applied shape transformation to his study of the human proportions ("Vier Bücher von Menschlicher Proportion", 1528). D'Arcy Thompson was inspired by Albrecht Dürer when he developed his famous fish transformations grids in "On Growth and Form" 1961. He showed that simple mathematical transformations could turn a silver hatchetfish (*Argyropelecus olfersi*) into a marine hatchetfish (*Sternoptyx diaphana*) (figure 1.5).

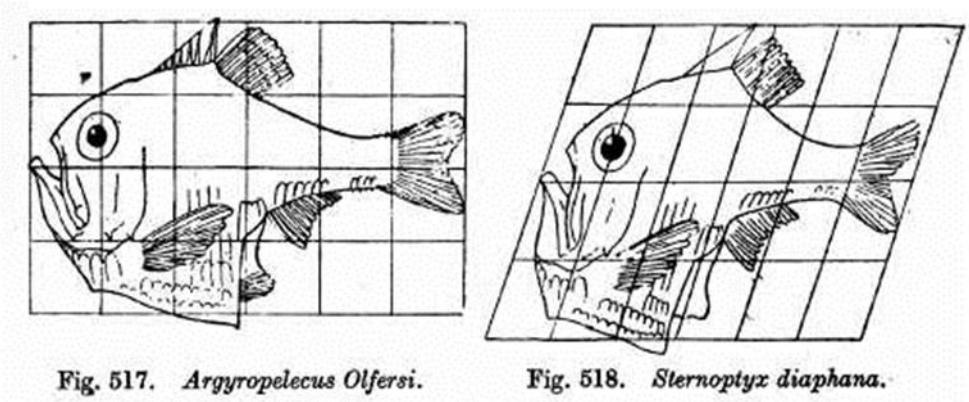

Figure 1.5: Mathematical transformation turns a silver hatchetfish (Argyropelecus olfersi) into a marine hatchetfish (Sternoptyx diaphana). This is an illustration from page 1062, volume II, chapter XVII, of On Growth and Form by D'arcy Wentworth Thompson.

Prior to molecular biology and sequencing technology taxonomic classification was entirely based on the comparison of the morphological form of organisms. The analysis of morphology went through a 'quantification revolution' in line with the transition seen in biology from a descriptive to a quantitative science (Adams et al., 2004). According to C. Klingenberg morphometric problems have been a motivation for the development of multivariate statistics, which then in turn provided new tools for morphometric analysis (Klingenberg, 2008).

The most common definitions of morphometrics are variations on the following:

Morphometrics is the quantitative study of biological shape, shape variation, and covariation of shape with other biotic or abiotic variables or factors (Webster and Sheets, 2010).

1.3.1 Landmark-based geometric morphometrics

Geometric morphometrics was hailed as a revolution in morphometrics and focussed on the coordinates of landmarks and the geometric information about their relative positions (Adams et al., 2004). When talking about morphometrics in this thesis we are exclusively looking at landmark-based geometric morphometrics.

Landmark data underlying geometric morphometrics can be extracted from 2 or 3 dimensions. 2D data generally consists of digital pictures while 3D data is often procured using MRI or CT scans and comes at considerable cost (Webster and Sheets, 2010). Primary landmarks are recognisable anatomical loci that should be recognisable on all specimens in the study, additionally semilandmarks or secondary landmarks can be employed spaced equidistant from a primary landmark along the sample outline (Zelditch et al., 2012; Webster and Sheets, 2010). The geometric value of semilandmarks (or sometimes referred to as type III landmarks) is controversial as their location depends on the geometric location of another landmark, however primary landmarks (type I), or type II landmarks which are defined as a mathematical point rather than a point of biological or anatomical significance (e.g. point of maximum width), are scarce and often difficult to locate precisely. The use of semilandmarks is by most considered to be a necessary evil, or concession to practicality (Zelditch et al., 2012; Webster and Sheets, 2010; Macleod, 2013).

Landmark-based morphometrics is frequently employed in the field of paleontology where access to intact specimen can be very difficult and care must be given to not damaging the specimen during data acquisition (Webster and Sheets, 2010). Leaves are particularly suitable for automated processing through landmark-based geometric morphometric methods as availability of samples is less likely to be a problem. Leaves have simple shapes which can be projected in two dimensions and provide a high contrast on a plain background (Weight et al., 2008).

Kendall's definition of shape, as given above, is central to almost all landmark-based morphometric studies (Adams et al., 2004; Webster and Sheets, 2010). To compare the configurations of the raw landmark coordinates superimposition is used to remove variation associated with differences in location, orientation and size (Webster and Sheets, 2010). The different methods of superimposition differ as to the degree in which they remove differences in location, scale and size. The relative value between using partial or full superimposition is debated in chapter 9 of this thesis. Superimposition requires several steps, translating all landmark configurations to a common location by calculating the centroid of each configuration and making the centroid the origin of a new coordinate system, rescaling all configurations to a unit centroid size, and rotating the configurations to an optimal fit (Klingenberg et al., 1998; Webster and Sheets, 2010).

Once location, scale, and rotational effects, or so called non-shape variation, has been eliminated the remaining variables are shape variation and the mean shape can be compared using statistical methods and graphical representations (Adams et al., 2004). One of the multivariate statistical methods used for the analysis of differences in mean shape is Principal Component Analysis (PCA). PCA reveals the structure of the data set in a way that best explains the variance; this is done through the reduction of a complex data set to a lower dimension (Smith, 2002; Shlens, 2005).

During chapter 4 of this thesis we will discuss the capabilities and limitations of landmark-based systems, specifically LeafAnalyser (Weight et al., 2008), for the comparative analysis of plant lines. We will be exclusively looking at LeafAnalyser (Weight et al., 2008) though other morphometrics methods have since been developed to analyse leaf shape such as Lamina (Bylesjö et al., 2008), LeafProcessor (Backhaus et al., 2010), and LeafJ (Maloof et al., 2013) each focussing on a different aspect or type of leaf.

1.3.2 Connecting shape to underlying gene expression and function

The real bottle-neck for this field lies in linking how a specific organ shape relates to the underlying pattern of gene activity. Cui et al., 2010 outlined three main reasons as to why this link is still poorly understood. The main method of identifying genes that modulate shape is through the phenotypic characterisation of wild-type and mutant lines making it difficult to isolate the effect on particular tissues or regions from the overall phenotypic effect. Even with more sophisticated morphometric methods shape is often defined in qualitative terms (e.g. rounder, more elongated) hindering the quantification and linking the shape change to differentially expressed genes. A modelling framework that allows the quantitative evaluation of how genes control morphogenesis is lacking.

1.4 Aims

The underlying genes of an organism influence the way an organism looks. Sometimes small changes to the DNA of the organism can have dramatic effect while other changes do not appear to vary the shape. In the medical domain the alteration of the shape of for instance the face, hands or feet can be an indication of a genetic abnormality and is increasingly used in diagnostic screening (Mankin et al., 2010; Liu et al., 2012).

Plants, and the leaf of the plant specifically, offer a unique opportunity to study the genetic component that determines the shape of an organism. The ethical implications of working with animals restricts what type of research can be carried out; most of these restrictions do not apply to plants making them an ideal organism to study shape. As mentioned earlier in this chapter, plants have an incredible potential for regeneration and high level of plasticity compared to animals, partly attributed to their sessile nature. Plant

have to grow their way out of trouble. Correspondingly leaf shape varies considerably across different plant species giving us an ideal organ to study.

The problem is challenging because there is the potential for a large portion of plant genes, proteins and processes to influence the final leaf shape. The question is which genes, proteins and processes are involved in determining leaf shape in a primary fashion and which genes have a secondary effect on leaf shape while primarily regulating another area of plant/leaf development (Tanksley 2004). The additional compounding factor that needs to be taken into account is the effect that the environment (biotic and abiotic) has on leaf shape.

This project focused on building an *Arabidopsis thaliana* leaf shape library, containing ten accessions defining the natural leaf shape variation in *Arabidopsis*. The stable reference set is designed to be used in concert with LeafAnalyser, creating a powerful quantitative imaging approach capable of characterizing leaf shape phenotypes. The capabilities of the software will be explored and tested on a number of case studies.

By applying the leaf shape reference set to a sub-clade of the class I *TCP* family of plant-specific transcription factors, this work aims to contribute to the understanding of the role of class I *TCP* genes in leaf development.

Analysing the functionality of class I *TCP* genes has been held back by the high level of genetic redundancy in this gene family, making the phenotypic characterization of mutant lines challenging. We will determine whether LeafAnalyser is a suitable method for analysing leaf shape phenotypes in a redundant background.

Chapter 2

Methods & Material

2.1 Plant material

All plant material used in this thesis is *Arabidopsis thaliana* (L.) Heynh. (*Arabidopsis*), unless otherwise stated the plant lines are obtained from the seed stock of Dr Richard Waites, University of York.

Dr Martin Kieffer kindly donated the *tcp14-4, tcp15-3, tcp14-4tcp15-3* and wild-type (ColO) lines.

The *Arabidopis thaliana* accessions (ecotypes), Ct-1, Hi-0, Kn-0, Mt-0, No-0, Oy-0, Po-0, Rsch-4, Wil-2, Wu-0, Bur-0, Can-0, Edi-0, Ler-0, Col-0, Sf-2, Tsu-0, Ws-0, Zu-0 were donated by the Leyser laboratory, with permission from Paula Kover.

SALK- (N654177, N643403) and SAIL T-DNA insertion lines (SAIL_64_D09, SAIL_387_A10, SAIL_443_F02) were purchased from Nottingham Arabidopsis Stock Centre (NASC).

2.2 Plant growing conditions

The greenhouse had natural light supplemented with artificial light to obtain long day (16 hours light) conditions at approximately 150 μmol m-2s-1. The temperature in the greenhouse varied between 15°C and 24°C. Plants are watered when necessary by the Horticultural Technicians of the University of York. All *Arabidopsis thaliana* lines were grown in p24 (Desch Plantpak, Maldon, UK) on F2 compost pre-treated with Intercept (both Levington

Horticulture, Ipswich, UK). Plants destined for LeafAnalyser or cell epidermal analysis were treated with two rounds of Intercept due to pest problems.

The plant growth chambers used had the following specifications:
Long day growth chamber: 16 hours light, temperatures between 19-22°C by day and 18-20°C at night, light intensity ~60-100 μmol $m^{-2}s^{-1}$.

2.3 In vitro culture

Sterile H_2O is prepared by autoclaving water micro filtered through a Purelab Ultra lab water system (ELGA, Marlow, UK).

2.3.1 Sterilizing Arabidopsis thaliana seeds

The required amount of seeds was placed in a square of Miracloth, folded and stapled shut (seed reference number written on the Miracloth cloth with pencil). Care was given not to overfill the squares. All further steps were carried out in the laminar flow. The packets were washed with 70% ethanol for 2 minutes and treated with bleach solution for 12 minutes.

For 50 ml bleach solution

30 ml 20 % Bleach (Sodiumhypoclorite 1°)
20 ml H_2O
0.05% Tween 20

The packets were rinsed with sterile H_2O till the pH was in the range of 6.5 – 7.0. Seeds were incubated in sterile water for at least 1 hr (preferably overnight); this step can be combined with stratification if the seeds are placed at 4ºC.

2.3.2 Growth media

2.3.2.1 Composition of ATS (Arabidopsis thaliana salts)

Per 1L 800 ml H_2O

10 g Sugar

5 ml 1M KnO_4

2.5 ml 1M KPO_4 pH 5.5

2 ml 1M $MgSO_4$

2 ml 1M $Ca(NO_3)_2$

2.5 ml 20mM FeEDTA

0.5 ml micronutrients

Add 8 g of Agar per liter for solid medium

Medium was autoclaved on the same day. If not used immediately ATS medium can be stored at room temperature and subsequently melted using a hot water bath.

2.3.2.2 Composition of LB medium

Per 1L 950 ml H_2O

10 g Bacto-tryptone

5g Bacto-yeast

10 g NaCl

Adjust to pH 7.0 with NaOH if necessary

Adjust volume to 1L

Add 8 g of Agar per liter for solid medium

Medium should be autoclaved on the same day. Medium can be stored and melted using the hot water bath.

2.3.3 List of antibiotics

Antibiotics are dissolved and prepared in sterile H_2O. A stock solution of 1000 times working concentration is made and the solution filter sterilised.

Phosphinothricin 50 mg/ ml (PPT)
Kanamycin monophosphate 50 mg/ml (Kn_{50})
Hygromycin 25 mg/ml ($Hygro_{25}$)
Gentamycin 25 mg/ml (G_{25})

Antibiotics were added to LB medium just before being poured into plates (cooled down to a temperature where the bottle could be handled without gloves).

2.3.4 Bacterial culture

Plates (Petri dishes, Sterilin®, Thermo Fisher Scientific Inc., Massachusetts, USA) are prepared in the laminar flow. Bacterial colonies are grown on LB plates containing the appropriate antibiotics.
Bacterial growth plates are placed in incubators. *E. coli* was grown at 37°C overnight, and *A. tumefaciens* at 28°C for 2-3 days or in some cases up to a week.

2.4 DNA extraction from plants

2.4.1 For use in plant genotyping

The Quick *Arabidopsis* DNA miniprep method below was kindly provided by (now) Dr Lynne Armitage from the Leyser Laboratory and is suitable for genotyping of plants.

2 X CTAB buffer (per 250 ml) is made according to the following instructions (final concentrations are given):

5 g	2% CTAB
25 ml of 1M stock	100 mM Tris pH8.0
5 ml of 1M stock	20 mM EDTA pH8.0
20.45g	1.4 M NaCl
2.5 g	1% PVP (polyvinyl-pyrrolidone Mr 40000)

1 or 2 rosette leaves (or other tissue) are placed in an Eppendorf tube. Tissue frozen in liquid nitrogen is suitable for long term storage (-80ºC). Tissue was ground using a grinding machine, handruhrer or by hand using a small Eppendorf pestle. Tissue should not defrost, 300µl 2 X CTAB buffer wa added immediately and sample vortexed. Samples were placed in a 65ºC water bath for at least 5 minutes. This step can be done overnight if lots of samples are processed simultaneously. 300µl of chloroform was added, vortex and spun for 2 minutes. The top layer was transferred to a fresh Eppendorf tube being careful not to take the interface. 800µl of 100% ethanol was added and tubes placed at -20°C for at least 20 minutes. This step can be done overnight if lots of samples are being processed simultaneously. The samples were centrifuged for 5 minutes and the supernatant removed. The pellet was washed in 70% ethanol and subsequently dried (Eppendorf tube placed in the laminar flow cabinet to speed up the process) and resuspended in 50µl water or TE buffer. For downstream analysis 0.5 or 1µl DNA was used in a10 or 20µl PCR reaction.

2.4.2 For use in molecular cloning

For use in molecular cloning and preparation of high quality plant DNA the DNeasy Plant Mini Kit from Qiagen (Qiagen N.V., Venlo, Limburg, Netherlands) was used. DNA concentration was checked on the Nanodrop™

ND-1000 spectrophotometer (Thermo Fisher Scientific Inc., Massachusetts, USA).

2.5 RNA extraction

Tissue is ground using a grinding machine, handruhrer or by hand using a small Eppendorf pestle. Tissue can be frozen in liquid nitrogen for long term storage (-80ºC). For RNA extraction the Qiagen RNeasy Plant Mini Kit was used (Qiagen N.V., Venlo, Limburg, Netherlands), according to the manufacturer's specification. All optional steps were carried out. RNA concentration was checked on the Nanodrop™ ND-1000 spectrophotometer (Thermo Fisher Scientific Inc., Massachusetts, USA).

2.6 cDNA synthesis

cDNA was synthesised from total RNA using Superscript™ II reverse Transcriptase from Invitrogen (Life Technologies, Carlsbad, CA, USA) according to manufacturer's instruction. RNA concentration was checked on the Nanodrop™ ND-1000 spectrophotometer (Thermo Fisher Scientific Inc., Massachusetts, USA) and 500ng RNA was used as starting material for RT-PCR.

A minus-reverse transcriptase (-RT) control is included in the RT-PCR to test for any remaining genomic DNA in the RNA sample. The -RT control contains all the RT-PCR reagents, except the reverse transcriptase. The presence of an amplification product in the -RT control indicates DNA contamination in the sample.

2.7 Plasmid DNA extraction

Plasmid DNA was extracted using the QIAprep Spin Miniprep Kit (Qiagen N.V., Venlo, Limburg, Netherlands) according to manufacturer's instructions. A 4ml LB culture grown overnight was used as the starting material. Plasmid DNA was eluted (50µl) with 1/5 EB Buffer (also Qiagen).

2.8 DNA Analysis

2.8.1 Restriction enzyme digestion

All restriction enzymes (New England BioLabs Inc., Massachusetts, USA) were kindly provided by the Leyser laboratory and used with the appropriate buffer (also NEB). The digestion was carried out as per the instructions of the manufacturer.

The following restriction enzymes were used:

Dra I (5' TTT*AAA)
EcoRV (5' A*GATCT)
Bgl II (5' GAT*ATC)
Rsa I (5' GT*AC)
Bcl I (5' T*GATCA)
Sph I (5' GCATG*C)
Pvu I (5' CGAT*CG)
Hind III (5' A*AGCTT)
Xba I (5' T*CTAGA)

The reaction was incubated at 37ºC for 1 to 2 hours. Restriction digestions were visualised by gel electrophoresis.

2.8.2 Polymerase Chain Reaction (PCR)

2.8.2.1 Standard PCR

A standard PCR was used for genotyping plants, and adapted to be used for bacterial colony selection (colony PCR) and semi-quantitative reverse-transcription PCR (RT-PCR) to estimate differences in cDNA quantity (visualised using gel electrophoresis). A master mix was used to prepare the reactions, typically carried out in a volume of 10µl. The reaction mix is given in table 2.1 and a typical programme in table 2.2. The programme would have been adjusted based on the primers, and purpose of the reaction. All PCR reactions were carried out using a DNA Engine DYAD® PCR machine (BIO-RAD, Hercules, CA, USA) and subsequently visualized using gel electrophoresis.

Type of PCR	**Standard**	**Colony**	**RT-PCR**
Template DNA	0.4µl Genomic DNA	1 µl* bacterial culture	2 µl cDNA
Primer 1 (10 µM)	0.2 µl	0.2 µl	0.2 µl
Primer 2 (10 µM)	0.2 µl	0.2 µl	0.2 µl
Taq DNA polymerase (5U/µl)	0.05 µl	0.05 µl	0.05 µl
Thermopol® buffer	1 µl	1µl	1µl
dNTP (10 mM)	0.2 µl	0.2 µl	0.2 µl
Final volume made up with sterile H_2O	10 µl	10 µl	10 µl

Table 2.1: PCR reaction mix for standard PCR. All reagents from New England BioLabs Inc. (Massachusetts, USA). * For the colony PCR, 15 - 20 colonies were selected and used to each inoculate 1 ml of LB (containing appropriate antibiotic) and placed in the 37ºC incubator for 1 hour. 1µl of the culture is used as template for the PCR.

	Standard
Initiation step	95ºC – 2 min
Denaturation step - Cycle	95ºC – 30 sec
Annealing step - Cycle	Tm – 45 sec
Elongation step - Cycle	72ºC – 1 min per 1kb
Number of cycles **Standard** **Colony** **RT-PCR**	 30 – 35 40 25* – 35
Optional: Final extension step	72ºC – 5 min

Table 2.2: Standard PCR programme. The programme would have been adjusted based on the primers, and purpose of the reaction (e.g. expected length of product). *For the RT-PCR a standard was created with a housekeeping gene (e.g. TUB) and run for 25 cycles.

2.8.2.2 Error-free PCR*

Error-free PCR was used when PCR products were subsequently needed for cloning (using PCR products); in this case the *Pfu* (Promega Corporation, Madison, Wisconsin) proof-reading polymerase or Phusion™ High-fidelity DNA Polymerase (New England Biolabs Inc., Massachusetts, USA) was used. The annealing temperature for the error-free PCR was optimised using a gradient PCR. In the case of Phusion™ High-fidelity DNA Polymerase the annealing temperature is optimised starting from T_m + 3ºC. All PCR reactions were carried out using a DNA Engine DYAD® PCR machine (BIO-RAD, Hercules, CA, USA) and subsequently visualized using gel electrophoresis.

* Error-free PCR is the name of the method, this does not imply that no errors are present.

Reaction mixture for PCR	**Final volume 10 µl**
Buffer	2 µl
dNTP (10 mM)	0.2 µl
Each primer (10 µM)	0.5 µl
Template DNA	0.2 µl
Pfu or Phusion DNA polymerase	0.1 µl
Final Volume made up with dH_2O	6.5 µl

Table 2.3: PCR reaction mix for error-free PCR.

	Pfu (Promega)	**Phusion (NEB)**
Initiation step	95ºC - 2 min	98ºC - 30 sec
Denaturation step - Cycle	95ºC - 30 sec	98ºC - 8 sec
Annealing step - Cycle	Optimized - 45 sec	Optimized - 20 sec
Elongation step - Cycle	72ºC - 1 min per 1kb	72ºC - 30 sec per 1kb
Number of cycles	40	33
Optional: Final extension step	72ºC - 10 min	72ºC - 10 min

Table 2.4: Error-free PCR programme. The PCR programme would have been adjusted based on the primers, and purpose of the reaction (e.g. expected length of product).

The concentration of the PCR product is estimated using the Quick-Load® 1 kb DNA Ladder (New England Biolabs Inc., Massachusetts, USA).

2.8.2.3 Reducing non-specific amplification

In an attempt to reduce non-specific amplification a touchdown PCR protocol adapted from Hecker and Roux (1996) was performed. In a touchdown PCR the annealing temperature is reduced incrementally (in this case per 2ºC for 5 cycles) in progressive cycles designed to bracket the melting temperature (Tm) of the reaction.

A second strategy to reduce non-specific amplification was an improvised Hot Start & Enrichment error-free PCR method. The PCR programme was

started without any tubes in the PCR machine; tubes were added once the machine reached 98ºC. A temperature gradient was applied to the annealing step with two replicates for each temperature. The two replicates were combined and half the sample (10µl) used for gel electrophoresis (section 2.8.2). For the sample that yielded the strongest amplification 1µl of the remaining PCR product (PCR product 1) was placed back in the machine in a new 20µl reaction (PCR product 2) for an additional 10 cycles.

2.8.3 PCR Primers

Primers were constructed with the aid of Primer3 (http://primer3.ut.ee/) and checked for specific binding using NCBI Primer-BLAST (http://www.ncbi.nlm.nih.gov/tools/primer-blast/). Primers were synthesized by VH Bio (Gateshead, United Kingdom) or Sigma Aldrich Corporation (St. Louis, Missouri, USA).

2.8.4 Gel electrophoresis

Gel electrophoresis was carried out using gels made from 1% molecular grade agarose (Sigma Aldrich Corporation, St. Louis, Missouri USA) dissolved in TBE buffer and run in gel tanks at 2-6V/cm.

5X TBE (Tris-Borate-EDTA) solution
108 g/L Tris base
9.2 g/L 0.5M EDTA pH 8.0
55 g/L Boric Acid

1-2µl of SYBRSafe dye (Invitrogen, Life Technologies, Carlsbad, CA, USA) was added per 100ml of gel, and visualisation carried out with a SafeImagerTM (also Invitrogen). Gels were photographed using GeneSnapTM software (Syngene, Biocon, Bengaluru, India).

Where applicable purification of PCR products and electrophoresis gels was carried out using the Illustra GFX™ PCR DNA and Gel Band Purification Kit from GE Healthcare (Amersham, United Kingdom), according to the manufacturer's instructions.

2.8.5 Sequencing & alignments

Sequencing was used to verify the constructs used in plant transformation, to determine the sequence of PCR products for cloning and to determine the exact insert point for T-DNA insertion mutants. Sequencing was carried out by the Technology Facility of the University of York using an Applied Biosystems 3130XL machine. The sequencing primers are described in Appendix A1. The results were analysed using Applied Biosystems Sequence Scanner Version 1.0 (Applied Biosystems, Life Technologies, Thermo Fisher Scientific Inc., Massachusetts, USA). Where verification of a sequence was needed the sample was additionally sent to GATC Biotech AG (Konstanz, Germany).

All sequence alignments were performed with Clustal W (2.1 - www.genome.jp/tools/clustalw).

2.9 Cloning from PCR products

The pENTR™ Directional TOPO® Cloning Kit, LR clonase II enzyme, *E. coli* (DH5α) and *A. tumefaciens* (GV3101) competent cells and both vectors (pENTR™/D-TOPO®, pMDC163) were kindly provided by the Leyser laboratory (Appendix A2).

The pENTR™ Directional TOPO® Cloning Kit (Invitrogen, LifeTechnologies, Carlsbad, CA, USA) was used to directionally clone a blunt-end PCR product into a vector to create an entry clone. The entry

clone is suitable for use in the Gateway® System (also Invitrogen). The entry vector used was pENTR™/D-TOPO®. The TOPO® cloning reaction was carried out using ½ the stated reaction volume; otherwise the kit was used as per manufacturer's instruction. The concentration of the PCR product was estimated using the Quick-Load® 1 kb DNA Ladder (New England Biolabs Inc., Massachusetts, USA). For use in the TOPO® cloning reaction a DNA concentration of 2.5 - 5 ng is desired. The entry clone is introduced into *E. coli* DH5α by *Escherichia coli* transformation (section 2.10.1).

Prior to the Gateway® LR recombination reaction plasmid DNA was extracted (section 2.7) and the vector verified using restriction enzyme digestion (section 2.8.1).

Gateway® LR Clonase® Enzyme mix was used to catalyze the *in vitro* recombination between the entry clone and a destination vector pMDC163 (Curtis and Grossniklaus 2003) to create an expression clone. The LR Recombination Reaction was carried out using ¼ of the recommended reaction volume and incubated for 4 hours; otherwise the kit was used as per manufacturer's instruction. The expression clone is introduced into *E. coli* DH5α by *Escherichia coli* transformation (section 2.10.1).

Prior to the *A. tumefaciens* transformation plasmid DNA was extracted (section 2.7) and the vector verified using restriction enzyme digestion (section 2.8.1).

2.10 Creation of transgenic organisms

2.10.1 Escherichia coli *transformation*

E. coli DH5α competent cells were prepared using the method of Inoue et al. as described by Sambrook and Russell (2001) and stored at -80°C in

aliquots of 100µl. *E. coli* transformation was carried out immediately after the TOPO® cloning reaction and the Gateway® LR Recombination reaction.

An aliquot of DH5α was thawed on ice. Cells were gently mixed using a pipette and 50µl of DH5α cells transferred into a 1.5ml Eppendorf tube. The TOPO® cloning reaction mix (all 3µl) or LR Recombination Reaction mix (all 2µl) is gently added to the DH5α cells and incubated on ice for 30 minutes. The mix was heat shocked for 30 seconds at 42ºC using a waterbath and placed on ice for a further 2 minutes. 950µl of room temperature liquid LB was added to the transformation and incubated for 1 hour at 37ºC in a shaker (225 rpm). The mixture (50µl, 200µl and the remaining mixture) is transferred to pre-warmed (30 minutes at 37ºC) LB plates containing appropriate antibiotics and left overnight at 37ºC. Positive transformants were verified by colony PCR using primers specific for the insert or plasmid (see section 2.8.2 and Appendix A1).

2.10.2 Agrobacterium tumefaciens *transformation*

Chemically competent *Agrobacterium tumefaciens* (GV3101) were prepared and transformed by a method modified from Höfgen and Willmitzer (1988). A 50µl aliquot of *A. tumefaciens* competent cells was thawed on ice and gently mixed with 1µl of plasmid DNA (vector pMDC163) and incubated on ice for 5 min. The mixture was cold shocked/flash frozen for 5 minutes using liquid nitrogen and subsequently incubated for 5 minutes in a water bath at 37ºC. Than 1ml of LB medium was added and the cells placed in the 28ºC shaker (250rpm) for 2-4 hours. The cells are transferred to LB plates (100µl, 300µl, and the rest of the cells) containing gentamycin and the appropriate antibiotic for the plasmid (kanamycin). The plates are incubated at 28ºC for 2-3 days.

2.10.3 Arabidopsis thaliana *transformation*

Arabidopsis thaliana transformation was performed using the floral dip method, adapted from Clough and Bent (1998). *Agrobacterium tumefaciens* culture was prepared by picking up a transformed colony into 10ml LB containing gentamycin and kanamycin and placed overnight in the 250 rpm shaker at 28ºC. Of this 10ml culture 0.9ml was added to an equal amount of 30% glycerol and flash frozen in liquid nitrogen for long term storage at -80ºC. The remaining culture was used to inoculate 400ml LB containing antibiotics and grown as above. 30 minutes before the transformation 100ml of fresh LB medium, 5g sucrose and 200µl Triton X-100 was added and the culture returned to the shaker.

Wild-type plants were grown in the green house until the first siliques had reached maturity. At an early stage the main inflorescence stem was cut to encourage more branching. The inflorescences were dipped in the *Agrobacterium* culture for approximately 1 minute. The plants are returned to the greenhouse covered overnight with a clear plastic bag, which is removed the next day, and plants are allowed to set seed.

Positive transformants were selected based on a method by Harrison et al. 2006. Arabidopsis seeds are sterilized and placed on ATS plates containing hygromycin (25µg/ml). The plates are stratified at 4ºC for 48 hours. The plates are placed in the plant growth chamber for a couple of hours. Plates are subsequently wrapped in aluminium foil and placed back in the growth chamber for 2 days. The aluminium foil is removed and the plates are left in the growth chamber for an additional week. The positive transformants will have elongated compared to the non-transformed plants.

2.11 GUS: Histochemical Staining with X-Gluc

The GUS histochemical staining with X-Gluc is based on a method described by Jefferson (1987).

A 2x GUS pre-stain stock solution is made and components added to make the 2 x GUS stain solution. Water and stain is added to tissue (seedlings) in small glass vials at 37°C for 16hr initially. A brief vacuum infiltration step is carried out. Length of staining can be increased or decreased depending on the construct.

To remove the GUS stain, the fluid is replaced with several changes of 70% ethanol. Tissue clearing is quicker at 37°C and can be carried out overnight. GUS stain can be reused, and is therefore captured in a separate foil wrapped bottle and kept in the fridge.

To make 2x GUS pre-stain stock solution:

20 ml 1M KPO_4 pH 7.0
400 µl Triton X-100
2 ml 200mM $K_4Fe(CN)_6$
2 ml 200mM $K_3Fe(CN)_6$
8 ml 0.5M EDTA pH 8.0
87.6 ml H_2O

To make 200 ml 2x stain solution add:

80 ml Methanol
240 mg X-Gluc dissolved in a small amount of DMSO

Note: 1M KPO_4 pH 7.0
61.5 ml K_2HPO_4 (1M = 17.42 g in 100 ml)
38.5 ml KH_2PO_4 (1M = 13.61 g in 100 ml)

Final concentration: store in dark (wrap bottle in foil) in the fridge

50 mM KPO_4 pH 7.0
0.1% Triton X-100
0.6 mg/ml X-Gluc
1 mM $K_4Fe(CN)_6$
1 mM $K_3Fe(CN)_6$

2.12 Leaf size and shape analysis

2.12.1 LeafAnalyser

LeafAnalyser is a high-throughput computational method that enables us to characterize leaf shape and size more efficiently than previously possible (Weight et al. 2008). The software encompasses an automated image processing, data analysis and data visualization. Leaves are scanned at 300 dpi resolution using a Scanjet 4370 scanner (Hewlett-Packard, www.hp.com) and loaded into LeafAnalyser in the form of a bitmap, JPEG or PNG. LeafAnalyser converts the images to a greyscale, scales the pixel values to the maximum possible dynamic range, and applies a Gaussian filter. The software generates an image histogram, and after thresholding, a fast edge detection method identifies the leaf margins. The image threshold can be adjusted manually for the best fitting margin detection (number of pixels on the x-axis and intensity on the y-axis). LeafAnalyser detects individual leaves by identifying a connected chain of pixels following a leaf margin. LeafAnalyser applies an object filtering method to back-trace any divergence from the margin, and removes any loops. Using a fill algorithm, LeafAnalyser identifies all of the pixels within the margin and calculates the leaf centroid, by averaging the x and y coordinates of all internal pixels. LeafAnalyser provides an estimate of the position of the leaf tip by automatically examining the contours of the pixel chain at the margin. The

position of the leaf tip can be manually adjusted. The indexes representing the nodes of the plants are estimated based on the position of the leaf in the bitmap; incorrect node indexes can be manually adjusted.

Once the node index has been validated LeafAnalyser distributes up to 256 landmarks evenly around the leaf margin starting and ending at the leaf tip, by automatically dividing the length of the pixel chain by the number of landmark points selected.

To generate leaf point models, LeafAnalyser automatically calculates the x and y coordinate values of each landmark, subtracts the value of the centroid from each landmark and saves a text file with one leaf per line expressed as comma-separated values. Text files share the same file name as the original image.

LeafAnalyser's data analysis and data visualization reads the generated text files and performs a Principal Component Analysis. The principal components (PC) are visualised based on standard deviations from the mean leaf. Data can be subdivided into custom groups making it easier to visualise differences between groups in 2-D or 3-D plots. The eigensystem can be exported for downstream analysis.

LeafAnalyser is freely available for download (http://leafanalyser.openillusionist.org.uk/ or http://www.plant-image-analysis.org/software/leafanalyser) with full user documentation outlining the method and functionality of the software.

2.12.2 LeafPredictor

A second software program to accompany LeafAnalyser, developed by Andrew Shofield (MRes Computational Biology, University of York, 2008), will aid us in predicting the leaf shape based on Principal Component Analysis. LeafPredictor imports the eigensystem from LeafAnalyser and

displays the mean leaf of the eigensystem in the plot window (figure 2.1). In either a 2-plot or 4-plot window principal components (PCs) can be manually adjusted starting from the mean leaf (defined by the LeafAnalyser eigensystem) by varying the slider associated with that principal component. In this fashion 4 PCs can be manipulated at any given time. The predicted leaf can be scaled to the mean leaf independently or manually. Predicted leaves can be saved as images or imported back into LeafAnalyser for further analysis. Additional features of the program include the option to use a custom leaf as the mean leaf or to overlay the mean leaf on the predicted leaf, as well as a leaf viewer for individual leaves and a tool to generate a principal component space grid. This feature makes it possible to populate an area in LeafAnalyser by importing a grid of predicted leaves into a particular part of the principal component space.

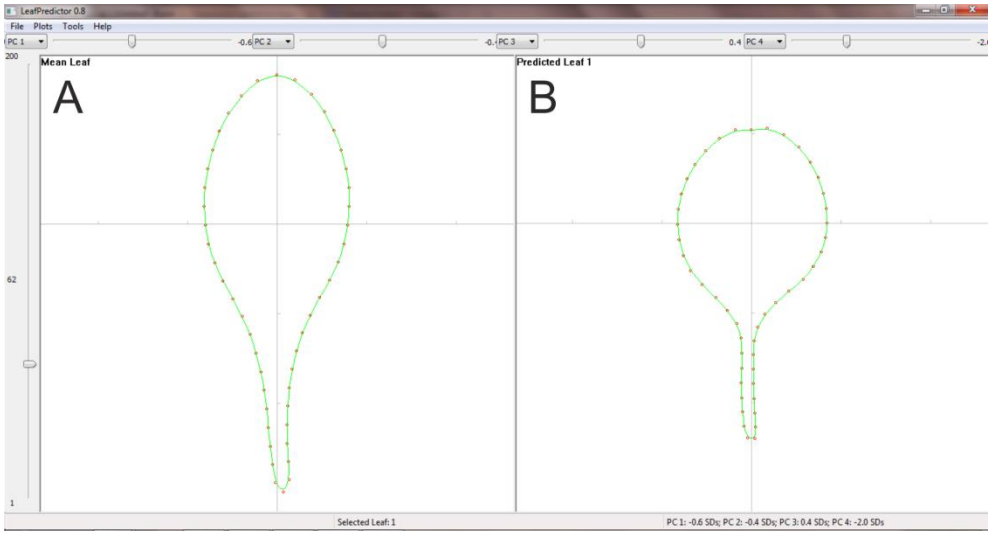

Figure 2.1: User interface of LeafPredictor. A. The mean leaf defined by the eigensystem that has been imported from LeafAnalyser. B. Predicted leaf has been altered from the mean leaf by adjusting the sliders for up to four Principal Components.

LeafPredictor is freely available for download (http://fire-salamander.co.uk/leafpredictor/) with full user documentation outlining the method and functionality of the software.

2.13 Epidermal cell analysis

The epidermal staining method was kindly provided by Dr. S. Bougourd.

Remove the leaf of interest from the plant using a scalpel and put the leaf into a glass vial containing 5% (v/v) Domestos. Place the glass vial(s) on a horizontal shaker on a speed that gently moves the liquid around the vial (approximately 200rpm). Change the bleach solution every day until the leaf is completely transparent (approximately 5 days). Any milky/cloudy areas will not stain properly. Prior to staining place the leaf in water to remove the bleach. Transfer the leaf to 0.1% (v/v) Methylene blue for 1-2 seconds, rinse briefly and mount in water. Note that the leaf is extremely fragile.
Epidermal cells are imaged using the microscope (Nikon optiphoto axiocam).

2.14 Root Growth Assay

Arabidopsis seeds are sterilised according to the method outlined in section 2.3.1. Individual seeds were placed in regular intervals (10 seeds per plate) on 100mm square petri dishes (Sterilin®, ThermoFisher Scientific Inc., Massachusetts, USA) containing ATS medium. The plates were stratified at 4 ºC for 48 hours before being placed in the growth room. The petri dishes were kept upright in a rack and imaged every 24 hours.

2.15 Statistics

Statistical analysis was carried out using PASW Statistics 18 (SPSS, IBM Corporation, New York, US) and R 2.15.2.

2.16 Graphs

Graphs were produced in PASW Statistics 18, LeafAnalyser, LeafPredictor or R 2.15.2 and annotated using CorelDRAW X5.

Chapter 3

The Arabidopsis Leaf Shape Library

3.1 Introduction

The aim of building an *Arabidopsis* Leaf Shape and Size Library is to be able to put any changes in leaf shape and size variation we observe between different *Arabidopsis* lines into context. By populating a leaf shape library with naturally occurring *Arabidopsis* accessions as well as developmental mutants we start to build up a picture of what changes (quantitative as well as directional differences) in leaf shape are possible and viable.

The initial idea was to make the library as large as possible with as much shape and size variation as possible. This chapter will detail how the *Arabidopsis* Leaf Shape Library was constructed and changed over time. A Principal Component Analysis of the leaf shape library with the percentage of variance will be shown at three different stages to illustrate the evolution of the library over time. The stages at which we show the library are not of any significance except to illustrate the changes in the library. In this chapter we look at the evolution of the Principal Components of the library rather than analyse the shape and size differences between the lines in the library; subsequent chapter will cover the shape and size analysis. It will be explained why the decision was made to define a stable reference set subsisting of *Arabidopsis* accessions that are part of the MAGIC lines (Kover et al., 2009; Gnan et al., 2014) narrowing down the selection by excluding ecotypes with significantly longer flowering time.

3.2 Building the library and the development over time

Arabidopsis thaliana plants were sampled after the first flowers had opened. The leaves were arranged on acetate OHP slides according to the phyllotaxis; these slides were scanned and loaded into LeafAnalyser as a bitmap file. The initial processing build into LeafAnalyser will select a threshold value. The histogram shows two peaks, the leaves and the background. When possible the threshold is placed in such a way that the two peaks are completely divided (Weight et al., 2008). The leaf outline will be shown in red. The centroid is calculated and the leaf tip estimated by examining the contours of the leaf margin. Using the histogram at the bottom of the screen the threshold can be manipulated to improve the leaf outline and if necessary the leaf tip can be adjusted manually. The image of the leaf is automatically rotated to vertically align the centroid and the leaf tip. The number of landmarks can be selected in the right-hand corner;

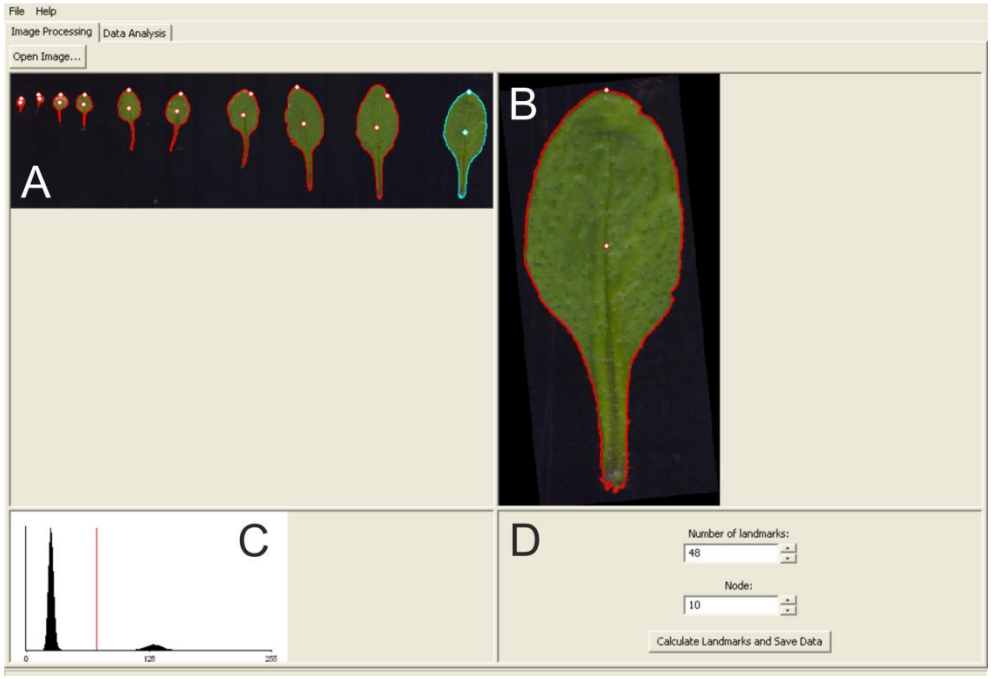

Figure 3.1: Screenshot of the image processing section of LeafAnalyser. A. full image with all leaves of 1 plant arranged from cotyledons on the left to the youngest leaf on the right. B. Close-up view of a selected leaf (blue outline in panel A), tip landmark can be manually

adjusted in this panel by dragging the point along the leaf perimeter. C. Image threshold histogram can be manually adjusted for best fitting margin detection. D. Number of landmarks can be chosen and node number adjusted if the software did not auto-assign the node correctly. Calculate Landmarks and Save Data.

The work carried out for this thesis has been exclusively on *Arabidopsis thaliana*, and the LeafAnalyser setup described below has been chosen for that purpose. Each image contains the complete set of leaves for one plant. As a convention the leaves on the slides are arranged such that the cotyledons are in the left-hand corner. Based on the arrangement of the leaves in the image LeafAnalyser assigned each leave to a node, this can be manually adjusted. In the case of *Arabidopsis* we have chosen to use 48 landmarks. The remaining 47 landmarks will be evenly distributed along the leaf outline when clicking *Calculate Landmarks and Save Data*. Per image a text file is generated with the leaf point models for each individual leaf. LeafAnalyser calculates the Principal Component values by multiplying the leaf point models by the eigenvector matrix. Each Arabidopsis line can be represented by a cloud of points (ellipsoid are a standard deviation). Using the leaf point model it is possible to calculate, and using LeafPredicter, visualize the leaf shape & size for each point in PC space, thereby creating leaf outlines representing the original leaves. A full description of the LeafAnalyser and LeafPredictor software is given in the material and methods section of this thesis (Chapter 2).

3.2.1 Version 1.0

The first version of the leaf shape library contains wild-type plants (Col-0) and the more auxiliary branching mutants (*max1-1*, *max 2-1*, *max3-9* and *max4-1*) (Stirnberg et al., 2002; Bennett et al., 2006). In total there are 1493 leaves from 184 plants. The first version of the library was constructed to test whether there was a difference in leaf size and shape between Col-0 and the *MAX* mutants.

Principal Component analysis (PCA) was applied to the leaf point models using LeafAnalyser. The first five PCs capture 96.52 % of the natural variance in leaf shape and size. The variation in leaf shape and size captured along the PCs is visualised as standard deviation from the mean leaf (figure 3.2). The PCs are numbered according to the amount of variation they explain; PC1 accounts for 74% of the total variation and has a major area effect (47%), higher PC1 values correspond to an increased leaf size. Variation along PC2 accounts for 9.80 % and captures leaf curvature, with the petiole aligned to the left at negative PC2 values and to the right with positive PC2 values. PC3 has an allometric effect capturing variation in leaf shape as well as leaf size; PC3 accounts for 7.15 % of the variation and 11.8 % area effect. 3.68 % of the variation is accounted for by PC4 which captures asymmetry of the blade. PC5 accounts for 1.67 % of natural variation and captures aspect ratio (leaf length: leaf width). Varying PC5 also had a noticeable allometric effect, though smaller than for PC1 and PC3.

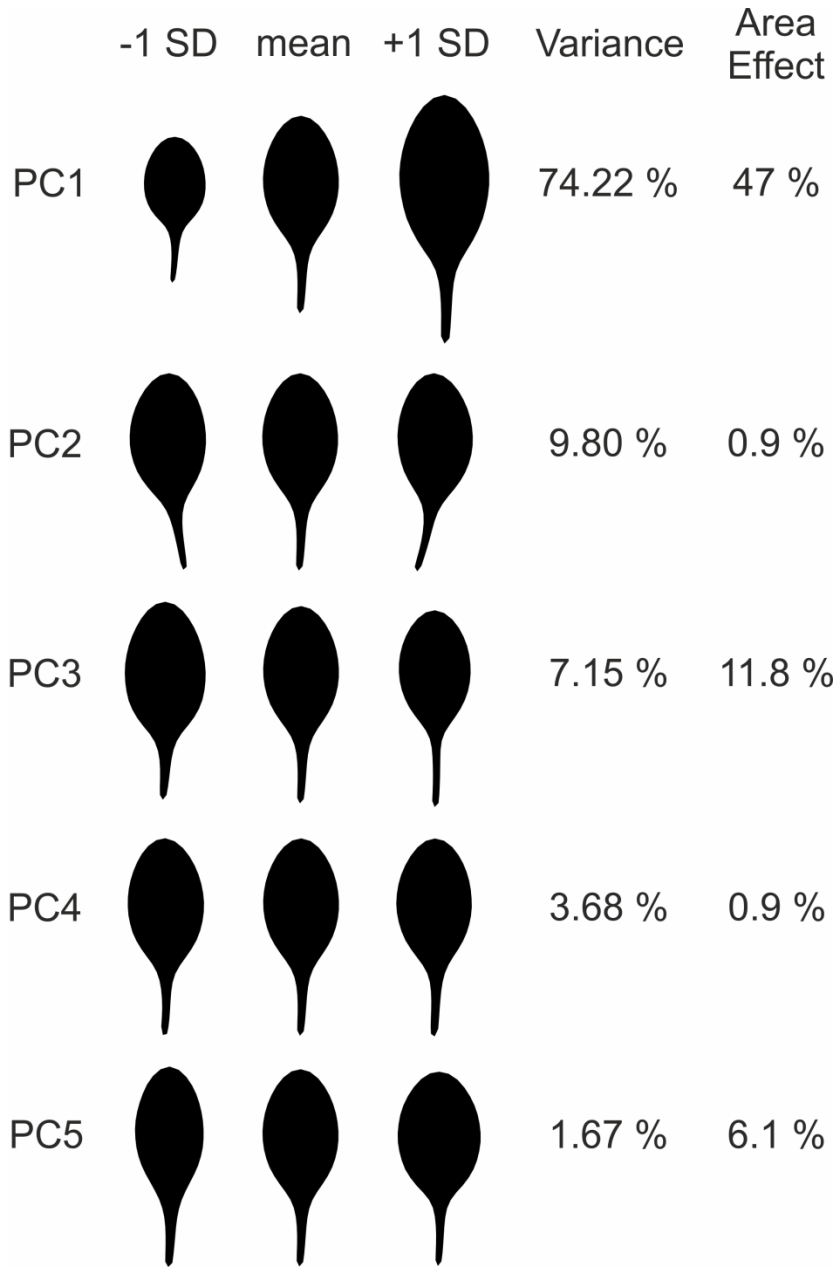

Figure 3.2: Version 1.0 of the Arabidopsis Leaf Size and Shape Library. Each graphically illustrated PC is shown as ±1 SD of the mean leaf, the percentage variance explained and the area effect (at 1 SD). Only the PCs with at least 1% variance are depicted.

3.2.2 Version 1.1

Version 1.1 of the leaf shape library contains 4711 leaves, an additional 15 *Arabidopsis* accession and leaf developmental mutant lines were added compared to version 1.0. The library was expanded to test whether we could quantify leaf size and shape differences between natural *Arabidopsis*

thaliana accessions as well as investigate the functional role of *TCP14* and *TCP15* (see chapter 5). In version 1.1 of the leaf shape library the first five PCs explain 98.5 % of the variation. Variation along PC1 accounted for 84.4 %, PC2 accounted for 6.66 %, PC3 accounted for 5.85 %, PC4 accounted for 0.87 % and PC5 accounted for 0.75 %. The variation in leaf shape and size captured along the PCs is visualised as standard deviation from the mean leaf and illustrated in figure 3.3. Similar to the first analysis PC1 captures leaf size; the percentage of variation explained by this PC has increased and has a 64% area effect. PC2 and PC 3 are mirror images of each other combining variation in leaf shape and variation in curvature with the petiole aligned either to the left or the right. Both PC2 and PC3 have a strong allometric effect, respectively 18 % and 13.8 %. PC4 captures asymmetry of the blade and has a negligible effect on area. PC5 had an allometric effect influencing aspect ratio (leaf length: leaf width) as well as area.

When visually comparing $PC2_{1.0}$ and $PC3_{1.0}$ (version 1.0) to $PC2_{1.1}$ and $PC3_{1.1}$ (version 1.1) it appears that $PC2_{1.1}$ and $PC3_{1.1}$ both show aspects of leaf curvature ($PC2_{1.0}$) and leaf shape ($PC3_{1.0}$) with an allometric aspect that is most pronounced in $PC2_{1.1}$. It is almost as if the second and third PC in version 1.1 are combinatorial forms of $PC2_{1.0}$ and $PC3_{1.0}$. We would predict that these PCs are unstable, what we mean by that is that these PCs are likely to be transitional, when additional leaves are added to the leaf shape library the PCs will likely resolve into PCs similar to the original $PC2_{1.0}$ and $PC3_{1.0}$. However, $PC2_{1.0}$ has hardly any effect on the area but $PC2_{1.1}$ and $PC3_{1.1}$ both carry significant allometric effects. It should also be noted that the orientation of the PC5 axis has been reversed, at -1 SD a leaf is rounder compared to the mean leaf, while a leaf is more elongated at +1 SD form the mean leaf.

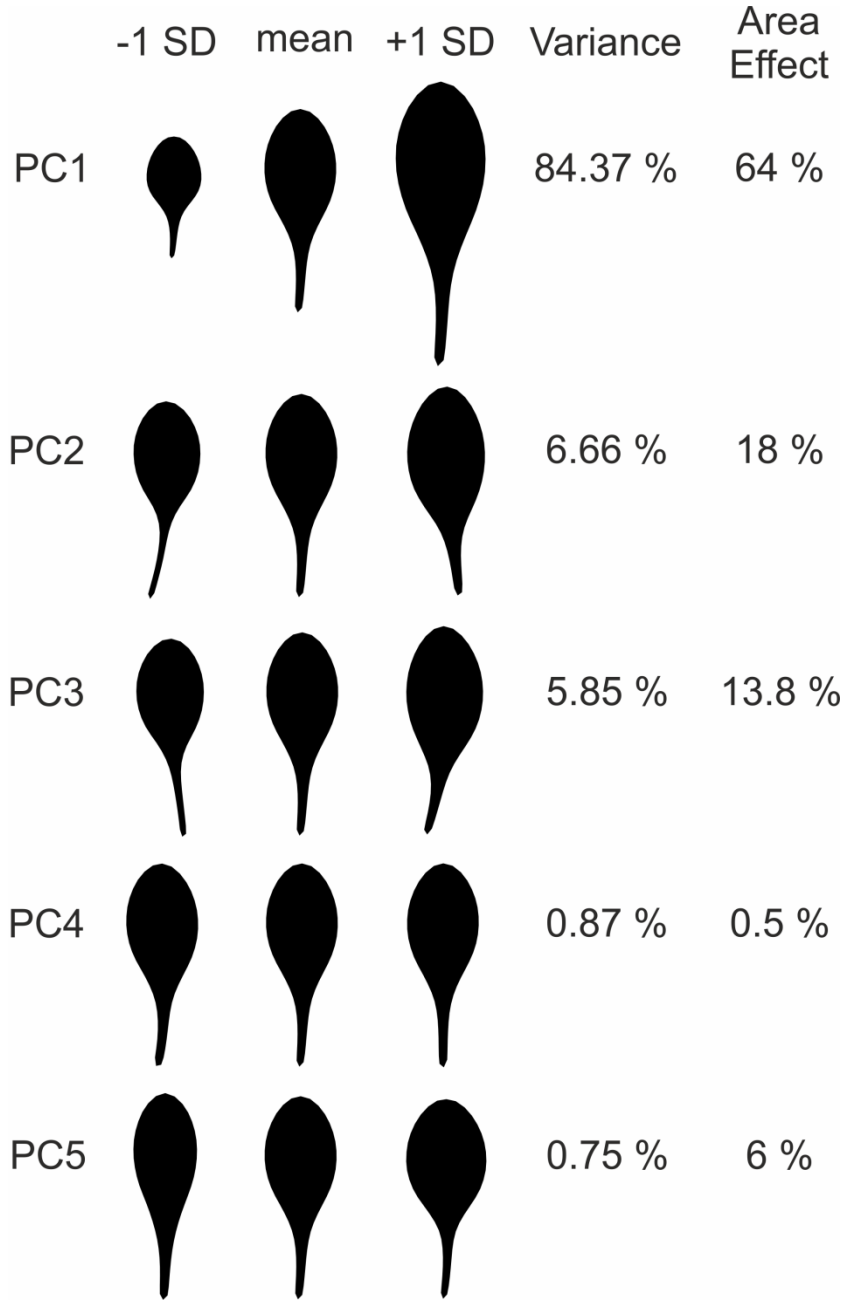

Figure 3.3: Version 1.1 of the Arabidopsis Leaf Size and Shape Library. Each graphically illustrated PC is shown as ±1 SD of the mean leaf, the percentage variance explained and the area effect (at 1 SD). Only the PCs with at least 1% variance are depicted.

3.2.3 Version 1.2

Version 1.2, or the full *Arabidopsis* Leaf Shape Library has a total of 6519 leaves, additional *Arabidopsis* accessions were added to the library which now accounts for a large part of the naturally available *Arabidopsis* leaf size

and shape. The PCA reveals that 98.48 % of the variation can be captured by investigating the first five PCs. Size is still the major source of variation in Version 1.2 of the leaf shape library. PC1 has a major effect on area and accounts for 84.26 % of the natural variation. PC2 accounts for 6.78% of the variation, PC3 accounted for 5.87 %, PC4 accounted for 0.88% and PC5 accounted for 0.69 % of the total variation. PC4 is the only principal component that has no significant allometric effect. The variation of each PC is visualised as standard deviations from the mean leaf. Their contribution towards the total variation and its corresponding area effects are illustrated in figure 3.4.

$PC2_{1.2}$ still shows a combinatorial effect on leaf shape and curvature, with the petiole aligned to the left at -1 SD and aligned to the right at +1 SD. PC2 and PC3 both have an allometric effect, though it is more pronounced in PC3. When we visually compare $PC2_{1.2}$ to PC2 from version 1.0 and version 1.1 it appears more similar to $PC2_{1.0}$ and captures more the aspect of curvature rather than variation in leaf shape though it still carries an allometric effect of around 11 %. PC3 has a slight aspect of curvature but mainly captures a variation in leaf shape and area. The orientation of PC5 axis has reversed again; higher values of PC5 have rounder leaves compared to the mean leaf while negative PC5 values have more elongated leaves.

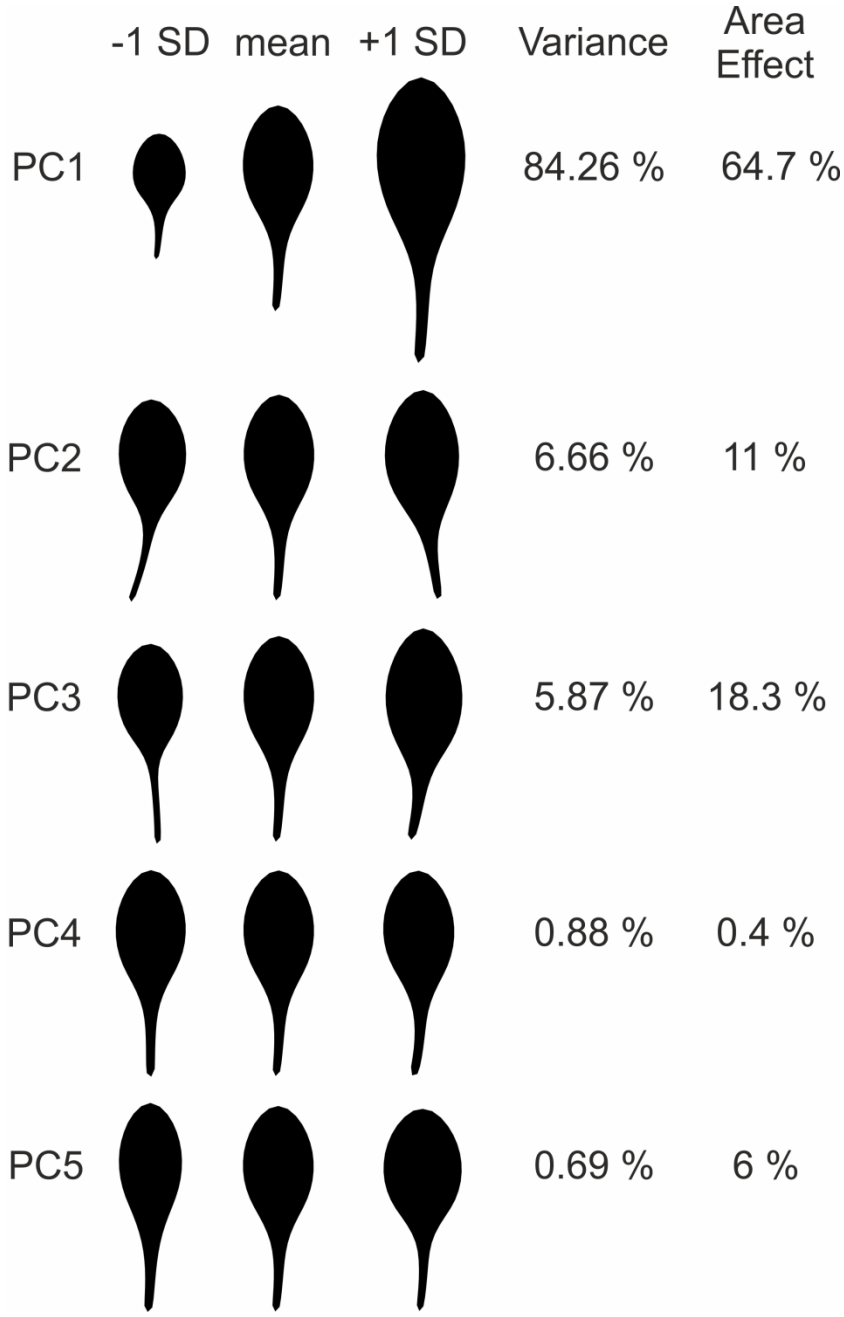

Figure 3.4: Version 1.2 of the Arabidopsis Leaf Size and Shape Library. Each graphically illustrated PC is shown as ±1 SD of the mean leaf, the percentage variance explained and the area effect (at 1 SD). Only the PCs with at least 1% variance are depicted.

3.3 Establishing a stable reference set

Version 1.0 through version 1.2 of the Arabidopsis Leaf Shape Library illustrates that adding additional leaves to the library changes the Principal Components. This is not surprising since the datasets (or number of leaves)

that are included in the analysis determine the major sources of variation, which is what the Principal Components are designed to highlight. For lack of a better way of describing this phenomenon we will say that the *Arabidopsis* Leaf Shape library can be considered to be unstable. If we want to compare or analyse different lines over a longer period of time it would be easier if the Principal Components stay fixed or stable. Though it is important to have sufficient data (e.g leaves) to produce a high quality principal component analysis we considered it preferable to maintain a stable reference set. This reference set could be used to construct a reference eigensystem making it possible to analyse new lines by PCA without integrating them into the eigensystem. The stable reference set is used to make an eigenvector matrix. The PC values for a line of interest are calculated by multiplying the leaf point models generated by LeafAnalyser with the reference eigenvector matrix.

The stable reference set contains 1050 leaves from 10 *Arabidopsis* accessions (figure 3.5). The 10 *Arabidopsis* accessions in the stable reference set were chosen because they have similar flowering times and are a subset of the Multiparent Advanced Generation Inter-Cross (MAGIC) lines described by Paula Kover (Kover et al., 2009; Gnan et al., 2014), making the downstream analysis of these lines easier. We are exclusively looking at the PCs that account for more than 1% of the natural shape and size variance. The variation in leaf shape and size captured by the PCs are shown as standard deviations from the mean leaf. The first four PCs account for 97.53 % of the total variance. Variation along PC1 accounts for 80.92 % of the natural variance in leaf shape and size, and captures variation in leaf size. Higher PC1 values correspond to an increased leaf size. PC2 explains 8.95 % of the total variation and describes a variation in leaf shape. Curvature of the leaf is captured by PC3, with the petiole aligned to the left or to the right, and accounts for 6.61 % of the total variation. The average leaf has a petiole that is aligned slightly to the left. Compared to the average leaf lower PC3 values will have a petiole curving more strongly to the left and higher PC3 values will curve to the right. Neutral petiole position is

attained with an approximate PC3 score of 0.2. PC4 accounts for 1.05 % of the variance and captures aspect ratio (leaf length: leaf width).

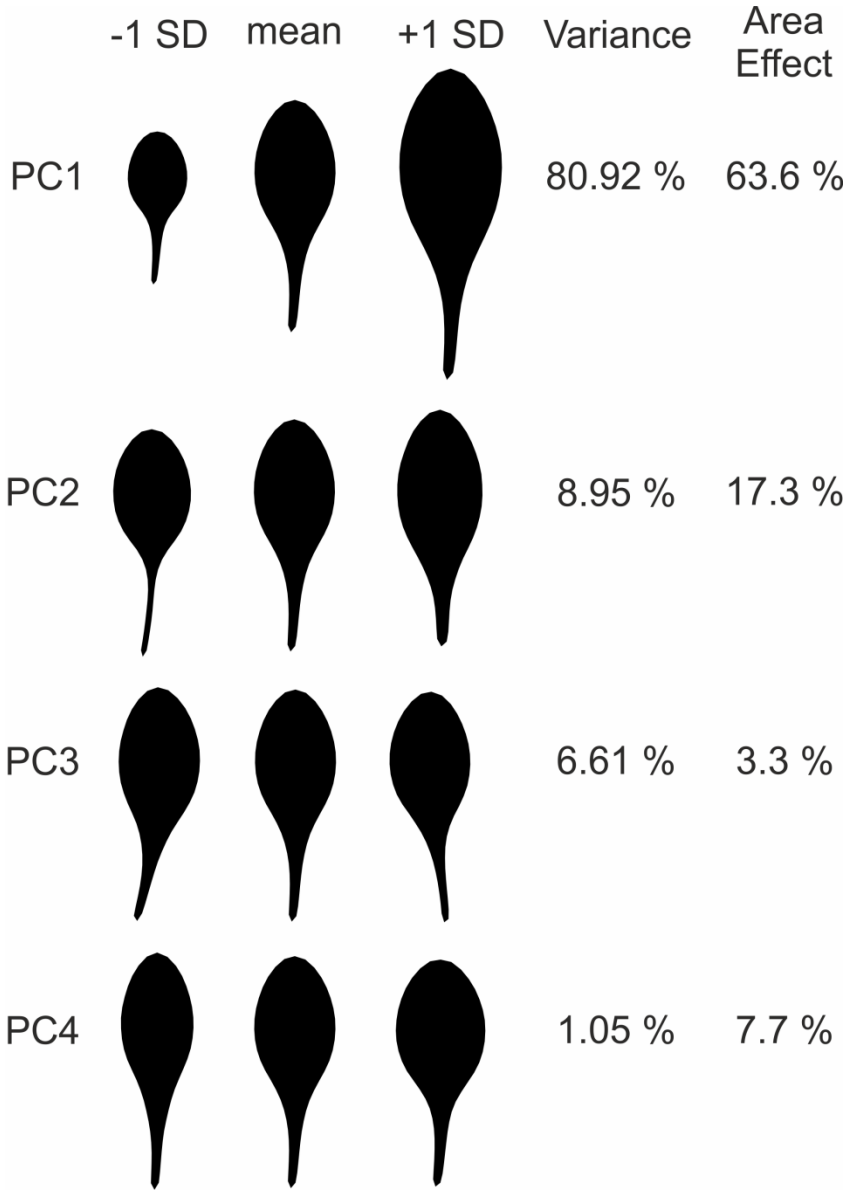

Figure 3.5: The stable reference set or version 2.0 of the Arabidopsis Leaf Size and Shape Library. Each graphically illustrated PC is shown as ±1 SD of the mean leaf, the percentage variance explained and the area effect (at 1 SD). Only the PCs with at least 1% variance are depicted.

3.4 Leaf shape and size analysis for the Arabidopsis reference set

To determine whether any of the PCs are significantly different between the 10 *Arabidopsis* accessions in the reference set a Kruskal-Wallis test was performed. The test revealed that there are significant differences between the 10 accessions for PC1, PC2, PC3 and PC4 (figure 3.6 and 3.7). A pairwise comparison (Wilcoxon rank sum test) was carried out to determine the differences between the lines (table 3.1).

The pairwise comparisons show that between the accessions there is a difference in leaf size, captured by PC1. With the largest average leaf size Po-0 has the highest mean PC1 score while Mt-0 and Wil-2 have lower average PC1 scores which reflect that their leaf size is smaller than the mean leaf. Ct-1, Kn-0, Hi-0 and No-0 have similar PC1 scores and their leaf size closely resembles the mean leaf.

There is a large amount of variation visible between the accessions along the PC2 axis. Looking at the pairwise comparison in table 3.1, we can see that the leaf shape of the majority of the accessions are significantly different from each other. The most extreme difference is between Po-0 (mean PC2 = -0.9961) and No-0 (mean PC2 score = 0.9831), and Ct-1 most closely resembles the leaf shape of the mean leaf. Most of the lines are significantly different from the mean leaf, either by a shift to a more positive PC2 value or to a negative PC2 value.

Though the Kruskal-Wallis test indicates that there was a significant difference between the lines for PC3 the pairwise comparison shows that only a few lines have statistically significantly different mean PC3 scores. Hi-0 is significantly different from Mt-0 and Oy-0 ($p < 0.05$), and Mt-0 significantly different from Wil-2. Hi-0 and Wil-2 have lower PC3 scores and correspondently their petiole curves to the left, while Mt-0 has a higher PC3 score and the petiole aligns to the right.

Similar to PC2, there is a large amount of variation visible between the accessions along the PC4 axis. PC4 describes leaf aspect ratio (leaf length: leaf width), a leaf with a more positive PC4 value will be narrower and more elongated. Hi-0 has the highest mean PC4 value (mean PC4 = -0.9259), No-0 the lowest (mean PC4 = -1.367), Rsch-4 has a mean PC4 value just above (mean PC4 = 0.274) the mean leaf and Wil-2 just below (mean PC4 = -0.0734) the mean leaf.

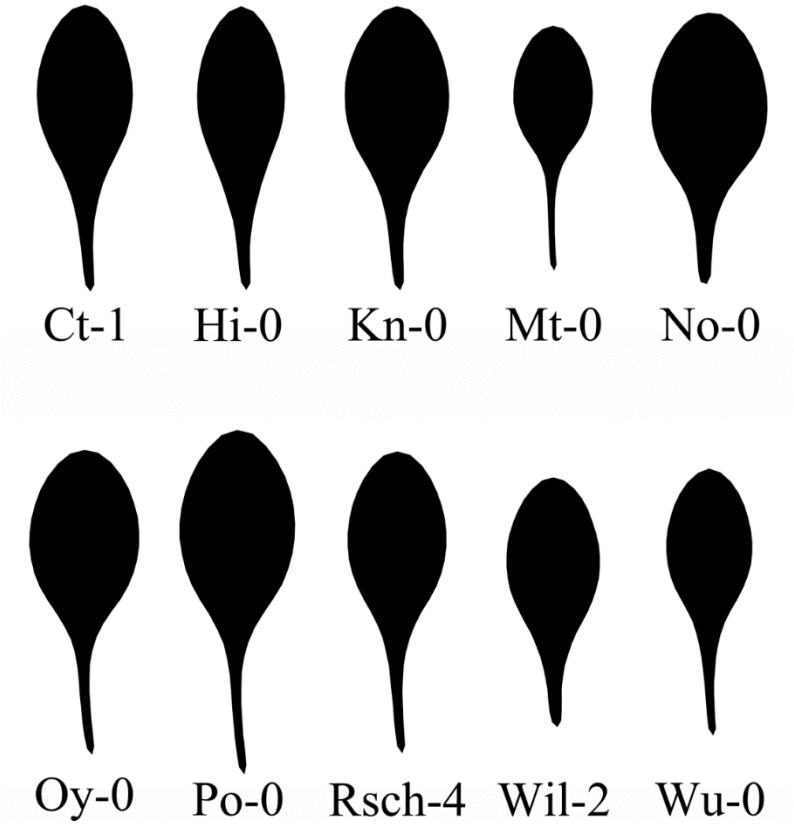

Figure 3.6: Comparison of leaf point models for nodes 5–11 for leaves from the *Arabidopsis* reference set. The mean PC score is calculated from mean PC1, PC2, PC3 and PC4 scores, visualising the mean size and shape of the leaves for each line. These leaves were constructed using LeafPredictor and the eigensystem of the reference set.

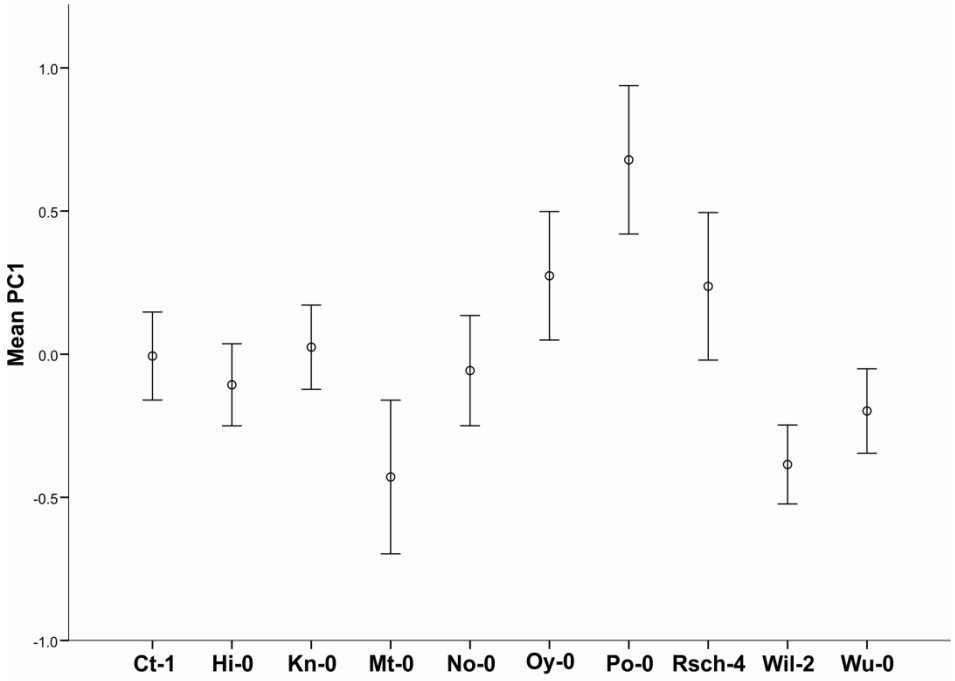
Mean PC1
1.0
0.5
0.0
-0.5
-1.0
Ct-1
Hi-0
Kn-0
Mt-0
No-0
Oy-0
Po-0
Rsch-4
Wil-2
Wu-0

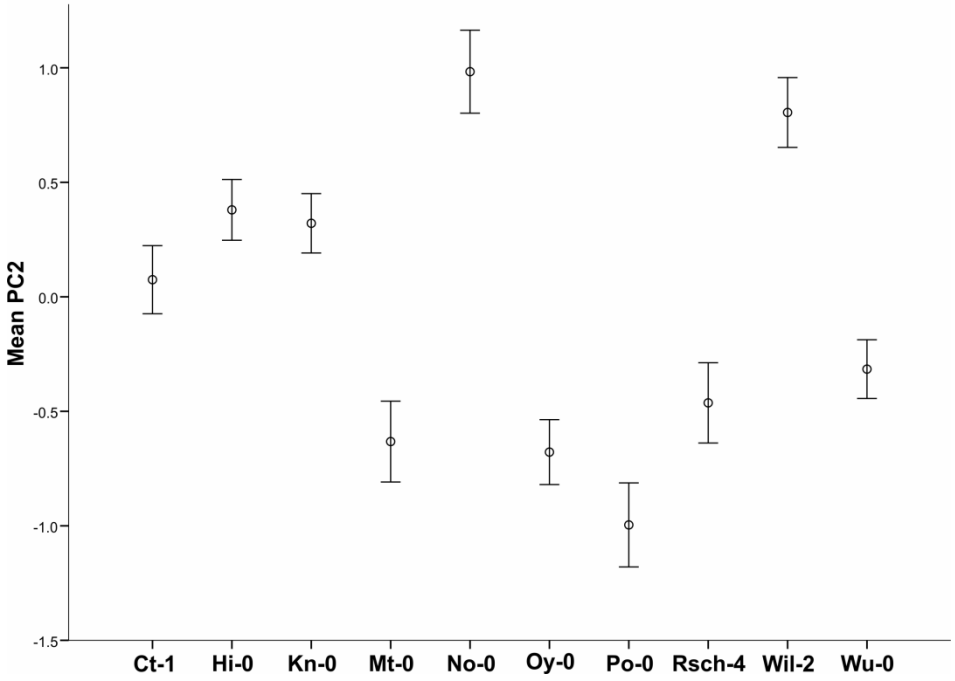
Mean PC2
1.0
0.5
0.0
-0.5
-1.0
-1.5
Ct-1
Hi-0
Kn-0
Mt-0
No-0
Oy-0
Po-0
Rsch-4
Wil-2
Wu-0

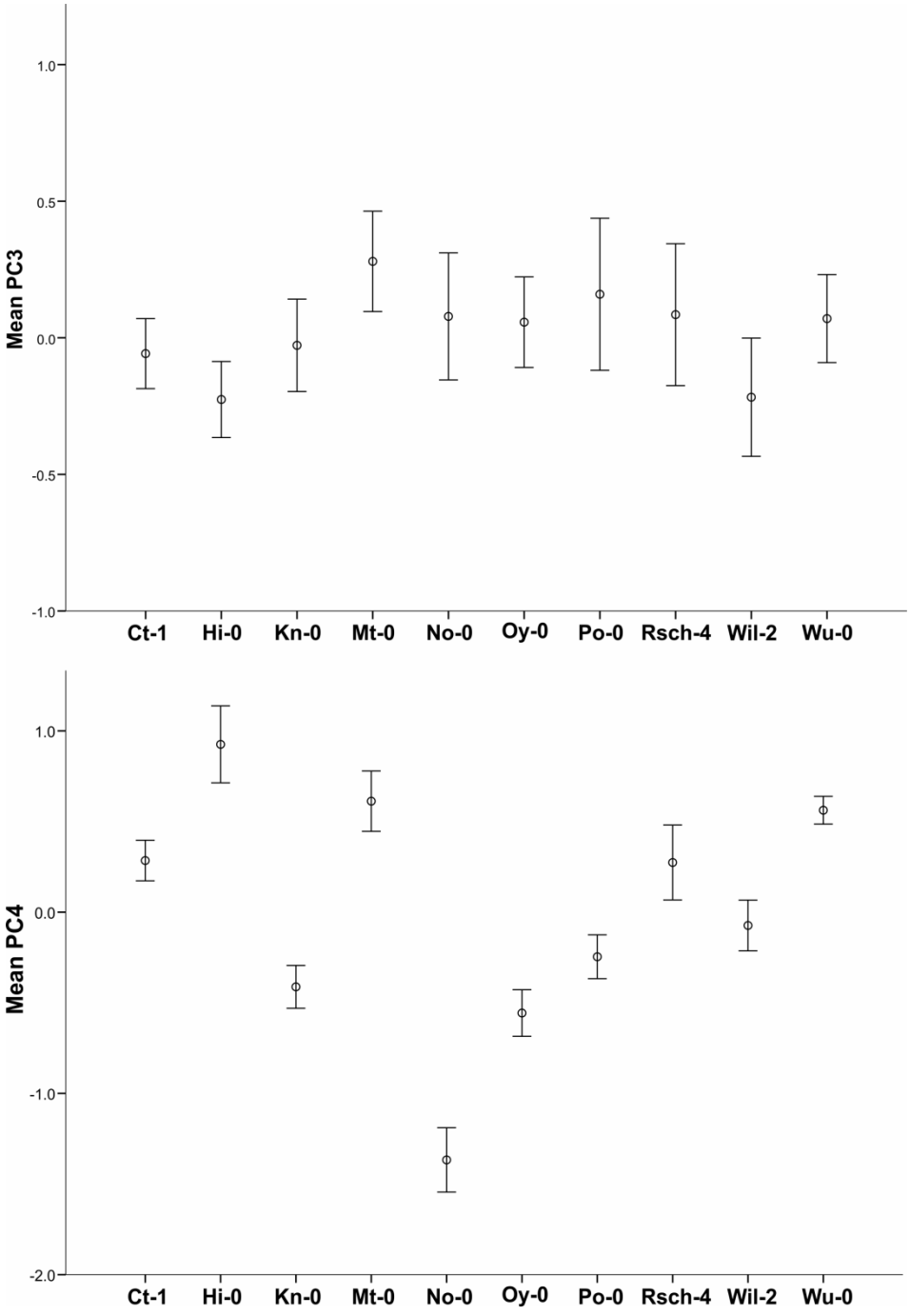

Figure 3.7: Leaf shape and size analysis for the *Arabidopsis* reference set of 10 natural accessions containing 1050 leaves. The mean PC scores for PC1, PC2, PC3 and PC4 for all leaves for the 10 Arabidopsis accessions. Error bars represents 95% confidence intervals.

PC1	Ct-1	Hi-o	Kn-0	Mt-0	No-0	Oy-0	Po-0	Rsch-4	Wil-2
Hi-o	1.00000	-	-	-	-	-	-	-	-
Kn-0	1.00000	1.00000	-	-	-	-	-	-	-
Mt-0	0.06073	0.25171	0.02557	-	-	-	-	-	-
No-0	1.00000	1.00000	1.00000	0.31727	-	-	-	-	-
Oy-0	1.00000	0.24228	1.00000	0.00588	0.95637	-	-	-	-
Po-0	0.00373	0.00012	0.00304	1.2e-05	0.00137	0.48391	-	-	-
Rsch-4	1.00000	1.00000	1.00000	0.01762	1.00000	1.00000	1.00000	-	-
Wil-2	0.01854	0.14072	0.00295	1.00000	0.06891	0.00066	1.6e-07	0.02557	-
Wu-0	1.00000	1.00000	1.00000	1.00000	1.00000	0.05710	8.7e-06	0.37860	1.00000

PC2	Ct-1	Hi-o	Kn-0	Mt-0	No-0	Oy-0	Po-0	Rsch-4	Wil-2
Hi-o	0.00204	-	-	-	-	-	-	-	-
Kn-0	0.00522	1.00000	-	-	-	-	-	-	-
Mt-0	2.9e-05	1.6e-13	3.8e-13	-	-	-	-	-	-
No-0	1.1e-11	6.2e-06	7.0e-08	< 2e-16	-	-	-	-	-
Oy-0	2.0e-08	< 2e-16	< 2e-16	1.00000	< 2e-16	-	-	-	-
Po-0	1.3e-13	< 2e-16	< 2e-16	0.01062	< 2e-16	0.03535	-	-	-
Rsch-4	0.00512	9.3e-10	5.6e-09	1.00000	< 2e-16	0.40272	0.00098	-	-
Wil-2	3.6e-10	0.00053	5.1e-06	< 2e-16	0.96815	< 2e-16	< 2e-16	2.9e-16	-
Wu-0	0.00038	1.3e-13	2.1e-13	0.73188	< 2e-16	0.01561	1.1e-07	1.00000	< 2e-16

PC3	Ct-1	Hi-o	Kn-0	Mt-0	No-0	Oy-0	Po-0	Rsch-4	Wil-2
Hi-o	1.0000	-	-	-	-	-	-	-	-
Kn-0	1.0000	1.0000	-	-	-	-	-	-	-
Mt-0	0.0818	0.0020	0.9594	-	-	-	-	-	-
No-0	1.0000	0.2101	1.0000	1.0000	-	-	-	-	-
Oy-0	1.0000	0.0482	1.0000	1.0000	1.0000	-	-	-	-
Po-0	0.8561	0.0645	1.0000	1.0000	1.0000	1.0000	-	-	-
Rsch-4	1.0000	1.0000	1.0000	1.0000	1.0000	1.0000	1.0000	-	-
Wil-2	1.0000	1.0000	0.8951	0.0017	0.1606	0.0549	0.0934	0.9594	-
Wu-0	1.0000	0.9242	1.0000	1.0000	1.0000	1.0000	1.0000	1.0000	0.3402

PC4	Ct-1	Hi-o	Kn-0	Mt-0	No-0	Oy-0	Po-0	Rsch-4	Wil-2
Hi-o	0.00113	-	-	-	-	-	-	-	-
Kn-0	6.6e-14	< 2e-16	-	-	-	-	-	-	-
Mt-0	0.00507	1.00000	8.3e-16	-	-	-	-	-	-
No-0	< 2e-16	< 2e-16	1.1e-14	< 2e-16	-	-	-	-	-
Oy-0	1.9e-15	< 2e-16	1.00000	< 2e-16	2.8e-10	-	-	-	-
Po-0	2.4e-07	2.3e-14	0.25460	2.5e-11	< 2e-16	0.02042	-	-	-
Rsch-4	1.00000	0.00605	6.5e-07	0.03883	< 2e-16	4.1e-08	0.00114	-	-
Wil-2	6.6e-05	4.2e-12	0.00761	1.2e-08	< 2e-16	0.00049	1.00000	0.03432	-
Wu-0	1.4e-05	1.00000	< 2e-16	1.00000	< 2e-16	< 2e-16	< 2e-16	0.00761	1.7e-13

p < 0.05
p < 0.001

Table 3.1: Pairwise comparison of PC1 to PC4 of the accessions in the reference dataset using Wilcox rank sum test. P value adjustment method: Holm. Light grey indicates a p value lower than 0.05, dark grey a p value lower than 0.001.

3.5 Discussion

In this chapter we have introduced the LeafAnalyser software and described the evolution of the *Arabidopsis thaliana* leaf shape library culminating in the stable reference set containing 10 *Arabidopsis* accessions. Initially the library was envisioned to contain as many accessions and leaf shape mutants as proved feasible. When new lines were analysed using LeafAnalyser the

leaves were integrated into the library in the process of the analysis. The mean leaf would therefore be calculated based on a set of leaves that contains the lines that we wish to analyse. From a statistical point of view this is not ideal; it is true that a PCA needs sufficient number of replicates to be valid but with the number of leaves available to us that is not a consideration (Number of samples = (2x number of landmarks) +2). We have additionally seen that when continuously adding leaves to the library the PCs become unstable. There are points when two PCs seem to merge, are mirror images of each other, before they separate again, and generally have changed position in the process (PC2 has become PC3 and vice versa). The downside of this situation is that PC2 may depict leaf shape in one analysis but in an extreme case could potentially be leaf aspect ratio in another. Though not technically a problem, it is nonetheless not ideal.

Using a stable reference set solves these problems and thereby is a far more elegant and user-friendly solution. The reference set defines the natural leaf shape variation in *Arabidopsis thaliana*. We will use the reference set as a standard for any further leaf shape and size analysis in this manuscript.

The *Arabidopsis thaliana* accessions represent naturally occurring genetic variation in Arabidopsis, however, the genetic basis of the natural variation remains unclear. Most traits of interest (e.g. economically important traits such as seed dormancy, flowering time and fruit production), including leaf shape and size, are quantitative traits and their phenotypic expression is dictated by the combination of many genetic (complex genetic inheritance) and environmental factors (Kover et al., 2009).

To discover the underlying genetic basis for the variation in leaf shape and size between the *Arabidopsis* accessions it will be necessary to conduct quantitative trait loci (QTL) mapping or genome-wide association study (GWAS); similar to the work carried out by Gnan et al. (2014) and Filiault and Maloof (2012) in *Arabidopsis* and Chitwood et al. (2013) in tomato. To facilitate the analysis of the underlying genetic basis of the variation in leaf shape and size in the *Arabidopsis* reference set the decision was made to

define a stable reference set subsisting of *Arabidopsis* accessions that are part of the MAGIC lines produced by Kover et al. (2009). The MAGIC lines are derived from an advanced intercross of *Arabidopsis thaliana* produced by intermating 19 natural accessions for four generations and then inbreeding for 6 generations. The resulting nearly homozygous lines form a stable panel of recombinant inbred line (RIL) that do not require repeated genotyping in each QTL study (Kover et al., 2009).

Further investigation of the *Arabidopsis thaliana* accessions has been taken up by Joseph Vaughan as a separate PhD also funded by a White Rose Studentship.

Chapter 4

Exploring the *Arabidopsis* Leaf Shape Library

4.1 Exploring the Arabidopsis Leaf Shape Library

4.1.1 Identifying outliers in the dataset

As indicated in the Material and Methods of this thesis (Chapter 2), it was decided not to include the cotyledons and first pair of leaves into the leaf shape and size analysis due to the fact that these leaves are often in a state of decomposition or partially eaten by thrips or sciarid larvae. An initial test of the database included all leaves regardless of the condition of the leaves. LeafAnalyser's built in visualisation tool can be used to identify outliers (Figure 4.1) in the dataset. Outliers can be interesting in order to investigate what the extremes in shape and size are within a given accession. The mouseover feature of LeafAnalyser will identify the corresponding text file for a given data point. All text files are named to reflect the accession and individual leaf (e.g. Hi-0_1) in order to facilitate tracing the data point back to the source. As illustrated in figure 4.1, in most cases the extreme outliers are either leaves malformed during development or damaged. The main source of damage is due to pest larvae which has been a considerable problem during this thesis. In general it is believed that LeafAnalyser is robust enough not to worry about having a number of damaged leaves in the database, however, to maintain a clean database only leaves deemed to be in acceptable condition were added to the database.

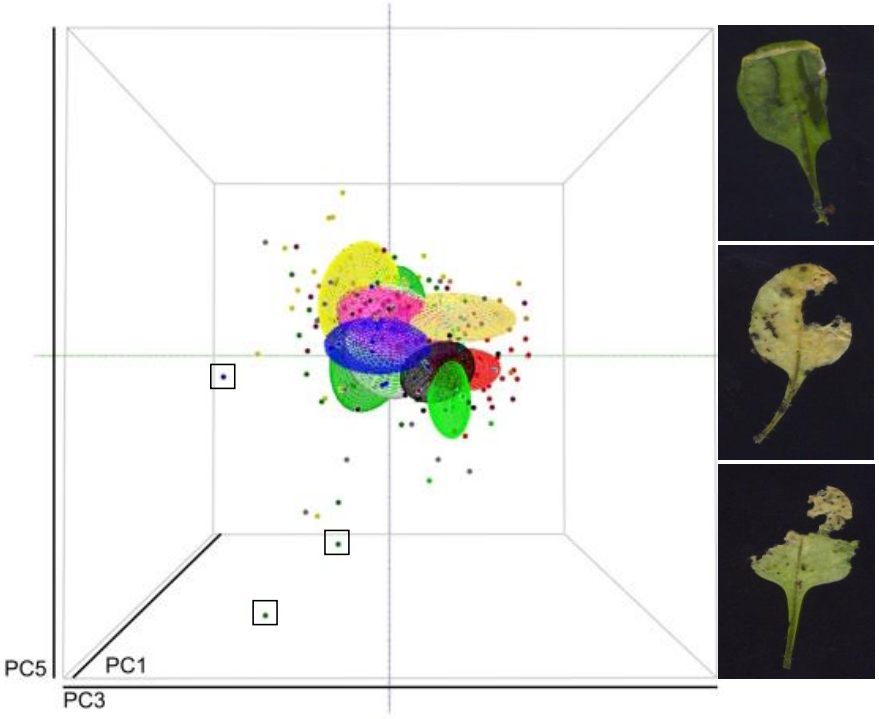

Figure 4.1: Detection of outliers. Outliers can be detected and traced back to the image database to determine whether or not these represent damaged leaves or genuine outliers. This figure was created using an initial test version of the *Arabidopsis* Leaf Shape Library and depicts leaves at node 6. Each plant line (different colours on the figure) is represented by a cloud of points and an ellipse representing 1 SD (standard deviation from the mean).

4.1.2 Comparing wild-type lines from different research groups

Columbia (Col-0) wild-type plants from different research groups have been integrated in the *Arabidopsis* leaf shape library. A first wild-type (Col-0) control set was kindly donated by the Leyser Laboratory and grown and analysed at the same time as the *MAX* mutants, a second set of wild-type (Col-0) seeds was received from the laboratory of Brendan Davies and grown simultaneously with the *tcp14-4*, *tcp15-3* and *tcp14-4tcp15-3* T-DNA insertion lines, the remaining Col-0 wild-type plants are sourced from the Waites group seed stock. Though there is a considerable degree of overlap the wild-type populations from the Leyser (pale blue) and Davies (grey) stock separate into distinct groups. The third population (black) was sourced from the Waites group seed stock and is almost completely separated from

the other wild-type populations (figure 4.2). In the case of the Waites Col-0, a large proportion of the effect is believed to be caused by the diseased state of the plants rather than the seed stock origin. It should be noted that the three Col-0 wild-type lines were not grown at the same time. To verify if the difference in leaf shape and size (or a proportion thereof) of the three Col-0 wild-type lines are due to the origin of the seed stock the lines should be regrown at the same time in the same conditions. If the differences we see are maintained it would indicate that the different seed stocks have become genetically different, potentially through 'genetic contamination' of the seed stock by other *Arabidopsis* lines.

4.1.3 Healthy versus diseased plant populations

The Leyser and Davies wild-type plants displayed in figure 4.2 were healthy plant populations, the Waites plant population failed to thrive due to unknown causes. There is a clear separation of the plant populations as well a marked decrease of leaf nodes.

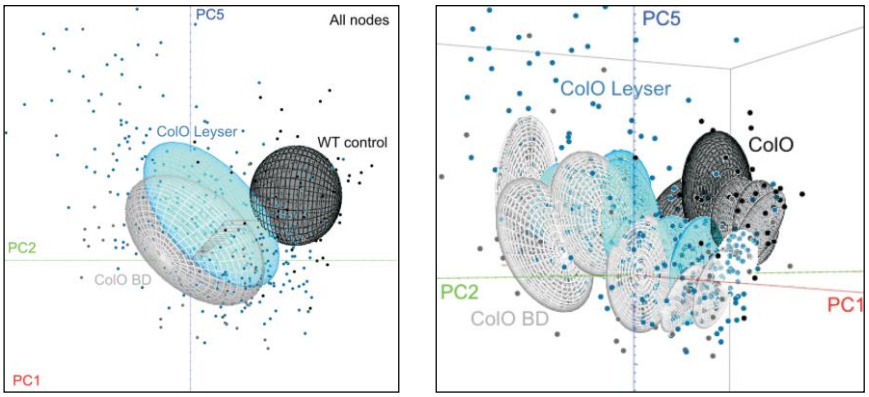

Figure 4.2: Comparison of leaf size and shape of Colombia wild-type plants from different seed stocks and in different health conditions. Grey = Col-0 plants grown from seeds donated by the Davies Laboratory, Pale blue = Col-0 plants grown from seeds donated by the Leyser Laboratory, Black = unhealthy population of wild-type plants (Waites stock). The left panel shows the 1 SD ellipse for all nodes, the right panel has an ellipse per leaf node.

4.1.4 Tracking a seed line across multiple seasons

During the course of this thesis the plant line Landsberg *erecta* (Ler-0) was grown at different times of the year. Figure 4.3 illustrates that the leaf shape of an accession subtly changes throughout the season. With LeafAnalyser we are able to pick up on these changes which would be impossible to pick up by eye alone.

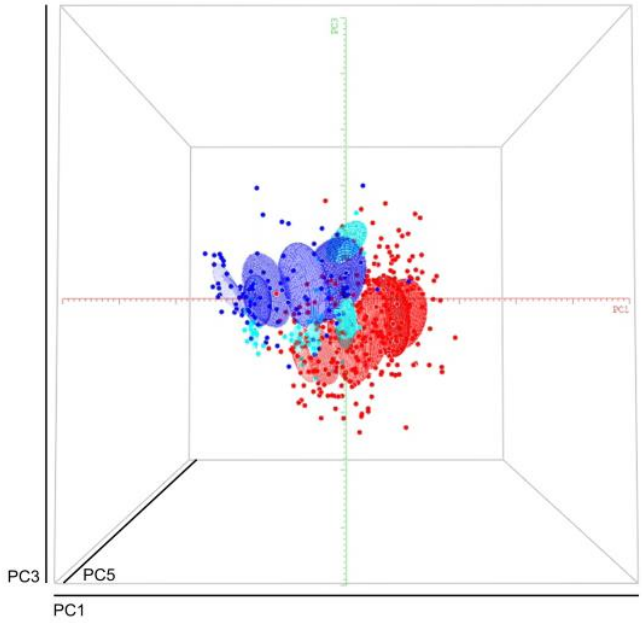

Figure 4.3: Landsberg *erecta* (Ler-0) populations grown at different times of the year (colours are different populations). This figure is for illustration purposes only and was created using an initial test version of the Arabidopsis Leaf Shape Library.

4.2 Exploring natural *Arabidopsis* PC space

The accessions in the Arabidopsis Leaf Shape Library provide an idea of the natural *Arabidopsis* PC space and provides a good overview of the possible variation in leaf shape and size in *Arabidopsis thaliana* (figure 4.4 and 4.5). If damage and malformation have been ruled out outliers show the widest margins of variation present in the *Arabidopsis* accessions. Not all *Arabidopsis* accessions are represented in the library but it nonetheless provides a solid overview. Such an overview is interesting because it allows

us to ask the following questions – what kind of leaf occurs naturally and why do leaves in certain other PC coordinates not exist? As mentioned earlier, LeafPredicter enables us to visualize the leaf shape and size for each point in PC space thereby allowing the creation of hypothetical leaves where no leaf exists in nature or so called null spot (personal communication J. Vaughan and Richard Waites).

The variation in the accessions is very large, along PC1 and PC2 there is a difference of more than three standard deviations. The accession with the largest leaf size is Sf-2 (mean PC1 = 2.14), Ct-1 leaf size (mean PC1 = -0.007) is closest to the mean leaf and Ler-0 has the smallest leaf size (mean PC1 = -1.338) of all the accessions. The Sf-2 accession is extreme in a number of the PCs, it accounts for the lowest PC2 value (mean PC2 = -2.766) and largest mean PC4 value (mean PC4 = 1.409). Along the PC2 axis, which illustrates a difference in leaf shape, No-0 accounts for the most positive PC2 value (mean PC2 = 0.9831) and Kn-0 (mean PC2 = 0.0748) is most similar to the mean leaf. The variation along the PC3 axis (petiole alignment) is markedly lower compared to variation along the other PCs though a few of the pairwise comparisons do show significant differences (data not shown). PC4 variation captures aspect ratio (leaf length: leaf width) and as mentioned Sf-2 shows the upper PC4 value while No-0 (mean PC4 = -1.367) has the largest negative mean PC4 value.

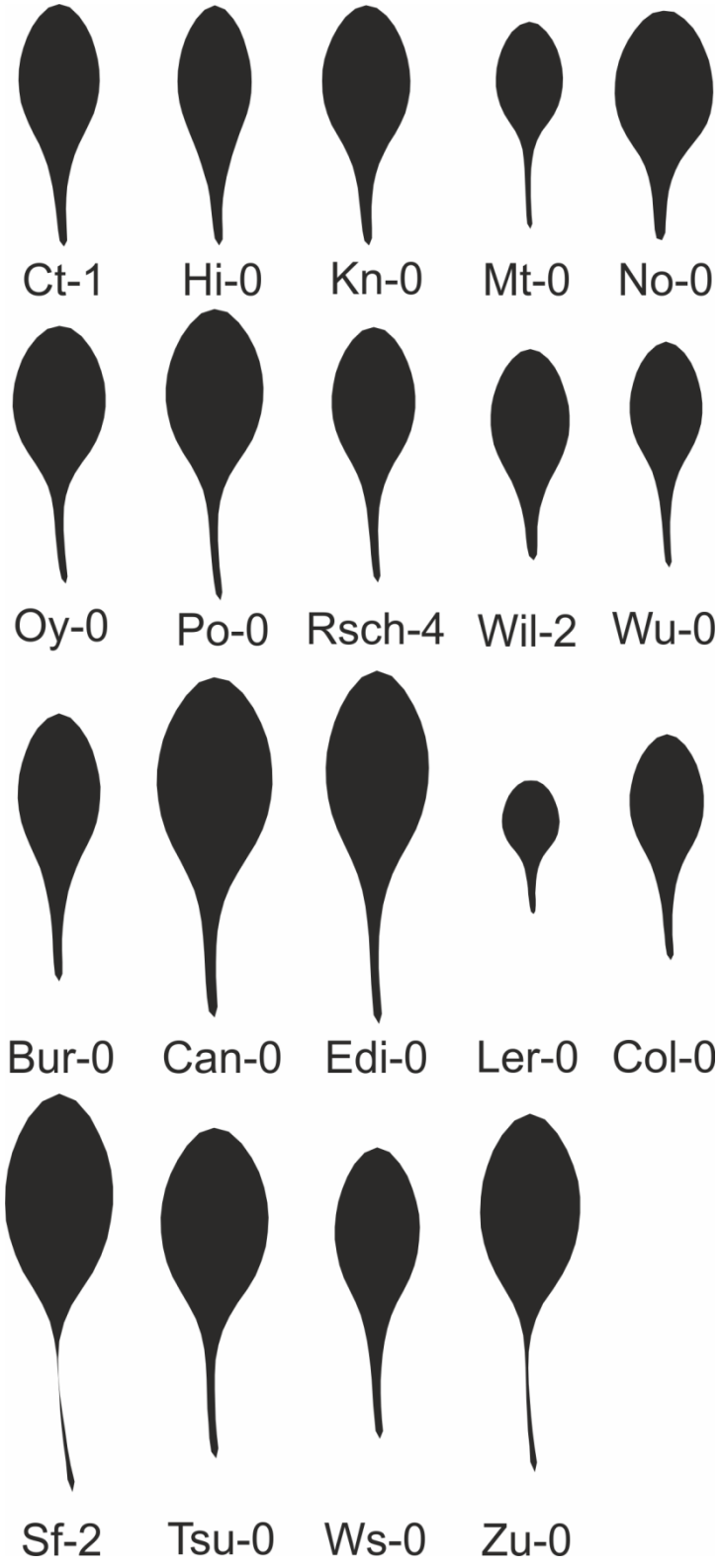

Figure 4.4: Comparison of leaf point models for nodes 5–11 for *Arabidopsis* accession leaves. The mean PC score is calculated from mean PC1, PC2, PC3 and PC4 scores, visualising the mean size and shape of the leaves for each line. These leaves were constructed using LeafPredictor and the eigensystem of the reference set.

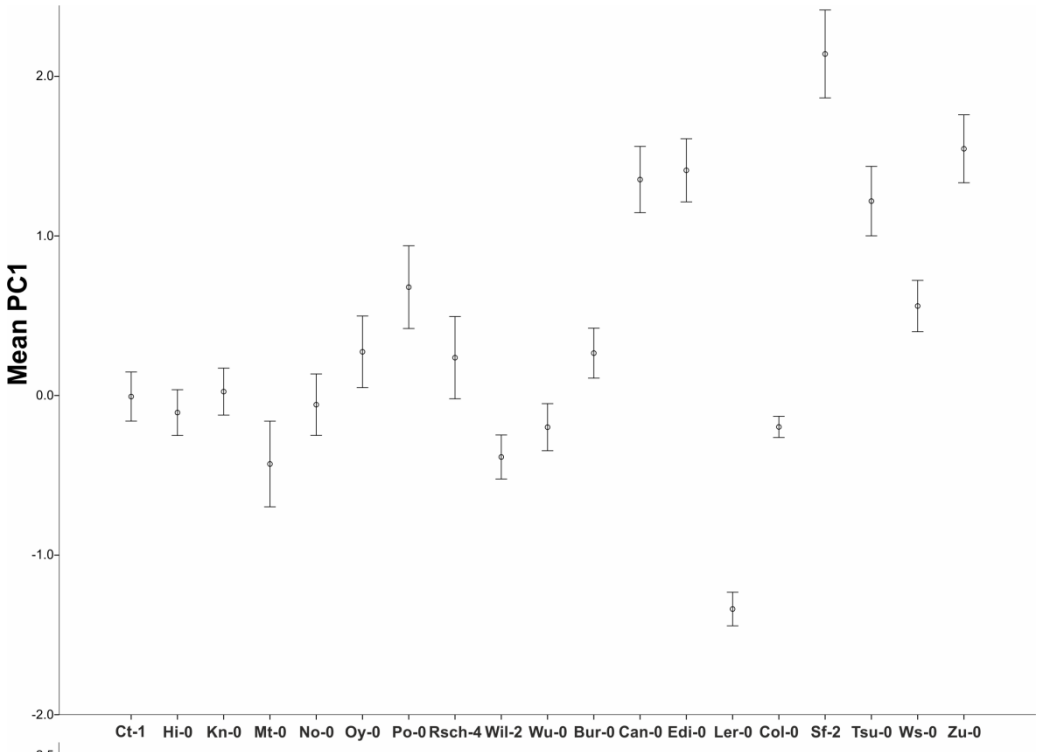
Mean PC1
2.0
1.0
0.0
-1.0
-2.0
Ct-1 Hi-0 Kn-0 Mt-0 No-0 Oy-0 Po-0 Rsch-4 Wil-2 Wu-0 Bur-0 Can-0 Edi-0 Ler-0 Col-0 Sf-2 Tsu-0 Ws-0 Zu-0

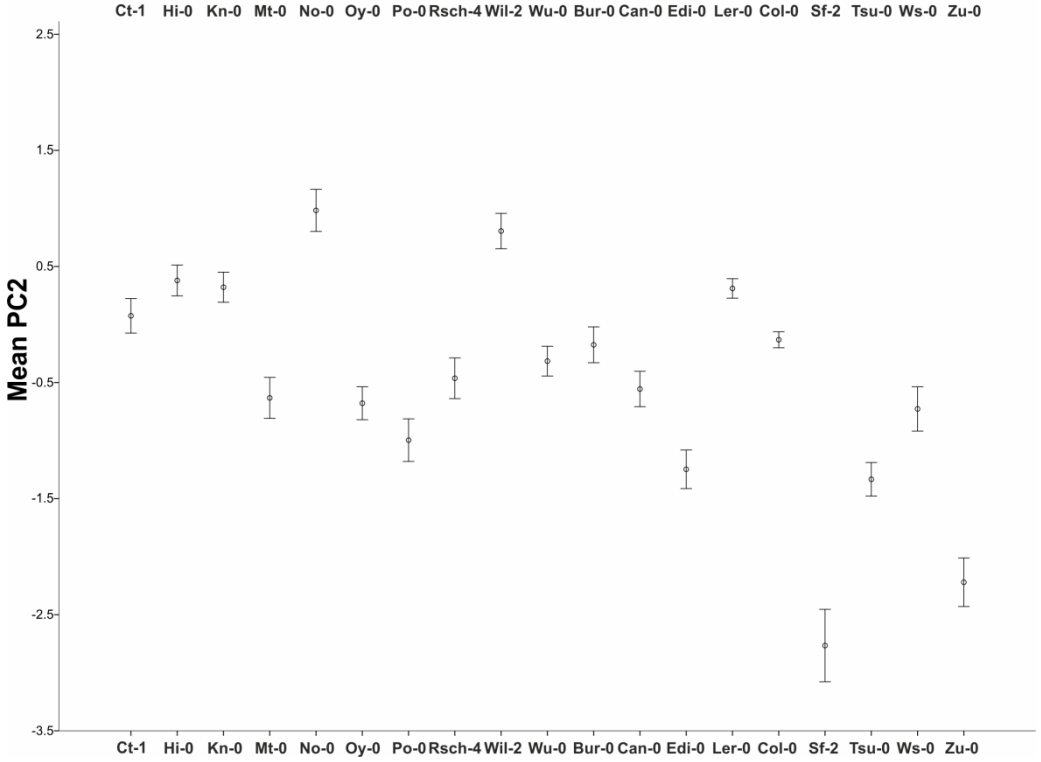
Mean PC2
2.5
1.5
0.5
-0.5
-1.5
-2.5
-3.5
Ct-1 Hi-0 Kn-0 Mt-0 No-0 Oy-0 Po-0 Rsch-4 Wil-2 Wu-0 Bur-0 Can-0 Edi-0 Ler-0 Col-0 Sf-2 Tsu-0 Ws-0 Zu-0

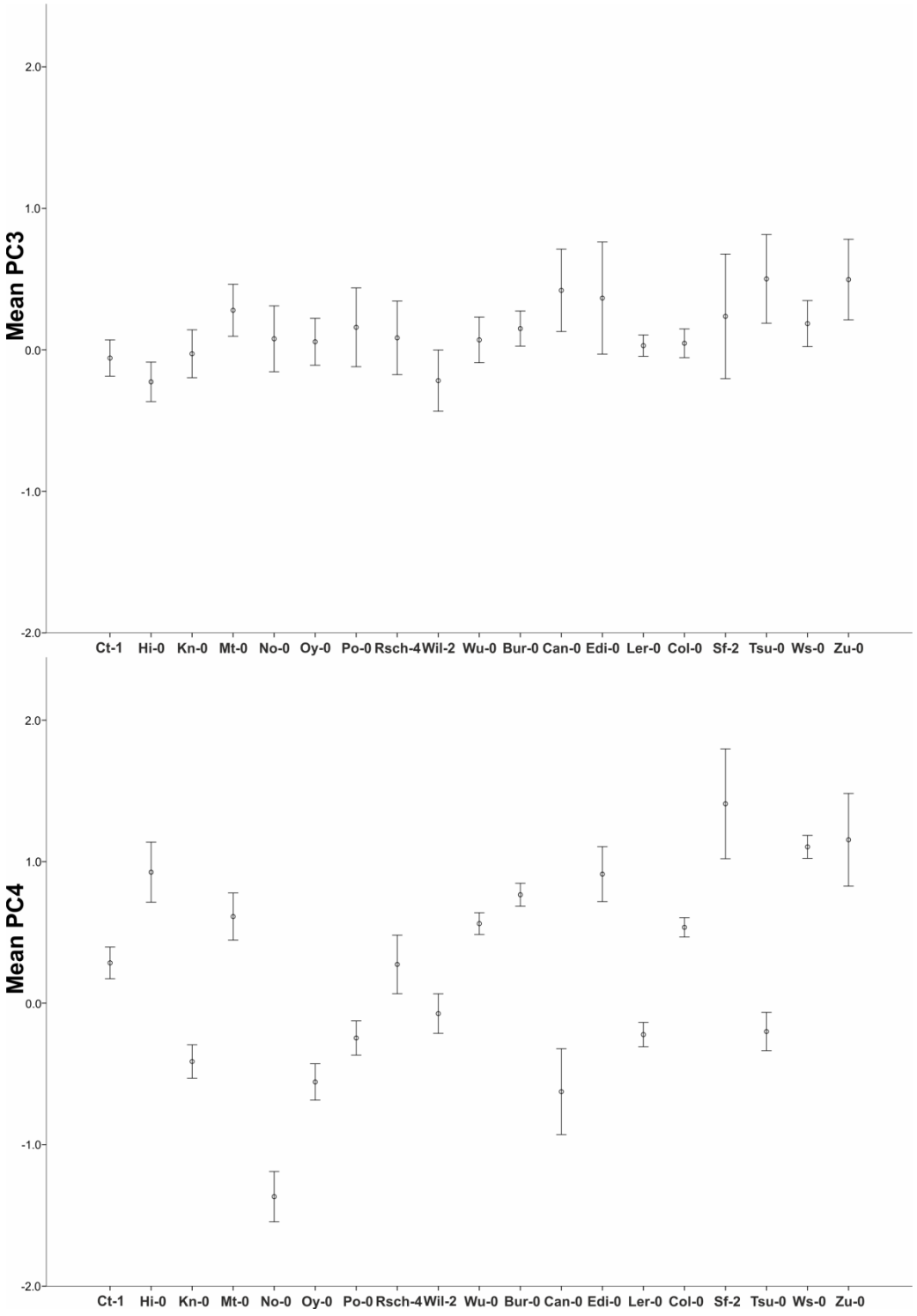

Figure 4.4: Exploring natural Arabidopsis PC space. Leaf shape and size analysis for the *Arabidopsis* accessions. The mean PC scores for PC1, PC2, PC3 and PC4 for the *Arabidopsis* accessions. Error bars represents 95% confidence intervals.

4.3 Case Studies

In this, and the previous chapter, we have examined the features of LeafAnalyser and the *Arabidopsis* reference set as well as explored the natural leaf shape and size variation in *Arabidopsis thaliana*. The next step is to use the *Arabidopsis* leaf shape and size library to analyse a number of well-known leaf development mutants. The aim of the case studies is to provide a quantitative analysis of the leaf shape and size and compare the results to what is currently known about these genes in the literature. The genes or gene families chosen are known to be involved in leaf development and are therefore interesting as candidate genes for a direct involvement in the regulation of leaf shape and size. For each mutant line discussed below the corresponding wild-type background line (same seed stock) was grown in the same environment and they were imaged as one large batch. For the case studies below the data was tested for normality and found to have a non-normal distribution (Shapiro-Wilk Test).

4.3.1 MORE AXILLARY GROWTH (MAX)

The Arabidopsis *MAX* pathway controls shoot branching by regulating auxin transport and strigolactones synthesis (Bennett et al., 2006; Crawford et al., 2010). The *MAX* mutants were characterised as a contribution in kind to the Leyser Laboratory. The *MAX* mutants are an interesting case study because they work in a hormone pathway and so far only two of the four *MAX* genes are known to cause a leaf shape and size phenotype when disrupted. Previous studies have shown that leaf shape and size is affected in *max1.1* and *max2.1* as well as branching, but a clear quantification of the changes in leaf shape and size is missing. Seedling growth is affected in *max2.1* but not *max1.1* (Stirnberg et al. 2002). The branching mutants *max1.1, max2.1, max3.9* and *max4.1* were characterized with regards to their leaf shape and size.

We have determined that there is a significant difference between the wild-type, *max1.1, max2.1, max3.9* and *max4.1* lines by carrying out a Kruskal-Wallis test. There is a significant difference in leaf size, shape and aspect ratio, captured by PC1, PC2 and PC4, between the lines. A pair-wise comparison identifies the differences between the individual lines (figure 4.5 & table 4.1). Along the PC1 axis there is a significant difference between the wild-type line and *max1.1, max2.1* and *max4.1* ($p<0.001$). The wild-type and *max3.9* do not differ, though *max3.9* significantly differs from *max1.1* ($p<0.001$), *max2.1* ($p<0.05$) and *max4.1* ($p<0.001$). Compared to wild-type and *max3.9, max1.1, max2.1*and *max4.1* have a lower mean PC1 value, indicating that they have smaller leaves.

There is a clear separation between the wild-type line and the MAX mutants along the PC2 axis ($p<0.001$). There are significant differences between the *MAX* mutants but these are smaller compared to the difference with the wild-type line (table 4.1). Along the PC4 axis there is a significant difference between the wild-type and the *MAX* mutants, the *MAX* mutants have a shift towards a lower PC4 value ($p<0.001$). Only the difference between *max1.1* and *max3.9* is not significantly, the other pair-wise comparisons are significant either at the $p<0.001$ or $p<0.05$ level.

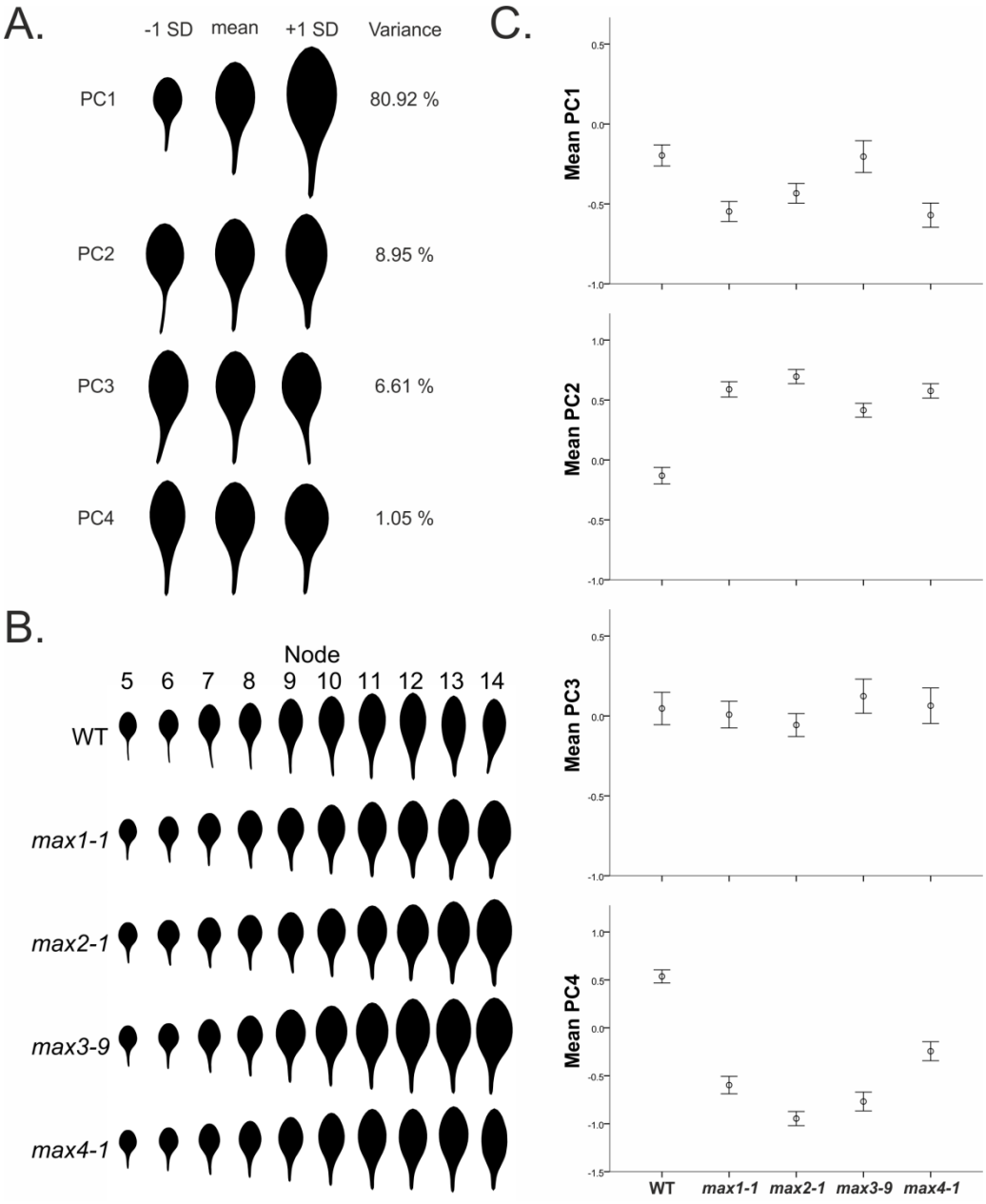

Figure 4.5: Leaf shape and size analysis for wild-type, *max1.1, max2.1, max3.9* and *max4.1* plants.

A. Leaf size and shape according to variation along the first four PCs for the *Arabidopsis* stable reference set of 1050 leaves.

B. Comparison of leaf point models for nodes 5–11 for WT, *max1.1, max2.1, max3.9* and *max4.1* plants. The mean node PC score is calculated from mean PC1, PC2, PC3 and PC4 node scores, visualising the mean size and shape of the leaves for each line. These leaves were constructed using LeafPredictor and the eigensystem of the reference set.

C. Mean PC scores for all leaves for wild-type, *max1.1, max2.1, max3.9* and *max4.1*. Error bars represents 95% confidence intervals. Wilcoxon Rank Sum test was used to determine the differences between the lines (table 4.1).

PC1	WT	*max1.1*	*max2.1*	*max3.9*
max1.1	7.8e-11	-	-	-
max2.1	6.9e-06	0.0919	-	-
max3.9	1.0000	3.4e-06	0.0028	-
max4.1	1.8e-10	1.0000	0.0405	3.4e-06

PC2	WT	*max1.1*	*max2.1*	*max3.9*
max1.1	< 2e-16	-	-	-
max2.1	< 2e-16	0.0575	-	-
max3.9	< 2e-16	0.0022	1.2e-08	-
max4.1	< 2e-16	0.9828	0.0575	0.0019

PC4	WT	*max1.1*	*max2.1*	*max3.9*
max1.1	< 2e-16	-	-	-
max2.1	< 2e-16	9.8e-10	-	-
max3.9	< 2e-16	0.0531	0.0027	-
max4.1	< 2e-16	9.8e-10	< 2e-16	7.8e-12

	p<0.05
	p<0.001

Table 4.1: Leaf shape and size analysis for wild-type, *max1.1*, *max2.1*, *max 3.9* and *max4.1* plants. Pair-wise comparison (Wilcoxon Rank Sum test) of leaf size and shape analysis for wild-type, *max1.1*, *max2.1*, *max 3.9* and *max4.1*.

4.3.2 CUP-SHAPED COTYLEDON (CUC)

CUP-SHAPED COTYLEDON (CUC) genes, *CUC1*, *CUC2*, and *CUC3* are members of the NAC transcription factor family and are expressed in the organ boundary. The partially redundant *CUC* genes are essential in the formation and maintenance of the shoot meristem and the specification of the organ boundary domain (Aida et al., 1999; Aida et al., 2006; Vroemen et al., 2003). Most single *cuc1* and *cuc2* mutant seedlings look phenotypically normal, but occasionally some seedlings have fused cotyledons on one side, called heart-shaped seedlings. The double mutant *cuc1cuc2* has fused cotyledons shaped like a cup, sepals and stamens and show severe defects in the embryonic and adventitious shoot apical meristems (SAM) (Aida et al., 1997; Aida et al., 1999).

As previously discussed, LeafAnalyser is not the right tool to analyse mutant lines with a severe leaf phenotype. As such, it is not necessary to analyse the leaf shape of these mutants because in the severe phenotypes there is no "real" leaf shape to analyse. From the point of view of this study we are more interested in the single *cuc1* and *cuc2* mutants reported to be phenotypically normal. With the aid of LeafAnalyser and the reference set we want to analyse the single *cuc1* and *cuc2* mutants to investigate whether the single mutant are indeed phenotypically normal or whether a leaf shape phenotype is visible in these mutant lines but has not previously been reported. Analysing the single mutant can tell us if the *CUC* genes are potential candidate genes to control leaf shape and size; their expression domain would support such an involvement (Aida et al., 1997; Aida et al., 1999; Hibara et al., 2006; Takada et al., 2001).

We use a Kruskal-Wallis test to determine whether there are any significant differences between the lines. The analysis reveals that there are significant difference between wild-type, *cuc1* and *cuc2*, the differences are captured by PC1 ($p<0.05$), PC2 ($p<0.001$), PC3 and PC4 ($p <0.05$) (figure 4.6). A pair-wise comparison is needed to establish the differences between the individual lines. The Wilcoxon test reveals that there is a significant difference between the wild-type line and *cuc1* and *cuc2* ($p<0.05$) along the PC1 axis. The mutant *cuc1* and *cuc2* lines have larger leaf sizes (higher PC1 score) than the wild-type line but there is no difference in leaf size between the two mutants. The situation is similar along the PC2 axis, there is a significant difference in leaf shape between the wild-type and *cuc1* and *cuc2* ($p< 0.001$), but no difference between the mutant lines. Along PC2 there is a shift to a higher PC2 value for *cuc1* and *cuc2*. The petiole of *cuc2* has a slightly more pronounced curvature to the left ($p<0.05$) compared to the wild-type. Along the PC4 axis there is a significant difference between wild-type and *cuc2* ($p<0.05$), as well as between *cuc1* and *cuc2* ($p<0.05$) but not between wild-type and *cuc1*.

Taken together our analysis reveals that *cuc1* and *cuc2* are not phenotypically normal as previously reported but show a subtle but distinct leaf shape and size phenotype. The *cuc1* and *cuc2* mutants have slightly larger leaves, with a more elongated leaf blade and a shorter, broader petiole. In the case of *cuc2* the petiole aligns slightly further to the left and the leaf is slightly narrower (figure 4.6). The observed phenotypes are consistent with the *CUC* genes not working in a fully redundant fashion, but sharing overlapping functions.

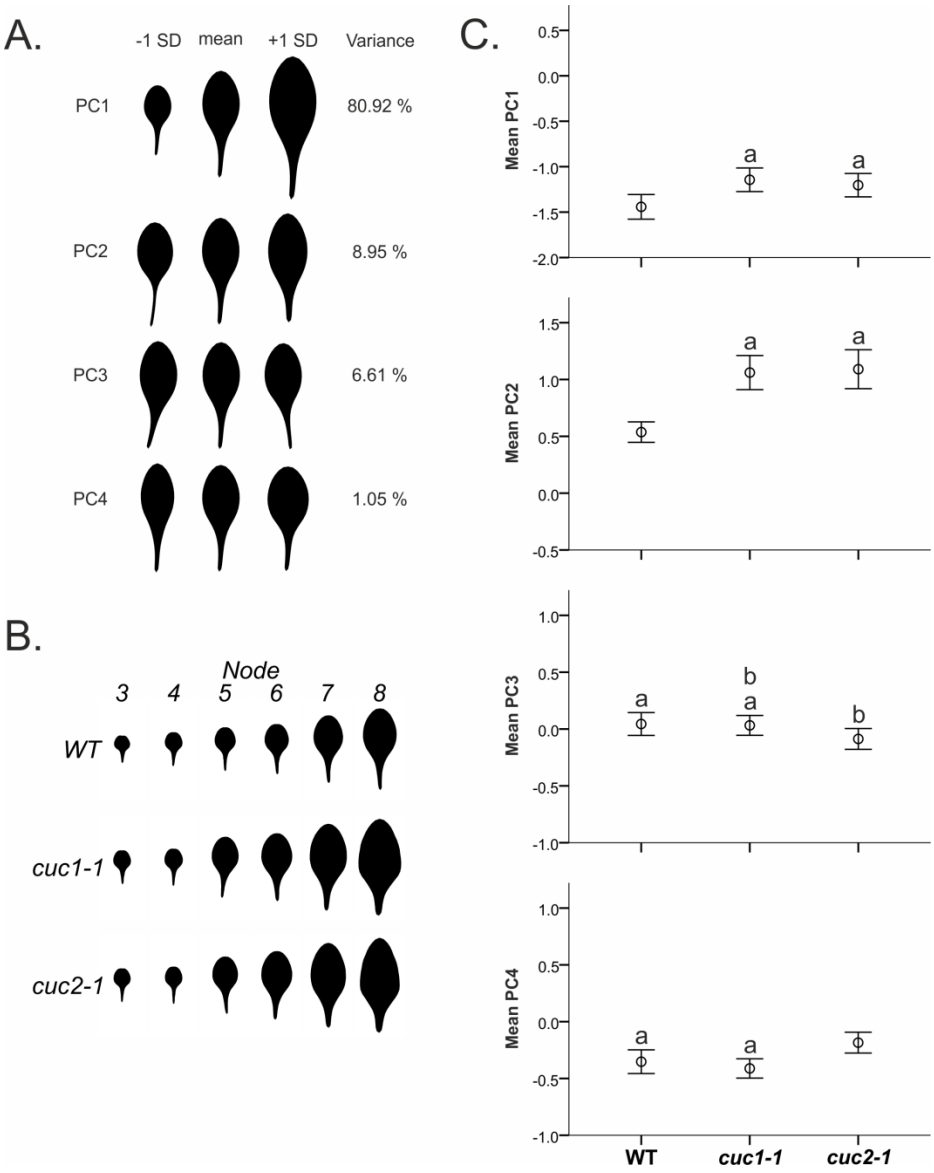

Figure 4.6: Leaf shape and size analysis for wild-type, *cuc1* and *cuc2* plants.

A. Leaf size and shape according to variation along the first four PCs for the *Arabidopsis* stable reference set of 1050 leaves.

B. Comparison of leaf point models for nodes 5–11 for WT, *cuc1* and *cuc2* plants. The mean node PC score is calculated from mean PC1, PC2, PC3 and PC4 node scores, visualising the mean size and shape of the leaves for each line. These leaves were constructed using LeafPredictor and the eigensystem of the reference set.

C. Mean PC scores for all leaves for wild-type, *cuc1* and *cuc2*. Error bars represents 95% confidence intervals. Wilcoxon Rank Sum test was used to determine the differences between the lines. The letters 'a' and 'b' indicate that there is no significant difference between genotypes.

4.3.3 YABBY Gene family

Four members of the *YABBY* family *FILAMENTOUS FLOWER (FIL), YAB2, YAB3* and *YAB5* are expressed in the abaxial domain of leaf primordia. Polar expression of *YABBY* genes is required for the maintenance of leaf polarity and abaxial/adaxial juxtaposition-mediated lamina expansion (Eshed et al., 2004; Yamaguchi et al., 2012). The expression domain of the *YABBY* family and their known involvement in leaf polarity make this an interesting family to study. For some of the family members limited leaf phenotype information is available but to date no quantitative analysis has been conducted. We are using LeafAnalyser to establish which of the family members exhibit a leaf phenotype and have the potential to be directly involved in establishing the final leaf shape..

4.3.3.1 CRABS CLAW (CRC)

For *CRABS CLAW (CRC),* a member of the YABBY gene family required for nectary and carpel development we have analysed the strong allele *crc-1* and the weak *crc-2* allele (Bowman and Smyth 1999; Eshed et al. 2001).

Kruskal-Wallis test was used to determine whether any of the PCs are significantly different between the lines. The analysis reveals that there is a significant difference in leaf size and leaf shape between wild-type, *crc-1* and *crc-2*, captured by PC1 and PC2 ($p<0.001$). There is no difference in PC3 and PC4, meaning that there is no difference in leaf curvature of leaf aspect ratio between the lines. Pair-wise comparison for PC1 shows that there is a significant difference in leaf size. A positive shift along the PC1 axis indicates that *crc-1* and *crc-2* leaves are larger in size than the wild-type ($p<0.001$). This positive shift is more pronounced in *crc-1* which is significantly different from *crc-2* ($p<0.05$) (figure 4.7). There is no difference in leaf shape between *crc-1* and *crc-2*, but both mutant lines show a significant difference in leaf shape compared to the wild-type line ($p<0.001$).

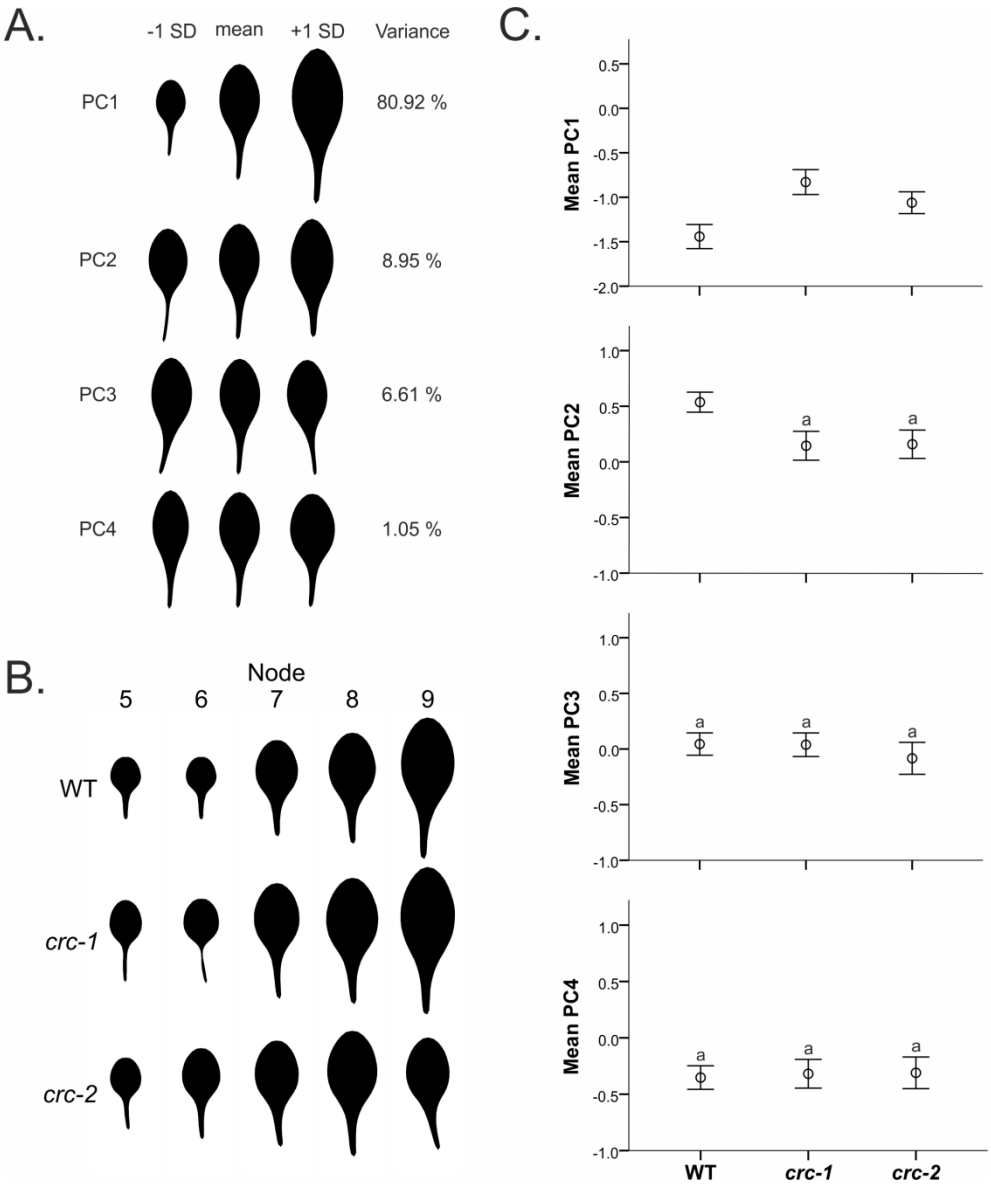

Figure 4.7: Leaf shape and size analysis for wild-type, *crc-1* and *crc-2* plants.

A. Leaf size and shape according to variation along the first four PCs for the Arabidopsis stable reference set of 1050 leaves.

B. Comparison of leaf point models for nodes 5–11 calculated for WT, crc-1 and crc-2 plants. The mean node PC score is calculated from mean PC1, PC2, PC3 and PC4 node scores, visualising the mean size and shape of the leaves for each line. Note that crc-2 node 9 only has 2 leaves in the dataset. These leaves were constructed using LeafPredictor and the eigensystem of the reference set.

C. Mean PC scores for all leaves for wild-type, crc-1 and crc-2. Error bars represents 95% confidence intervals. Wilcoxon Rank Sum test was used to determine the differences between the lines. The letter 'a' indicates that there is no significant difference between genotypes.

4.3.3.2 YABBY 3 (YAB3)

The second member of the *YABBY* gene family that we have investigated is *YAB3*. The *YAB3* null allele *yab3-2* is reported to be indistinguishable from wild-type plants under normal growth conditions (Golz et al. 1999).

To determine whether there is a difference between *yab3-2* and the wild-type line we have carried out a Kruskal-Wallis test. Since there are only two lines in this analysis a further pair-wise comparison is not necessary. There is a significant difference between the wild-type line and *yab3-2,* the differences are captured by PC1, PC2 ($p<0.001$), PC3 and PC4 ($p<0.05$). Compared to the wild-type line *yab3-2* has a higher mean PC1 and PC4 value but lower mean PC2 and PC3 values.

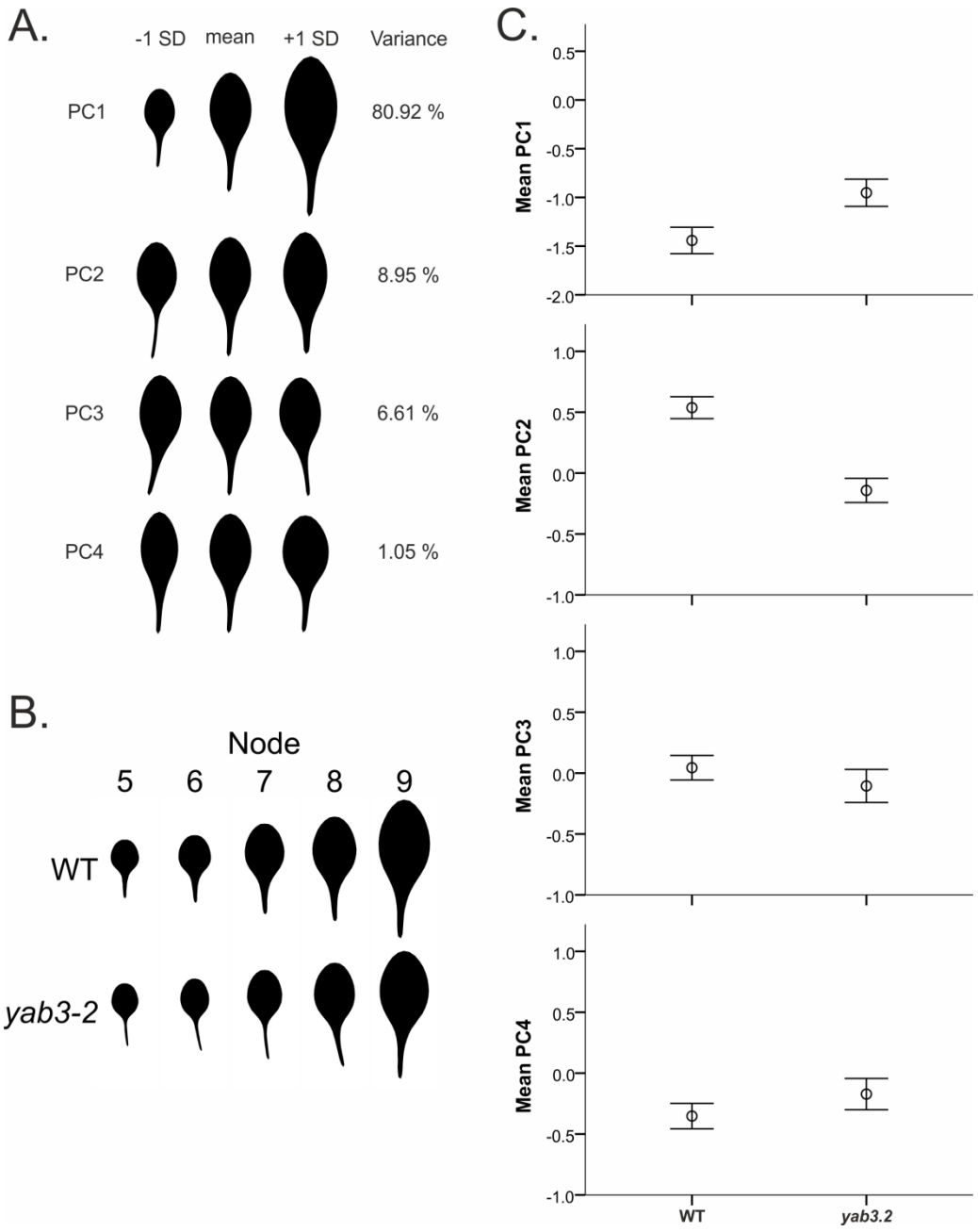

Figure 4.8: Leaf shape and size analysis for wild-type, and *yab3-2* plants.

A. Leaf size and shape according to variation along the first four PCs for the Arabidopsis stable reference set of 1050 leaves.

B. Comparison of leaf point models for nodes 5–11 for WT and *yab3-2* plants. The mean node PC score is calculated from mean PC1, PC2, PC3 and PC4 node scores, visualising the mean size and shape of the leaves for each line. These leaves were constructed using LeafPredictor and the eigensystem of the reference set.

C. Mean PC scores for all leaves for wild-type, and yab3-2. Error bars represents 95% confidence intervals. Kruskal-Wallis test was used to determine the differences between the lines.

4.3.4 KANADI (KAN) & ERECTA (ER)

KANADI regulates organ polarity in Arabidopsis, and is required for abaxial identity in both leaves and carpels. The first two leaves of *kan12* are curled upwards and stay curled throughout their development. In contrast to Col-0 wild-type leaves (curl downwards) higher node *kan12* leaves are reported to emerge in-rolled but flatten out almost completely during maturation (Kerstetter et al. 2001). Kerstetter et al. 2001 report that the difference in leaf expansion is not associated with a change in leaf size. LeafAnalyser should be able to confirm whether leaf size (and shape) is indeed not affected. The original *kan12* was isolated in Landsberg erecta (Ler) and crossed into Colombia (Col). We report here the leaf shape and size analyses for *kan12* in a Ler background as well as in a Col background. Due to the availability of the *kan12* mutant in two separate backgrounds it allows us the opportunity to investigate if the presentation of a leaf phenotype is consistent across genetic backgrounds or not.

There are significant differences between the lines based on the Kruskal-Wallis test. The differences are described by PC1, PC2 and PC4 indicating a difference in leaf size, shape and aspect ratio (leaf length: leaf width) ($p<0.001$) between wild-type Col-0, wild-type Ler-0, *kan12* (Col-0) and *kan12* (Ler-0). No difference was observed in leaf curvature (PC3).

To determine the differences between the lines a pair-wise comparison was carried out for PC1, PC2 and PC3 (figure 4.9). Along the PC1 axis all four lines are significantly different from each other ($p<0.001$). The Col-0 wild-type line has the highest mean PC1 score, *kan12* (Col-0) has a negative shift along the PC1 axis indicating smaller leaf size compared to the wild-type line. Ler-0 leaves have the smallest leaf size (lowest mean PC1 score), in the Ler background *kan12* has a positive shift along the PC1 axis indicating that the *kan12* (Ler-0) leaves are larger than the Ler wild-type leaves, though still significantly smaller than Col-0 and *kan12* (Col-0) leaves.

There is no significant difference in leaf shape between the wild-type Col-0 line and *kan12* (Col-0) line, though both are significantly different (lower PC2 value) from Ler-0 and *kan12* (Ler-0) ($p<0.001$). Ler-0 has a significantly higher PC2 value than the *kan12* (Ler-0) ($p<0.05$), indicating that Ler-0 has rounder, more compact leaves. Both the Col-0 / *kan12* ($p<0.001$), as well as the Ler-0 / *kan12* ($p<0.05$) wild-type versus mutant combination show a shift toward a lower PC4 value, though this shift is much more pronounced in the Col-0 background. There is no significant difference between the *kan12* (Col-0) and the *kan12* (Ler-0).

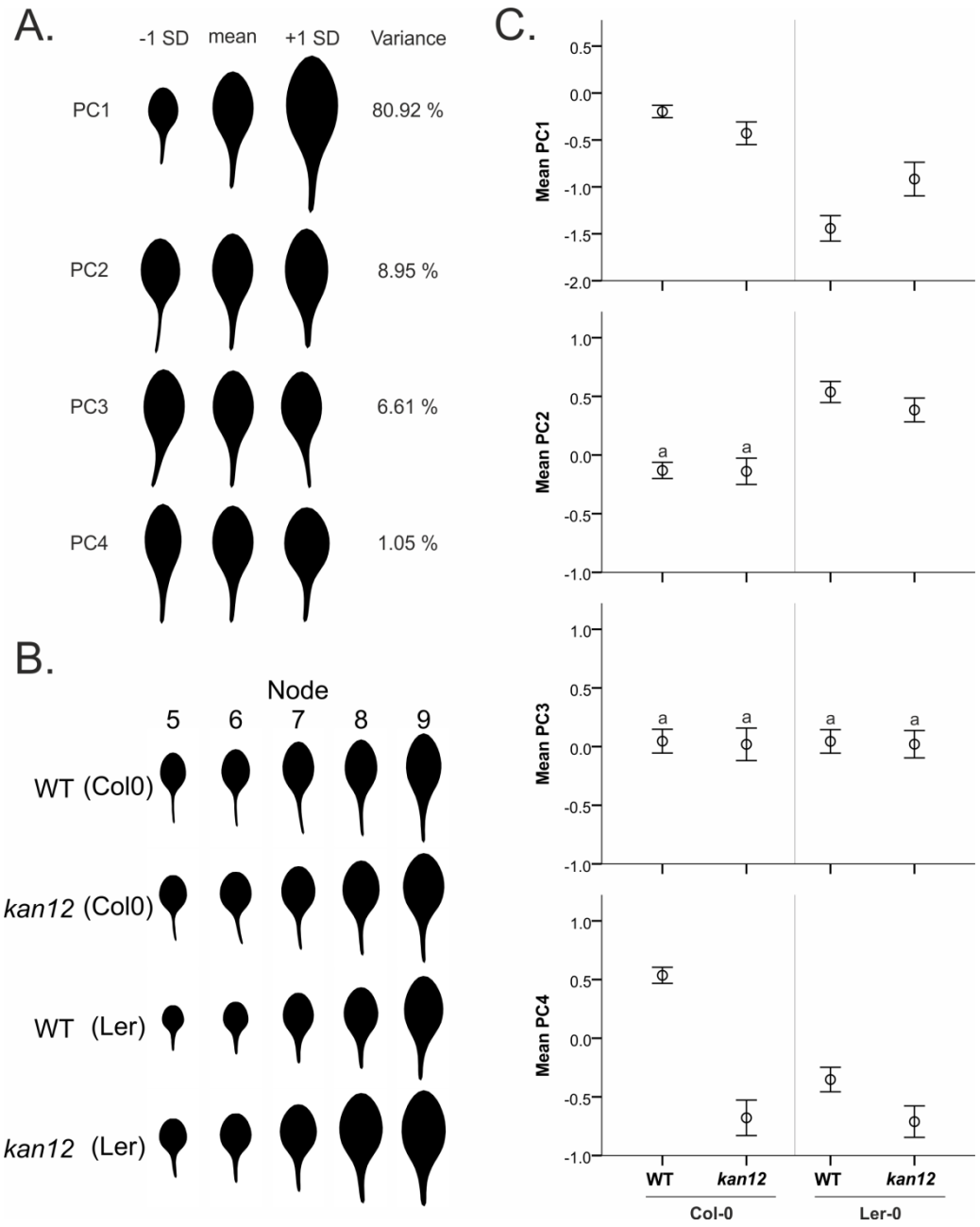

Figure 4.9: Leaf shape and size analysis for wild-type (Col-0), *kan12* (Col-0), wild-type (Ler-0) and *kan12* (Ler-0).
A. Leaf size and shape according to variation along the first four PCs for the *Arabidopsis* stable reference set of 1050 leaves.
B. Comparison of leaf point models for nodes 5–11 for WT (Col-0), *kan12* (Col-0), WT (Ler-0) and *kan12* (Ler-0) plants. The mean node PC score is calculated from mean PC1, PC2, PC3 and PC4 node scores, visualising the mean size and shape of the leaves for each line. These leaves were constructed using LeafPredictor and the eigensystem of the reference set.
C. Mean PC scores for all leaves for WT (Col-0), *kan12* (Col-0), WT (Ler-0) and *kan12* (Ler-0) plants. Error bars represents 95% confidence intervals. Wilcoxon Rank Sum test was used to determine the differences between the lines. The letter 'a' indicates that there is no significant difference between genotypes.

4.4 Discussion

4.4.1 Limitations of the LeafAnalyser tool and experimental method

Previously in this chapter and throughout this thesis the effectiveness of LeafAnalyser in determining leaf shape and size variation has been illustrated. It should however be acknowledged that LeafAnalyser as a landmark-based geometric morphometrics tool has a number of downsides and limitations; most of which are shared by the alternative tools developed by other research groups.

The main downside to the LeafAnalyser technique is that it is destructive to the plants that are being analysed. Though it might be possible to scan the leaves and subsequently isolate the DNA from the leaves it would not be advisable, certainly RNA extraction under these circumstances would not be feasible due to the stress responses in the leaves alone. The plant is processed at or shortly before terminal flowering, it thus follows that seed cannot be taken from plants that have been analysed by LeafAnalyser. While building up the leaf shape library or analyzing the leaf shape and size

of homozygous mutant lines not being able to isolate seed is of lesser concern. However, there are situations where the usefulness of LeafAnalyser is reduced due to the destructive processing workflow. From our experience is seems feasible to use LeafAnalyser as a method to distinguish wild-type, heterozygous and homozygous mutants in a segregating population. The inability to identify the homozygous plants and isolate seeds from that same plant is a decided handicap. For the same reason it is not really possible to analyse leaf shape as well as epidermal cells on the same leaf.

During the LeafAnalyser workflow leaves are flattened or allowed to flatten over time and subsequently scanned. Leaves with a slight convex or concave leaves will flatten out naturally when the leaves lose their firmness after having been detached from the main plant. Plants that have more extensively curled leaves like the Arabidopsis mutant curly leaf are almost impossible to analyse with LeafAnalyser as are the more extreme leaf shape mutants such as pin-formed mutant (Kim et al., 1998; Okada et al., 2001). LeafAnalyser is a 2D landmark-based method and is therefore restricted to leaves that are more or less flat. A number of research groups are researching the possibilities of three-dimensional (3D) imaging and the analysis of (living) plant leaves. Positron Emission Tomography (PET), Magnetic resonance imaging (MRI), optical coherence microscopy (OCM), high-resolution X-ray computed tomography (HRCT) and optical projection tomography (OPT) have all been used to accomplish 3-D imaging of leaves and make it possible to take into account the internal structure of the leaf (Wuyts et al., 2010; Pajor et al., 2013). While 3D imaging can still be considered in its infancy in the field of experimental biology, four-dimensional imaging (4-DI) is being proposed and includes visualising dynamic processes throughout an organism's developmental cycle or in response to external pressures (e.g. environmental and/or experimental) (Domozychi, 2012).

LeafAnalyser is unable to detect serrations or lobes, increasing the number of landmarks that are placed around the perimeter of the leaf does not negate

this technical limitation. Exactly why the software does not pick the serrations is unclear. The lack of ability to detect serrations is a real shortcoming because serration has proven to be an indication for underlying biological processes (Bilsborough et al., 2011). If serrations are of specific interest it would be advisable to choose a different system to analyse the leaf shape. In contrast to a number of other morphometric tools LeafAnalyser distributes the landmarks equidistant across the leaf outline rather than fixing landmarks to discrete anatomical loci. Langlade et al. 2005 describe in their experimental method the placement of 19 points along the leaf margin and mid-vein, including six primary points placed at recognizable (anatomically recognisable) landmarks. An example of landmarks fixed to anatomical loci is the work of Klingenberg and Zaklan (2000), where landmarks are placed on the intersections of major veins on the *Drosophila* wing. The remaining points are secondary and distributed at equidistance intervals. It is possible that complex leaves or serrated leaves may be analysed by fixing landmarks to recognisable positions but adding these anatomically recognisable landmarks places a different set of constraints on the system and is therefore not as such a more sophisticated system than LeafAnalyser, merely limited by different factors. Even though the primary landmarks are placed on anatomically recognizable loci, in practice there is a considerable variation in leaf shape which does not always make it easy to determine these loci. In the authors opinion this type of method increases the subjective sampling. It does not take a great deal of imagination to envisage leaf shapes where placing these primary points is not as self-evident as suggested. From experience we can state that it is sometimes difficult to keep the base of the petiole perfectly intact, the base of the lamina is not always an easily identifiable point, and the maximum leaf width could be at more than one point or marred by leaf imperfections.

During the LeafAnalyser workflow the leaves of the plant are severed and arranged on an ohp slide with the phyllotaxis of the plant as a guide. Consistency in the placement of the leaves is important especially if differences across the nodes are going to be compared. A mutant with an alteration in the phyllotaxis would need to be detected prior to dissection,

and as such the method requires a certain level of experience with plant development.

During the exploration of the capability of LeafAnalyser and the reference library we highlight that the quantitative imaging method can pick up differences between wild-types from different labs (section 4.1.2), track a line across different seasons (section 4.1.4) and distinguish growth conditions/ healthy versus diseased populations (section 4.1.3). On the one hand this illustrates how powerful the technique is and the case studies described above show how we have been able to report leaf size and shape phenotypes for mutants previously reported as phenotypically normal. On the other hand it also shows that the critical interpretation of the data is vital. If we were to analyse the three wild-type Colombia lines sourced from different research groups, the Landsberg *erecta* populations tracked across seasons, or the diseased versus healthy Colombia populations it is possible, probably even likely, that we would find statistically significant differences. The question is whether the fact that we could find statistically significant differences would invalidate any of the results we find in for instance the case studies or analyses later in this study.

The question whether any differences described in section 4.1 are biologically significant is a related but distinct and no less important question. As such it is the belief of this author that these differences are significant; it is a well-known fact that stress biotic or abiotic, and environmental conditions can have an impact on leaf size, shape and number. Therefore we would expect to find differences in the leaf shape of healthy and diseased (or growth retarded) population; it is the interpretation of the results that is essential.

Our *Arabidopsis* reference set is a control on which to base our analysis, the established experimental method for the LeafAnalyser leaf size and shape analysis is to grow a number of wild-type plants simultaneously with the lines of interest. As such this is the reason why we have wild-type Colombia plants from three different research groups. Growing wild-type plants in the

same condition will eliminate any changes due to growing conditions, seasons and as far as we can control biotic or abiotic stress.

The *Arabidopsis* accessions show just how extensive the natural variation in leaf size and shape is. An interesting line of investigation would be to display all *Arabidopsis* accessions in the library and colour code them based on factors like climate, geographic location etc. and see what kind of pattern emerges if there is one. This may provide a starting point for an analysis on what drives changes in leaf size and shape.

4.4.2 Case studies

The case studies we have chosen highlight how valuable the combination of LeafAnalyser and the *Arabidopsis* reference set is. With the aid of the reference set we have analysed the leaf size and shape in mutant lines of *MORE AXILLARY GROWTH (MAX 1-4), CUP-SHAPED COTYLEDON (CUC),* two members of the YABBY Gene family, *CRABS CLAW (CRC)* and YABBY3 (YAB3) and have conducted an analysis of a KANADI mutant in a Col-0 and Ler-0 background. The ultimate aim of a phenotypical analysis is to tie the changes we see in shape to gene function. However, as discussed in chapter 1 of this thesis (section 1.3.2) this is the real bottle-neck of the field in general. The second half of this thesis tries to investigate the relationship between shape and gene function for a subgroup of TCP genes, it is regrettably not within the premise of these case studies to attempt the same level of interpretation. In the case of transcription factors the added difficulty with the interpretation is that often the direct (or indirect) transcriptional targets are not known, are tissue-dependent or the transcription factor is known to be part of a multicomponent regulatory complex or regulatory network, thereby making it harder to tie the phenotypic effect to the gene function. Where possible we have tried to highlight what line of investigation could be a starting point for further exploration of this fundamental question.

A previous publication by Stirnberg et al. 2001 outlined that a mutation in *MAX1* and *MAX2* also had an impact on leaf shape as well as shoot branching. In this manuscript we can report a full analysis of the leaf size and shape of the MAX mutants (*max1.1, max2.1, max3.9* and *max4.1*) not just compared to wild-type but also to each other.

Our analysis shows that *cuc1* and *cuc2* are not phenotypically normal as previously reported but have a subtle but distinct leaf shape and size phenotype. *CUC1* and *CUC2* are NAC transcription factors and are presumed to be transcriptional activators, but exactly what their function is in the formation and maintenance of the SAM and establishment of the organ boundary domain is unclear (Aida et al., 1999; Aida et al., 2006; Vroemen et al., 2003; Takeda et al., 2011). The double *cuc1cuc2* mutant line has fused cotyledons shaped like a cup, and the more severe *cuc1* and *cuc2* phenotype displays heart-shaped seedlings. We can now reveal that the weaker *cuc1* and *cuc2* mutants display a subtle but distinct leaf shape and size phenotype resulting in slightly larger leaves, with a more elongated leaf blade and a shorter, broader petiole. In the case of *cuc2* the petiole aligns a little further to the left and the leaf is slightly narrower. More information is needed about the direct transcriptional targets of *CUC1* and *CUC2* to formulate a hypothesis as to how they perform their function and thereby influence leaf shape and size.

To the authors knowledge a leaf size and shape phenotype has not previously been attributed to *CRC* mutants. *CRC* expression is largely limited to carpels and nectaries (Bowman and Smyth 1999) and is involved in establishing abaxial cell fate in the carpel (Eshed et al. 2001). In line with the observed nectary and carpel development phenotype, *crc-1* exhibits a leaf phenotype that is stronger that *crc-2*. Without further investigation it is unclear how *CRC* specifies leaf size and shape.

Similar to *cuc1* and *cuc2* we can report that *yab3-2* exhibits a leaf size and shape phenotype rather than as previously reported indistinguishable from wild-type. Compared to the wild-type plants *yab3-2* leaves are larger, and

the centre of the leaf is shifted upwards producing a rounder more compact leaf blade. The *yab3-2* petiole is longer and narrower and curves slightly more to the left.

Arabidopsis Landsberg *erecta* is one of the most commonly used ecotypes for both molecular and genetic studies. Ler is the background line for all the mutants produced by Feenstra, Van der Veen and Koornneef at Wageningen University (http://arabidopsis.info/CollectionInfo?id=94). Landsberg *erecta* harbors the *erecta* mutation in a Landsberg background (La-0), and displays a compact inflorescence, blunt fruits, and short petiole (Torii et al. 1996). It can be questioned whether producing and analysing mutant lines in a background that harboured an uncharacterised mutation is a sensible idea. Ler was previously described as having round leaves with a short petiole (Rédei, 1992; Bowman, 1993).

In a Columbia background *kan12* leaves show a significant difference in leaf aspect ratio producing a smaller much narrower leaf. In the Landsberg *erecta* background *kan12* leaves are larger, less round and only slightly narrower than the wild-type leaf. It is interesting that in the Ler-0 background there is a significant difference in the PC2 value while there is not in the Col-0 background. This result indicates that rather than being absolute, the effect of the *kan12* mutation is dependent on the background in which the mutation has been produced. This phenomenon has been observed in other species and is presumed to be the effect of modifier genes acting in combination with the causative gene (Montagutelli, 2000).

Chapter 5

Phenotypic analysis of class I TCP genes

5.1 Investigating the role of *TCP14* and *TCP15*

The previous chapters of this thesis have outlined how LeafAnalyser provides a sophisticated computer-aided morphological analysis tool which can be used to visualization of phenotypes. In this chapter we apply the quantitative imaging approach to the difficulty of obtaining mutant phenotypes in a gene family that exhibits extreme genetic redundancy (Koyama et al. 2010b).

The *Arabidopsis* TCP genes belonging to the class I sub-family are less well characterized than the class II genes. Class I TCP genes were thought to promote cell proliferation, while class II have a negative effect on cell proliferation. For a detailed description of *Arabidopsis TCP* genes the author refers to the introduction of this thesis. Genetic redundancy has significantly hampered mutant phenotyping of this class of genes. Out of the 13 *Arabidopsis* class I genes only two have characterized mutant phenotypes. *TCP14* shows delayed germination (Tatematsu et al. 2008) and *TCP15* protein-protein interactions with various components of the circadian clock (Giraud et al. 2010). *TCP14* and *TCP15* are expressed in leaf primordia. *TCP14* is expressed throughout the leaf blade, including young trichomes and developing leaf vascular bundles. *TCP15* expression is primarily restricted to the primordial leaf margin. The expression of both genes is repressed in a basiplastic or apical to basal manner during leaf maturation (Kieffer et al. 2011).

TCP14 and *TCP15* are the closest relatives of the Antirrhinum TCP factor *TIC*, which interacts with the organ boundary NAC-domain transcription factor *CUPULIFORMIS* (*CUP*) to establish lateral organ boundaries (Weir et al., 2004). For this reason, and due to the known role of *TCP* genes in the control of cell proliferation and the complex and dynamic expression patterns of *TCP14* and *TCP15* during leaf development (kieffer et al., 2011) we have chosen to investigate the role of *TCP14* and *TCP15* in leaf development. A detailed quantitative imaging analysis will be conducted for lines carrying a mutation(s) in *TCP14* or *TCP15*. We will ascertain whether these plant lines have an altered leaf size and/or shape by using LeafAnalyser and the stable reference set from the *Arabidopsis* leaf size and shape library. Based on our result we hope to be able to predict whether these closely related genes work in a redundant fashion or not, to this purpose we will also analyse the double mutant line.

T-DNA insertion mutants for *TCP14* (*tcp14-4*) and *TCP15* (*tcp15-3*) were received from the Davies laboratory. Kieffer et al. (2011) report that the *tcp14-4* mutant line caused a reduction in transcript levels, results in the production of truncated transcripts and thereby significantly altering the *TCP14* transcript. The position of the *tcp14-4* insertion lies in the coding region. Though the *tcp14-4* mutant is not a null allele, Kieffer et al. (2011) conclude that the *TCP14* expression is likely to be compromised. Northern blot analysis showed that the *tcp15-3* insertion destabilised the mutant transcript, hence, no transcript levels were detected (Kieffer et al., 2011).

The mutant lines were subjected to intense scrutiny but by visual inspection alone, no leaf development phenotype could be perceived in the single or double mutant (Figure 5.1).

Figure 5.1: Image of wild-type, *tcp14-4*, *tcp15-3* and *tcp14-4tcp15-3* (right to left).

5.1.1 Applying the Arabidopsis reference library to TCP lines

As described in Chapter 3 the *Arabidopsis* reference leaf shape library contains 1050 leaves from 10 *Arabidopsis* accessions. The first four Principal Components (PCs) account for 97.23% of the variance in leaf shape and size (figure 5.2). To determine whether there are differences in leaf shape and size between wild-type, *tcp14*, *tcp15* and *tcp14tcp15* the leaves (node 5 to 11; N = 427) of 20 plants of each line were analysed. LeafAnalyser was used to construct leaf-point models for each of the leaves. Standardised PC scores were generated for each leaf by applying the principal component analysis from the *Arabidopsis* reference library to the TCP leaf-point models. Based on these PC scores, it was possible to construct mean leaves and calculate mean PC values for each line (figure 5.2).

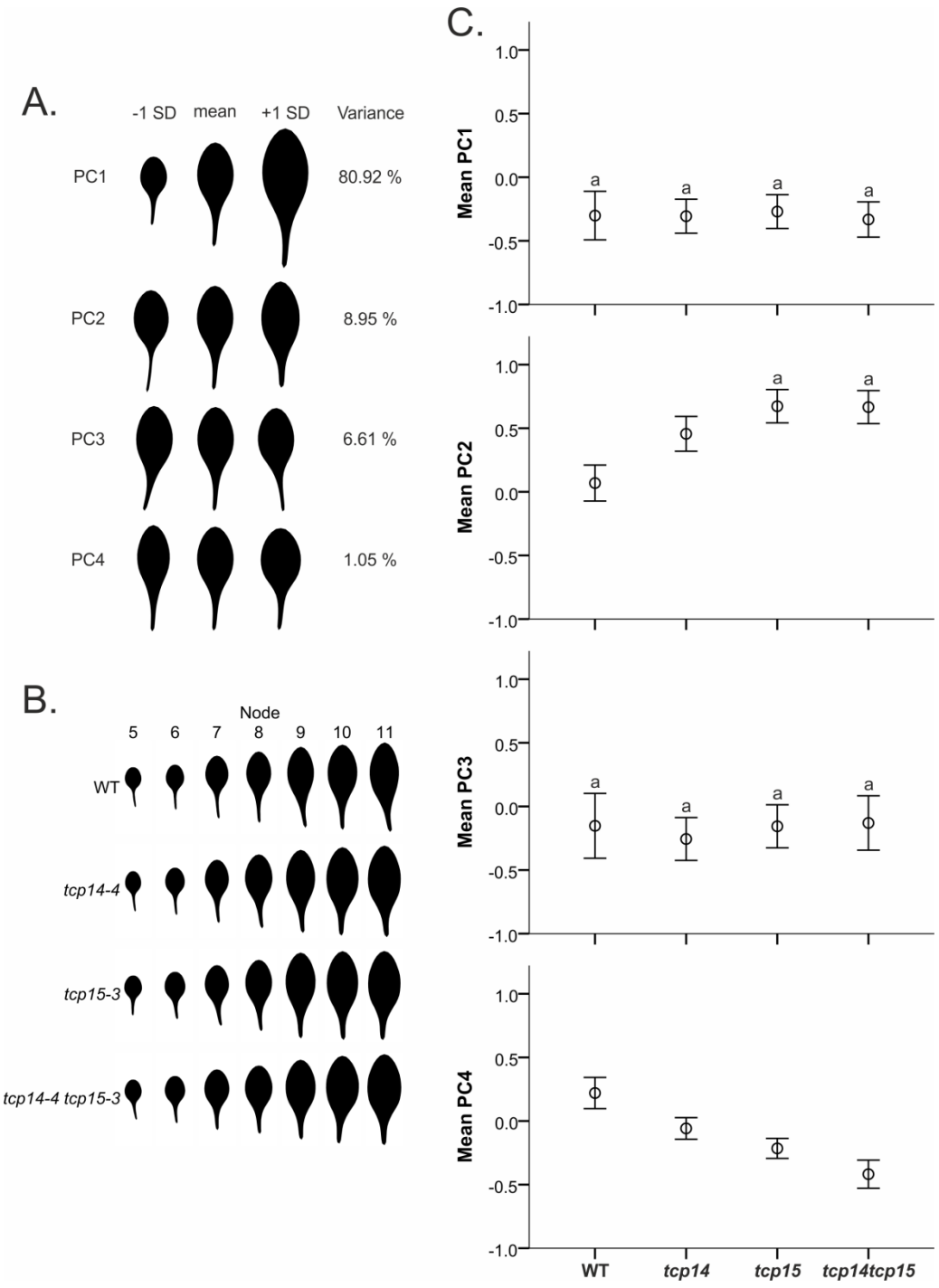

Figure 5.2: Leaf shape and size analysis for wild-type (WT), *tcp14-4, tcp15-3 and tcp14-4tcp15-3* plants.

A. Leaf size and shape according to variation along the first four PCs for the *Arabidopsis* stable reference set of 1050 leaves.

B. Comparison of the leaf point models for nodes 5–11 for WT, *tcp14-4, tcp15-3 and tcp14-4tcp15-3* plants. The mean node PC score is calculated from mean PC1, PC2, PC3 and PC4 node scores, visualising the mean size and shape of the leaves for each line. These leaves were constructed using LeafPredictor and the eigensystem of the reference set.

C. Mean PC scores for all leaves for wild-type, *tcp14-4, tcp15-3 and tcp14-4tcp15-3*. Error bars represents 95% confidence intervals. The letter "a" indicates that there is no significant difference between the genotypes; calculated using the Mann-Whitney test.

5.1.2 TCP14 and TCP15 specify leaf shape

A Kruskal-Wallis test was used to determine whether any of the PCs were significantly different between the lines. The analysis revealed that there are significant differences in leaf shape and leaf aspect ratio between wild-type, *tcp14*, *tcp15* and *tcp14tcp15* ($p<0.001$). These differences are captured by PC2 and PC4. No significant differences were found for PC1 and PC3, indicating that there is no significant difference in leaf size and leaf curvature between the different lines. In the *Arabidopsis* reference library PC2 explains 8.95 % of the total variation and describes a variation in leaf shape. PC4 accounts for 1.05 % of the variance and captures aspect ratio (leaf length: leaf width).

To determine the differences between the lines a pairwise comparison was carried out for PC2 and PC4. The Mann –Whitney test reveals that along PC2 *tcp14*, *tcp15*, and *tcp14tcp15* significantly differ from the wild-type line ($p<0.001$), and *tcp14* is significantly different from *tcp15* and *tcp14tcp15* ($p<0.05$). Along PC4 the wild-type line significantly differs ($p<0.001$) from *tcp14*, *tcp15*, and *tcp14tcp15*. Additionally *tcp14* is significantly different from *tcp15* ($p<0.05$) and *tcp14tcp15* ($p<0.001$), and a significantly difference exists between *tcp15* and *tcp14tcp15* ($p<0.05$) (Figure 5.2).

5.1.3 Discussion

The leaves show a blade shape defect in the order wild-type > *tcp14* > *tcp15* > *tcp14tcp15*, this sequence mirrors the plant stature phenotype observed by Kieffer et al., 2011. The blade shape defect is characterised by

changes in PC2 and PC4. Compared to the wild-type line the mutant lines have a shift to a higher PC2 value and a lower PC4 value. The combination of these changes produces a leaf that is broader towards the base due to a shift of the centre of the leaf. The petiole shape of the mutant lines is broader and shorter compared to the wild-type line.

These differences in leaf shape and size, which were not visible by eye alone, have been detected by applying a quantitative imaging approach. Using this method it is possible to conclude that *TCP14* and *TCP15* regulate the overall leaf shape. This result highlights the necessity of using of advanced methods of phenotypic analysis, in this case computer-aided morphological analysis in order to characterize phenotypes.

Kieffer et al reported a complex, dynamic expression pattern for *TCP14* and *TCP15* throughout leaf development using GUS staining. *tcp15* had a mild reduction in inflorescence height as well as reduced fruit pedicel length. The double mutant *tcp14tcp15* showed a more severe reduction in inflorescence height and pedicel length highlighting the genetic redundancy between *TCP14* and *TCP15*. Our results add a leaf shape phenotype for *tcp14* and *tcp15* which is more pronounced in the double mutant *tcp14tcp15* and could be indicative of increased cell proliferation in the leaf blade.

The short EAR motif can be used in a fusion construct (SRDX fusion) to create a dominant repressor thereby causing a loss-of-function phenotype (Hiratsu et al. 2003), this method has been used to study the functions of a number of class II TCP genes (Koyama et al. 2007; 2010a). Investigation of *pTCP14:TCP14:SRDX*, shows an enhanced version of the *tcp14tcp15* double mutant phenotype and characterised by an excess of cell proliferation in the leaf blade (Kieffer et al. 2011). The results from Kieffer et al. 2011 indicate that *TCP14* and *TCP15* redundantly control cell proliferation in a tissue dependent manner, promoting cell proliferation in young stem internodes to control plant stature and repressing cell proliferation in leaf and floral tissues to control organ shape.

The observed results allow us to speculate that leaf shape is defined by the regulation of cell proliferation through the interplay of a range of TCP factors. Due to the high degree of redundancy in this group individual TCP mutants do not exhibit strong phenotypes.

5.2 Isolation of homozygous mutants for *TCP8*, *TCP22* and *TCP23*

We have characterised the leaf shape phenotypes for *tcp14-4, tcp15-3* and *tcp14-4tcp15-3* using quantitative imaging analysis. The phenotype and the values for PC2/PC4 were more severe in the double mutant suggesting *TCP14* and *TCP15* might have overlapping functions in the specification of leaf shape. It is likely that *TCP14* and *TCP15* repress cell proliferation in the leaf and through this process modulate leaf shape (Kieffer et al., 2011). Furthermore leaf shape, or any organ shape, is likely to be controlled by the interplay of a range of TCP factors. The phenotype of *tcp14-4 tcp15-3* indicates that other genes have a role in determining leaf shape. To investigate this hypothesis we decided to investigate whether other class I TCP genes, closely related to *TCP14* and *TCP15*, were involved in modulating leaf shape.

5.2.1 TCP14 and TCP15 are closely related to TCP8, TCP22 and TCP23

A BLAST (Basic Local Alignment Search Tool) search using the *TCP14* sequence and the list of *Arabidopsis* TCP genes collated by (Cubas et al. 1999) was used to construct a neighbour-joining tree of *TCP14*-like genes. There are three additional TCP genes, *TCP8, TCP22* and *TCP23* that may form a sub-clade with *TCP14* and *TCP15* and might also have a role in determining leaf shape (Figure 5.3).

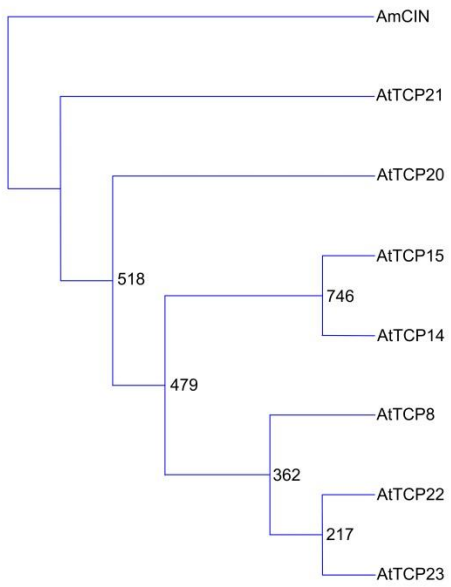

Figure 5.3: Neighbour-joining tree of TCP14-like genes. The *Arabidopsis* TCP genes, *TCP8, TCP14, TCP14, TCP20, TCP21, TCP22* and *TCP23* have been included. The *Antirrhinum majus* gene *CINCINNATA* was used as an outgroup. The length of the branches does not indicate genetic distance.

5.2.2 Isolation of T-DNA insertion mutants

5.2.2.1 Identification of suitable T-DNA insertion mutants

The primary focus will be on the TCP genes closely related to *TCP14* and *TCP15*. The neighbour-joining tree reveals that *TCP14* and *TCP15* are part of a sub-clade that also includes *TCP8*, *TCP22* and *TCP23*.

Initial investigation of the expression patterns of these TCP genes using Arabidopsis eFP Browser (http://bar.utoronto.ca/efp/cgi-bin/efpWeb.cgi - Winter et al. 2007) reveals that *TCP23* is expressed at a higher level in leaf tissue than *TCP8*. No information is available on the web for *TCP22*, this gene was not available on the Affymetrix chips at the time of this analysis. As is often the case for multi-gene families a number of the TCP-genes are clustered together on the chromosome. *TCP8*, *TCP22*, and *TCP23* are

clustered with *TCP15* on chromosome 1, while *TCP14* is located on chromosome 3. The close clustering of these genes will make the construction of multiple mutants more challenging. Another TCP genes that could be of interest is *TCP21*, which is highly expressed in leaves. To investigate the role of these class I TCP genes we have analysed T-DNA insertion mutants for *TCP8, TCP22, TCP23*.

Table 5.1 shows a list of the selected T-DNA insertion mutants.

5.2.2.2 Identifying insertion points for T-DNA insertion lines

The seeds received from the Nottingham Arabidopsis Stock Centre (NASC) were grown on the appropriate selection media (table 5.1) to assess antibiotic resistance. Plants not containing a T-DNA insertion will be sensitive to the antibiotic. It should be noted that after several generations some lines show silencing of the antibiotic resistance gene; it is therefore possible that a mutant plant does not express the antibiotic resistant phenotype. To isolate homozygous plants gene-specific primers were designed to amplify the wild-type gene. DNA was extracted and used in subsequent PCR analysis.

Reference	ID	Name	Approx. Insertion site*	Gene	AGI code	Selectable marker
tcp8-1	N817775	SAIL_387_A10	Promoter -region	TCP8	At1g58100	Kn
tcp8-2	N803036	SAIL_64_D09	Exon	TCP8	At1g58100	Kn
tcp22	N654177	SALK_045755	5’ UTR	TCP22	At1g72010	PPT
tcp23	N874232	SAIL_443	Exon	TCP23	At1g35560	Kn

Table 5.1: Overview of the ordered T-DNA insertion lines; Kn = Kanamycin, PPT Phosphinothricin/ BASTA. *Estimated insertion information available at time of order.

To determine the exact T-DNA insertion point the PCR product of the amplified gene/T-DNA boundary is sent for sequencing (Appendix 2). The orientation of the insertion is determined by whether the forward or the reverse gene-specific primer amplifies a PCR product when combined with the left-border T-DNA insertion primer. If both primer combinations amplify a PCR product the line carries an inverted tandem T-DNA insertion. The sequenced PCR product(s) are aligned with the genomic and the T-DNA sequence. By comparing the two alignments the exact insertion point can be determined.

Sequence alignments are carried out using Clustal W 2.1 (www.genome.jp/tools/clustalw) and within this thesis the insertion point will be given in reference to the start codon (ATG), minus will refer to sequences upstream of the start codon, such as five prime untranslated region (5'UTG) or promoter region. The insertion point will be directly after the mentioned base pair. In case of multiple insertion points the first insertion point will be the farthest upstream of the start codon; e.g. Insertion Point 1 is located in the 5'UTG of gene 1 at -235bp, Insertion Point 2 is located at 45bp.

5.2.2.3 Determining T-DNA insertion point for *tcp8-1*

For allele *tcp8-1* (N817775) both of the gene-specific/left-border T-DNA primer combinations yielded a PCR product and were consequently sent for sequencing (figure 5.4, figure 5.8 and table 5.2). Insertion point 1 was amplified by the forward gene-specific primer and insertion point 2 by the reverse gene-specific primer, indicating a right-border/right-border inverted repeat insertion. The first insertion point is located in the promoter region of *TCP8* at -678bp. The exact position of the second insertion point is ambiguous, and located in the sequence spanning location -674bp to -667bp. The 7bp sequence shows a high sequence similarity with the *TCP8* genomic sequence as well as with the T-DNA sequence. In the alignment with the

genomic sequence there is one mismatched base pair at -669bp (T/G). This mismatch could signal the end of the genomic sequence or be a sequencing error. The integration of the T-DNA resulted in a short deletion in the promoter region; the length of the deletion is minimum 4bp and maximum 11bp depending on the location of the second insertion point.

5.2.2.4 Determining T-DNA insertion point for *tcp8-2*

The second T-DNA insertion line, allele *tcp8-2* (N803036), has two insertion points located in the 5'UTR of *TCP8* and carries a right-border/right-border inverted repeat insertion (figure 5.5, figure 5.8 and table 5.2). Insertion point 1 has been narrowed down to a 3bp sequence (TAA) at position -215bp/-212bp which perfectly aligns with the *TCP8* genomic and T-DNA sequence. The second insertion point is located at -190bp. The integration of the T-DNA caused a deletion of minimum 22bp and maximum 26bp depending on the first insertion point. It should be noted that the quality of the sequence reads for the *tcp8-2* PCR products was not very good resulting in a number of gaps and single base pair mismatches in the alignments making the confidence level of this analysis less than for *tcp8-1*.

5.2.2.5 Determining T-DNA insertion point for *tcp22*

tcp22 (N654177) carries a right-border/right-border inverted repeat insertion in the 5'UTR (figure 5.6, figure 5.8 and table 5.2). The first insertion point is located between -326bp and -323bp (GAA). Base pair -326bp is a mismatch with the genomic sequence (G/A) which could signal the end of the genomic sequence. The second insertion point was narrowed down to a stretch of 6bp (TCCTGC), between positions -269bp and -263bp, aligning with the genomic as well as the T-DNA sequence. The T-DNA insertion resulted in a deletion of minimum 55bp and maximum 64bp in the 5'UTR.

5.2.2.6 Determining the T-DNA insertion point for *tcp23*

The TCP23 T-DNA insertion line, allele tcp23 has a right-border/right-border inverted repeat insertion in the exon (figure 5.7, figure 5.8 and table 5.2). The first insertion point is either at position 426bp or 428bp (AT), the second insertion point is located at 486bp or 488bp; in both cases the 2 base pairs align with the genomic as well as the T-DNA sequence. A deletion of 58bp to 62bp is the result of the T-DNA insertion.

Gene	AGI code	Reference	ID	IP	Comment
TCP8	At1g58100	*tcp8-1*	N817775	Promoter region	Deletion 4bp - 11bp
TCP8	At1g58100	*tcp8-2*	N803036	5'UTR	Deletion 22bp - 26bp
TCP22	At1g72010	*tcp22*	N654177	5'UTR	Deletion 55bp - 63bp
TCP23	At1g35560	*tcp23*	N874232	Exon	Deletion 58bp - 62bp

Table 5.2: Summary table of T-DNA insertion lines and their insertion points.

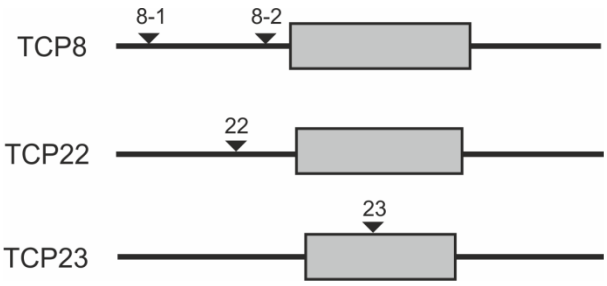

Figure 5.8: Graphical overview of the insertion points for the T-DNA insertion lines *tcp8-1, tcp8-2, tcp22,* and *tcp23*. The grey box represents the exon.

5.2.3 Creating multiple mutants

Double mutants are isolated by crossing the single T-DNA insertion lines to each other and selecting progeny on selective media. Homozygous double mutants (*tcp8-1tcp22, tcp8-2tcp22, tcp8-1tcp23, tcp8-2tcp23, tcp22tcp23*) have been successfully isolated. Identification of the double TCP mutants

was hampered by the position of *TCP8*, *TCP22* and *TCP23* on chromosome I. Due to the expected subtle phenotype, even of the double TCP mutants genotyping was carried out by PCR.

A. **Forward Gene-specific PCR product *tcp8-1***

TAGCAACCGATTCATAAATAATTTTTCGGGTTTGGGCCACAACA
GACCGGCCCATTTCAACCGGTTCATAAATTCTAAATACTAGAAA
ATTCCAAATTAGATAAGTTTTTGTCCATCCTTTCTTTGGGATTC
TTGACGAGTAACGTTTGATGTCTTTCTTAATTTGGTTGAATGAT
CAAATTTGTGATCCAAATTCTTACAAACTGATATGTTAATGAAT
CTATAACCAAAATAACGTCTAAAACAAAAAGCTGTAACGATTTG
AAA**AACACATTGCGGACGTTTTTAATGTACTGAATTAACGCCGA**
ATTGAATTCGATTTGGTGTATCGAGATTGGTTATGAAATTCAGA
TGCTAGTGTAATGTATTGGTAATTTGGGAAGTTATAAGGAAGCA
ATGGAGATACCTACTTCCGGGGGGGGGGGGGGGGGGGGAGAAAC
TTCGGGGGGGGGGGGGGGGGGGCTCTTAATGATCGCCACGCCGTG
AGGGCTGTTGCGATGGGCGCTCACCGTTCCTCGTACTGCTCCTG
CCTTGGCGACGGCTGCGGGACGGATCAGTCCTCAAGCGGTAAAG
GTATCACAAACAGGGATAACGAAGAAAAAGGAGAAAGGCAGAAA
GGCAAGAACATAAAAAGGCAGGTGTGGATTTTCTAGTCCCCCCT
AAAG

B. **Reverse Gene-specific PCR product *tcp8-1***

ATAAAAGTAGGGTTTGGTGAAGAGGAAGAACGGCCATGGAAGCT
CCGATTGTCGCCTTCAAGTTTGACTCTTGTCTTCTTCTTTGTCT
CGAGAAGAGAGAGAGAGAGATGAGAGAAAAAAAGGTTTGATGAT
GTAAAAGCAGGTGGATGACTTTTCCAGCAAGAGGATATTATTAT
TAAAATAAATAATATATATGCCGTCATTAACATTAAATAAAACG
TTTATTGATTTTTGATTAGTTATTATATAAATCAAAAAGTAATT
AGGGGAGAAAAATAACTTTTCACAATTATTTTAAGTCTTTTTTA
TCAAAATTCTACCCAAATATGAGTTATGTTATTTTTCAATTACA
TTATTTTCATCACAACATTATTGTTTACCAATTTTAGAGCACCA
ATAAAAAAAGGTTTAAAAAAGATTTGTGGATTAAGAAAGTTAGA
AAGAGAGAGATAAGCATCTTTCAGACAGTGAAGCGTGCGTATTT
TTGCAGGTGGGGACAGCTCATTACAATCCACCTCCGTATCTCCA
TTTCACTTTTGTCTTAAATATTTTTAGTTTTATAAGATTTTGTT
AAAAGTATATCCATTAGATAAATGACACTAAATTCTTTAATTAG
TTATATAGTTTTGGG**AACAAATTGACGCTTAGACAACTTAATAA**
CACATTGCGGACGTTTTTAATGTACTGAATTAACGCCGAATTGA
ATTCGATTTGGTGTATCGAGATTGGTTATGAAATTCAGATGCTA
GTGTAATGTATTGGTAATTTGGGAAGATATAATAAGGAAGCAA

C. **Alignment of *TCP8* and Forward Gene-specific PCR product**

```
TAAACCCAAAAAGACCCAAATACCCCAACGCCTTACCATATTAAATTAGGAGGAAACCCG
----------------------------------------------------TAGCAACCGA
                                                      * ****

TTCATAAATAATTTTTCGGGTTTGGGCCACAACAGACCGGCCCATTTCAACCGGTTCATA
TTCATAAATAATTTTTCGGGTTTGGGCCACAACAGACCGGCCCATTTCAACCGGTTCATA
************************************************************

AATTCTAAATACTAGAAAATTCCAAATTAGATAAGTTTTTGTCCATCCTTTCTTTGGGAT
AATTCTAAATACTAGAAAATTCCAAATTAGATAAGTTTTTGTCCATCCTTTCTTTGGGAT
************************************************************

TCTTGACGAGTAACGTTTGATGTCTTTCTTAATTTGGTTGAATGATCAAATTTGTGATCC
TCTTGACGAGTAACGTTTGATGTCTTTCTTAATTTGGTTGAATGATCAAATTTGTGATCC
************************************************************

AAATTCTTACAAACTGATATGTTAATGAATCTATAACCAAAATAACGTCTAAAACAAAAA
AAATTCTTACAAACTGATATGTTAATGAATCTATAACCAAAATAACGTCTAAAACAAAAA
************************************************************
             IP1  IP2
GCTGTAACGATTTGAAAG-TGGATTTTTTCCCAAAACTATATAACTAATTAAAG---AAT
GCTGTAACGATTTGAAAAACACATTGCGGACGTTTTTAATGTACTGAATTAACGCCGAAT
*****************  *****  *       ** **   ****** *   ***

TTAGTGTCATTTATCTAATGGATATACTTTTAACAAAATCTTATAAAACTAAAA-ATATT
TGAATTCGATTTGGTGTATCGAGAT-TGGTTATGAAATTCAGATGCTAGTGTAATGTATT
* * *   ****     ** ** **    ***  *** **  **   * *  **  ****

TAAGAC----AAAAGTGAAATGGAGATACGGAGGTGGATTGTAATGAGCTGTCCCCACCT
GGTAATTTGGGAAGTTATAAGGAAGCAATGGAGATACCTACTTCCGGGGGGGGGGGGGGG
    *      **  *  ** * **  * **** *   *  *   * *  *

GCAAAAATACGCACGCTTCACTGTCTGAAAGATGCTTATC--TCTCTCTTTCTAACTTTC
GGGGGAGAAACTTCGGGGGGGGGGGGGGGGGGCTCTTAATGATCGCCACGCCGTGAGGGC
*    * *    **       *   *   *   ****    ** *     *       *

TTAATCCACAAATCTTTTTTAAACCTTTTTTTATTGGTGCTCTAAAATTGG-TAAACAAT
TGTTGCGATGGGCGCTCACCGTTCCTCGTACTGCTCCTGCCTTGGCGACGGCTGCGGGAC
*    * *       *       ***  *  *  *  ***  *      ** *     *

AATGTTGTGATGAAA--ATAATGTAATTGAAAAATAACATAACTCATATTTGGGTAGAAT
GGATCAGTCCTCAAGCGGTAAAGGTATCACAAACAGGGATAACGAAGAAAAAGGAGAAAG
      **  * **    *** *  **   ***     *****  * *    **   **

TTTGATAAAAAAGA-CTTAAAATAATTG-TGAAAAGTTATTTTTCTCCCCTAATTACTTT
GCAGAAAGGCAAGAACATAAAAAGGCAGGTGTGGATTTTCTAGTCCCCCCTAAAG-----
   ** *   **** * *****     * **   * **  *  ** *******
```

Figure 5.4: Determining the T-DNA insertion point for *tcp8-1* (N817775)

A. Sequence of the PCR product obtained by the forward gene-specific and the T-DNA left-border primer combination. The non-bold sequence shows high sequence similarity with the gene-specific, TCP8, sequence while the bold sequence overlaps with the left-border T-DNA sequence.

B. Sequence of the PCR product obtained by the reverse gene-specific and the T-DNA left-border primer combination. The non-bold sequence shows high sequence similarity with the gene-specific, TCP8, sequence while the bold sequence overlaps with the left-border T-DNA sequence. The boxed sequence shows high sequence similarity to TCP8 sequence as well as left-border T-DNA sequence

C. Alignment of the TCP8 sequence and the PCR product obtained from the forward gene-specific primer and the T-DNA left-border primer. Insertion point 1 could be narrowed down to 1bp while the second insertion point was determined within 7bp (boxed sequence).

A. **Forward Gene-specific PCR product *tcp8-2***

ACTCCCTTTTCTACTTTCTTATCCACAAATCTTTTTTAAACCT
TTTTTTATTGGTGCTCTAAAATTGGTAAACAATAATGTTGTGA
TGAAAATAATGTAATTGAAAAATAACATAACTCATATTTGGGT
AGAATTTTGATAAAAAAGACTTAAAATAATTGTGAAAAGTTAT
TTTTCTCCCCTAATTACTTTTTGATTTATATAATAACTAATCA
AAAATCAATAAACGTTTTATTTAATGTTAATGACGGCATATAT
ATTATTTATTT**TAAACAAATTGACGCTTAGACAACTTAATAAC**
ACATTGCGGACGTTTTTAATGTACTGAATTAACGCCGAATTGA
ATTCGATTTGGTGTATCGAGATTGGTTATGAAATTCAGATGCT
AGTGTAATGTATTGGTAATTTGGGAAGATTATAAGGAAGCA

B. **Reverse Gene-specific PCR product *tcp8-2***

CATGGAGGAGCCGGTGGCCTGCGGCGGTGTTATTGTTGCTACT
ACTCTCCATTTGATTACCGGCCGTTGTCGGTACCGGAAGCATC
CAAAAAGTGTTCCCAGCACCAGACCTACTCGGCGGCGCAACCG
CCCACATCGGCGCCGCCGTAGGACCCGACGTTTCACTTTCTTT
CAAAGATTTATTCTCGTTCTGTTTCCGATCATCGTTTTCTTTA
GACAAATCAACCGATCTATACCGTTTCCTAGAGAAATTCTCAC
CTTCAGGAATAGTTTCCACCGGATCTTGATTCTGATTCTGGTT
CTGGTGGTGTTGAAGCTGATGATGAAACCCTAAAAGCGGCGAC
GTATGAGCAGCAAACACACCGCCGCCTCCTTGTTCATCATACT
GATGATGAGTCAATCCAAGAGCACCGTAAAGCGGCACCGATTT
CGACGGCGGAGCAGAGAGAGTCGATCCACTACTTCGTAACGAA
ACACTTAAAGTAGAGAAGTTCGCCGGAATAGTTCCTGTACCTG
TAGCAGCAACAATAGCTGGCTCAGCTTGTTGAAGAAGCCATTC
AATAGTTTCACCATCGGATTTATGACCTAACTCTCTCGTTAAC
TGAAAAACTCTAGCTGCACATAGCGCCGGCATACGAATCCGAC
GTCCTCTTCCGTCGACTTTCGTGTGACGGTCTTTAGTCGACCG
CTTCGTTGTAGTCGCCGTTGCCGTAGATGAGGTTGTTGCGAGT
GTTGAGTCTTCGGGAGGTGTAGATCTGGGAACGATTGAGAGAG
ATGCGTCAACTAGCTGTCTTGCTCCTCCTCCGGTGGCGACGGC
GGCGGTGTCGTTGTTGTTGTTTCGGATGTCGGAGAGATCCATT
TTCCGGTGAGAAAGAAGGGAAAAGAAGATGAAATTGAAATTAG
GGTTTGGTGAAAGAGGAAGAACGGCCATGGAAGCTCCGATTGT
CGCCTTCAGTTTGACTCTTGTCTTCTTCTTTGTCTCGAGAGAG
AGAGAGAGAGATGAGAGAAAAAAGGTTTGATGATGTAAAGCAG
TGGATGACTT**AATAACAACTGACGCTAGACACTTAATAACACA**
TGCGAACGTTTTATGTACTGACACGGCCGAATTGAATTCGAAT
TTGGTGGATCGAATGCTAGAATCCGATGCTAGGCAATGCAGTT
GTAACG

C. **Alignment of *TCP8* and Forward Gene-specific PCR product**

```
AGATGCTTATCTCTCTCTTTCTAACTTTCTTAATCCACAAATCTTTTTTAAACCTTTTTT
----------ACTCCCTTTTCTACTTTCTTA-TCCACAAATCTTTTTTAAACCTTTTTT
           *** ****   ********* ************************

TATTGGTGCTCTAAAATTGGTAAACAATAATGTTGTGATGAAAATAATGTAATTGAAAAA
TATTGGTGCTCTAAAATTGGTAAACAATAATGTTGTGATGAAAATAATGTAATTGAAAAA
************************************************************

TAACATAACTCATATTTGGGTAGAATTTTGATAAAAAAGACTTAAAATAATTGTGAAAAG
TAACATAACTCATATTTGGGTAGAATTTTGATAAAAAAGACTTAAAATAATTGTGAAAAG
************************************************************

TTATTTTTCTCCCCTAATTACTTTTTGATTTATATAATAACTAATCAAAAATCAATAAAC
TTATTTTTCTCCCCTAATTACTTTTTGATTTATATAATAACTAATCAAAAATCAATAAAC
************************************************************
                                                    IP1
GTTTTATTTAATGTTAATGACGGCATATATATTATTTATTTTAATAATAATATCCTCTTG
GTTTTATTTAATGTTAATGACGGCATATATATTATTTATTTTAAACAAATTGACGCTTAG
****************************************** * * *  *   * *
       IP2
----CTGGAAAAGTCATC-CACCTGCTTTTACATCATCAAACCTTTTTTTCTCTCATCTC
ACAACTTAATAACACATTGCGGACGTTTTTAATGTACTGAATTAACGCCGAATTGAATTC
    **  * **  ***  *    * *****    *   **           * *  **

TCTCTCTCTCTTCTCGA--GACAAAGAAGA--AGACAAGAGTCAAACTTGAAGGCGACAA
GATTTGGTGTATCGAGATTGGTTATGAAATTCAGATGCTAGTGTAATGTATTGGTAATTT
  * *      **  **  *   * ***    ***    ***  **  *   **  *

TCGGAGCTTCCATGGCCGTTTCTTCCTCTTTCACCAAACCCTAATTTCAATTTCATCTTC
GGGAAGATTATAAGGAAGCA----------------------------------------
  * ** **  * **  *

TTTTCCCTTCTTTCTCACCGGAAAATGGATCTCTCCGACATCCGAAACAACAACAACGAC
------------------------------------------------------------
```

Figure 5.5: Determining T-DNA insertion point for *tcp8-2* (N803036)

A. Sequence of the PCR product obtained by the forward gene-specific and the T-DNA left-border primer combination. The non-bold sequence shows high sequence similarity with the gene-specific, *TCP8*, sequence while the bold sequence overlaps with the left-border T-DNA sequence. The boxed sequence shows high sequence similarity to *TCP8* sequence as well as left-border T-DNA sequence

B. Sequence of the PCR product obtained by the reverse gene-specific and the T-DNA left-border primer combination. The non-bold sequence shows high sequence similarity with the gene-specific, *TCP8*, sequence while the bold sequence overlaps with the left-border T-DNA sequence.

C. Alignment of the *TCP8* sequence and the PCR product obtained from the forward gene-specific primer and the T-DNA left-border primer. Insertion point 1 was narrowed down to 3bp (boxed sequence) while the second insertion point was determined to within 1bp.

A. **Forward Gene-specific PCR product**

CAATTTATTTTTTATTTTATAAAGGTTCTTAATTA
CATCACTGATCTATAGGATTAGATACTCTAAGAAT
GTTCATGTTCCATTCTAATTAATTATATATTTAAA
AAACAAATCCGAAAATTAGCTTGCATAATTATCCA
AAAGTAACAATGATGATTTTTTTTTTTTTAACTGG
GTCAATTTTAATTTTAACCAGGGAAAAGCAAAAAA
ATGAAGGGTTTTCAACAAAAAAAAAAAACAGTGTA
A**AAAAACTTAATAACACATTGCGGACGTTTTTAAG**
GTACGGGGGGGGTTTTTCTTTTCCCCAGGGAAACG
GGCAACAGCTGATTGCCCTTCCCCCCCTGGCCCTG
AAAAAGTTGCAGCAAGCGGCCCACGCTGGTTTGCC
CCACCAGGCAAAAATCCTGTTTGATGGGGGTTCCA
AAATCGGCAAATAAA

B. **Reverse Gene-specific PCR product**

CAAGGTTTTTTACCGGGATTAAGCTGAGCGTCGCC
TCCGCAACAGAGGAATTCTGATTCATCTTCAAATC
CGTAAAAAGATATGATTTTTATGATTTTTAGACAA
AACCCATGTGAATTCTGTGTCTTGACATCGAATTC
TATATAATCTGGGGAAATCTGAAGCAAATCGATTG
AAGAAACAAAAGCAGAGAAAGAAGAGAAAGTGACT
GTGGAAGGAGGAGATCTAAGCTTGCTACTAAAATG
GAGTTTGAGAACAGAGAGGGAGAGAGAAGAGAGAA
TGATTGAGAAGGATAAAAACAAGTGGATATGAATG
GTGTGATT**GCAGGATATATTGTGGTGTAAACAAAT**
TGACGCTTAGACAACTTAATAACACATTGCGGACG
TTTTTAATGTACTGGGGTGGTTTTTCTTTTCACCA
GTGAGACGGGCAACAGCTGATTGCCCTTCACCGCC
TGGCCCTGAGAGAGTTGCAGCAAGCGGTCCACGCT
GGTTTGCCCCAGCAGGCGAAAATCCTGTTTGATGG
TGGTTCCGAAATCGGCAAAATAATG

C. **Alignment of TCP22 and Forward Gene-specific PCR product**

```
GATCACGGTTAAAGAAACTTAGATGGGAAAATCAAGGTTAAAAAAATTCACCTAATTTTA
----------------------------------------------------CAATTTAT
                                                     *****

TTTTTATTTTATAAAGGTTCTTAATTACATCACTGATCTATAGGATTAGATACTCTAAGA
TTTTTATTTTATAAAGGTTCTTAATTACATCACTGATCTATAGGATTAGATACTCTAAGA
************************************************************

ATGTTCATGTTCCATTCTAATTAATTATATATTTAAAAAACAAATCCGAAAATTAGCTTG
ATGTTCATGTTCCATTCTAATTAATTATATATTTAAAAAACAAATCCGAAAATTAGCTTG
************************************************************

CATAATTATCCAAAAGTAACAATGATGATTTTTTTTTTTTTAACTGTGTCAATTTTAATT
CATAATTATCCAAAAGTAACAATGATGATTTTTTTTTTTTTAACTGGGTCAATTTTAATT
****************************************** *************

TTAACCATGGCAAAGCAAAAAAATGAAGGGTTTTCGACAAGAAAGAAGAACAGTGTAAGA  IP1
TTAACCAGGGAAAAGCAAAAAAATGAAGGGTTTTCAACAAAAAAAAAAAAACAGTGTAAAA
******* ** ********************** **** *** ** **********  *

AACAAATAAGTCAATAAAGGTTGAATTGAATAGAGAATTTAGATGGATAGTTTCTTCCTG  IP2
AA--ACTTAAT-AACACATTGCGGACGTTTTTAAGGTACGGGGGGGGTTTTTCTTTTCCC
**  * * * * ** * *    * *     *  **      *  ** *  **  **  *

CAATCACACCATTCATATCCACTTGTTTTTATCCTTCTCAATCATTCTCTCTTCTCTCTC
CAGGGAAACGGGCAACAGCTGATTGCCCTTCCCCCCCTGG------CCCTGAAAAAGTTG
**   * **     * * *   ***   **  **  **        * **       *

CCTCTCTGTTCTCAAACTCCATTTTAGTAGCAAGCTTAGATCTCCTCCTTCCACAGTCAC
CAGCAAGCGGCCCACGCTGGTTTGCCCCACCAGGCAAAAATCCTGTTTGATGGGGGTTCC
*  *      * **  **   **     * ** **  * ***   *         **  *

TTTCTCTTCTTTCTCTGCTTTTGTTTCTTCAATCGATTTGCTTCAGATTTCCCCAGATTA
AAAATCGGCAAATAAA-------------------------------------------
    **  *
```

Figure 5.6: Determining T-DNA insertion point for *tcp22* (N654177)

A. Sequence of the PCR product obtained by the forward gene-specific and the T-DNA left-border primer combination. The non-bold sequence shows high sequence similarity with the gene-specific, *TCP22*, sequence while the bold sequence overlaps with the left-border T-DNA sequence. The boxed sequence shows high sequence similarity to *TCP22* sequence as well as left-border T-DNA sequence

B. Sequence of the PCR product obtained by the reverse gene-specific and the T-DNA left-border primer combination. The non-bold sequence shows high sequence similarity with the gene-specific, *TCP22*, sequence while the bold sequence overlaps with the left-border T-DNA sequence. The boxed sequence shows high sequence similarity to *TCP22* sequence as well as left-border T-DNA sequence

C. Alignment of the *TCP22* sequence and the PCR product obtained from the forward gene-specific primer and the T-DNA left-border primer. Insertion point 1 was narrowed down to 3bp (boxed sequence) and the second insertion point was determined to within 6bp (boxed sequence).

A. **Forward Gene-specific PCR product *tcp23***

AATTTAATAGGGTTTAAAAGTAAAAAATTCAGTACAAGTTTGTT
TGTTTGTTTATTCCATTTTCTTGTGTGTTTTTTTCCCCATAATT
TATAAATTTTATAAGCAATATGGAGTCCCACAACAACAACCAGA
GCAACAACAACACCACTGGTTCGGCCCATCTGGTCCCATCCATG
GGACCAATCTCCGGTTCAGTCTCATTAACCACCACTGCTCCAAA
CTCCACTACCACCACCGTCACCGCCGCTAAAACACCCGCAAAAC
GACCGTCCAAGGACCGTCACATCAAAGTAGACGGACGTGGCCGG
AGGATACGTATGCCGGCTATCTGCGCAGCACGTGTCTTCCAACT
AACACGTGAGTTACAACACAAATCGGACGGCAAGACTATAGAGG
GGCTGCTCCAACAAGCGGAGCCAGCTATCATCGCAGCCACCGGA
ACTGGAACCTTACCGGCAAATATCTCTACTTTGAACATCTCTCT
TCGAAGCAGTGGCTCTACTCTTTCAGCTCCACTGTCTAAATCTT
TCCAC**ATTGTGGTGTAAACAAATTGACGCTTAAACAACTTAATA**
ACACATTGCGAACGTTTTTAATGTACTGAATTAACGCCAAATTG
AATTCAATTTGGTGTATCAAGATTGGTTATGAAATTCAAATGCT
AGTGTAATGTATTGGTAATTTGGGAAGATATAATAGGGAAGAC

B. **Reverse Gene-specific PCR product *tcp23***

ATTGGAGTCTCACAAAGTTGCATAAATCACACATTCACACTTTT
TAAAAACCAAAGAAATCATGAAGTCTTTCAAGGAGAACCATCTA
TAGTAGGATTTTGGTCTCTAGTAGCATGATCACTCACTTGATGT
TGAGGCTTTTGCTCAAGACTCATTCCGAGACCAACCCGACCACC
GTCTCCTCCTCCGCCGGAAAATAGCCCCAAATTGTTATTTTCTG
CAACACCTAACCCTAACTGTTGACCTCCCACTAACATAGACCCT
AGCTGAACCGACCCGATTCGACCCGGGTAATGACCCGGATTAAA
CGCCCACATGTGCTGTGATGGATCCTGAACGTTAGCCGGACCTC
CTCCTCCTCCGACTGGTAACATCCAAAAAGCACTACCTCCGTTT
GTGGAGGCTGGCGTTGGCGCTAGTGCCCACATCGGCGGTATCAT
ATTTTGTGTTCTTGACCGGGTCGAACCCGGATCTTGATCAGGAG
CTTCGGATCCCGGTTTAGGTGATCTTGAACCGGGTTCTTGATCT
AGAAAATTAGGATCTTTAAAAAGATCTTCTTCACGGAATGTTTT
GGGAAGAGAAGAAGAAGAAGAATCTGTCGTGATATGA**TGGTGTA**
AACAAATTGACGCTTAGACAACTTAATAACACATTGCGGACGTT
TTTAATGTACTGAATTAACGCCGAATTGAATTCGATTTGGTGTA
TCGAGATTGGTTATGAAATTCAGATGCTAGTGTAATGTATTGGT
AATTTGGGAAGAAAA

C. **Alignment of *TCP23* and Forward Gene-specific PCR product**

```
GTGTTTTTTTCCCCATAATTTATAAATTTTATAAGCAATATGGAGTCCCACAACAACAAC
GTGTTTTTTTCCCCATAATTTATAAATTTTATAAGCAATATGGAGTCCCACAACAACAAC
************************************************************

CAGAGCAACAACAACACCACTGGTTCGGCCCATCTGGTCCCATCCATGGGACCAATCTCC
CAGAGCAACAACAACACCACTGGTTCGGCCCATCTGGTCCCATCCATGGGACCAATCTCC
************************************************************

GGTTCAGTCTCATTAACCACCACTGCTCCAAACTCCACTACCACCACCGTCACCGCCGCT
GGTTCAGTCTCATTAACCACCACTGCTCCAAACTCCACTACCACCACCGTCACCGCCGCT
************************************************************

AAAACACCCGCAAAACGACCGTCCAAGGACCGTCACATCAAAGTAGACGGACGTGGCCGG
AAAACACCCGCAAAACGACCGTCCAAGGACCGTCACATCAAAGTAGACGGACGTGGCCGG
************************************************************

AGGATACGTATGCCGGCTATCTGCGCAGCACGTGTCTTCCAACTAACACGTGAGTTACAA
AGGATACGTATGCCGGCTATCTGCGCAGCACGTGTCTTCCAACTAACACGTGAGTTACAA
************************************************************

CACAAATCGGACGGCGAGACTATAGAGTGGCTGCTCCAACAAGCGGAGCCAGCTATCATC
CACAAATCGGACGGCAAGACTATAGAGGGGCTGCTCCAACAAGCGGAGCCAGCTATCATC
*************** *********** ******************************

GCAGCCACCGGAACTGGAACCATACCGGCGAATATCTCTACTTTGAACATCTCTCTTCGA
GCAGCCACCGGAACTGGAACCTTACCGGCAAATATCTCTACTTTGAACATCTCTCTTCGA
******************** ******* ****************************
                                                  IP1
AGCAGTGGCTCTACTCTTTCAGCTCCACTGTCTAAATCTTTCCACAT---GGGAAGAGCG
AGCAGTGGCTCTACTCTTTCAGCTCCACTGTCTAAATCTTTCCACATTGTGGTGTAAACA
***********************************************   **    * *
                                                    IP2
GCTCAAAACGCTGCCGTTTTTGGGTTCCAGCAACAGCTTTATCATCCTCATCATATCACG
AATTGACGCTTAAACAACTTAATAACACATTGCGAACGTTTTTAATGTACTGAATTAACG
  *  *  *     *   **       **     * * ** * *   * * *  * ***
```

Figure 5.7: Determining T-DNA insertion point for *tcp23* (N874232)

A. Sequence of the PCR product obtained by the forward gene-specific and the T-DNA left-border primer combination. The non-bold sequence shows high sequence similarity with the gene-specific, *TCP23*, sequence while the bold sequence overlaps with the left-border T-DNA sequence. The boxed sequence shows high sequence similarity to *TCP23* sequence as well as left-border T-DNA sequence

B. Sequence of the PCR product obtained by the reverse gene-specific and the T-DNA left-border primer combination. The non-bold sequence shows high sequence similarity with the gene-specific, *TCP23*, sequence while the bold sequence overlaps with the left-border T-DNA sequence. The boxed sequence shows high sequence similarity to *TCP23* sequence as well as left-border T-DNA sequence

C. Alignment of the *TCP23* sequence and the PCR product obtained from the forward gene-specific primer and the T-DNA left-border primer. Insertion point 1 was narrowed down to 2bp (boxed sequence) and the second insertion point was determined to within 2bp (boxed sequence).

5.2.4 Expression levels

RNA expression levels of the T-DNA insertion mutants are analysed using reverse transcription-polymerase chain reaction (RT-PCR) and compared to wild-type plants (figure 5.9 and primers listed in Appendix A1). A minus-reverse transcriptase (-RT) control is added to check for any genomic DNA contamination in the sample. The double insertion lines have been included to rule out any interactions between the genes. Figure 5.8 shows that the *tcp23* insertion mutant could be a null-allele of *TCP23*. There is no transcript level detected in the RT-PCR, this result is confirmed in the *tcp8-1tcp23* double insertion mutant. The *TCP8* and *TCP22* insertion lines have transcription levels that appear similar to the wild-type line. The -RT controls were all negative indicating that there was no DNA contamination in any of the RNA samples.

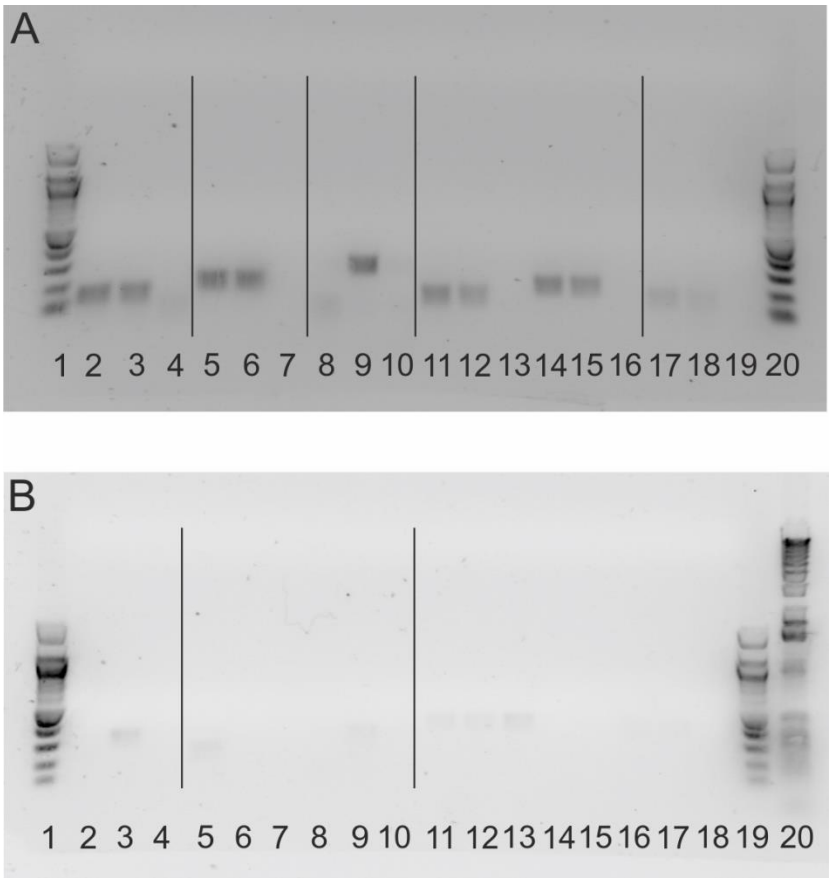

Figure 5.9: RT-PCR estimating the RNA expression levels of the single and double TCP T-DNA insertion mutants compared to wild-type. For each mutant the RNA expression for

the affected gene is analysed using three samples (adjacent lanes on the gel), mutant RNA sample, a wild-type RNA sample and a -RT control. For the double mutant each affected *TCP* gene was analysed separately (6 lanes per double mutant). Lane A1, A20, B1, B19, B20: DNA ladder (B19 Ladder with erroneous molecular weight), A2 = *tcp8-1*, A3 = wild-type plant, A4 = genomic control for tcp8; A5-A7 = *tcp22;* A8-A10 = *tcp23*; A11-A13 = *tcp8-1tcp22* (*TCP8* expression); A14-A16 = *tcp8-1tcp22* (*TCP22* expression); A17-A19 = *tcp8-1tcp23* (*TCP8* expression); B2-B4 = *tcp8-1tcp23* (*TCP23* expression); B5-B7 = *tcp22tcp23* (*TCP22* expression); B8-B10 = *tcp22tcp23* (*TCP23* expression); B11-B18 = internal standard using transcript level of *TUB9*.

5.2.5 Discussion

5.2.5.1 T-DNA insertion lines

T-DNA or Transfer-DNA insertion mutants are a common and highly effective method of linking genotype to phenotype. The Salk Institute Genome Analysis Laboratory (SIGnAL - http://signal.salk.edu/) produced a Sequence-Indexed Library of Insertion Mutations in the *Arabidopsis* Genome. SALK lines are T-DNA insertion lines, whose insertion sites have been analysed by the SALK institute using a high-through put sequencing method. The T-DNA transformed plants are derived from the Alonso/Crosby/Ecker collection (Alonso et al. 2003). The T-DNA insertion mutants and their related DNA sequence data can be located via a web accessible graphical interface, the SIGnAl Gene Mapping Tool (http://signal.salk.edu/cgi-bin/tdnaexpress). Seed stock can be ordered from NASC (The European Arabidopsis Stock Centre - http://arabidopsis.info/) or ABRC (Arabidopsis Biological Resource Center - https://abrc.osu.edu/). A second large T-DNA insertion collection was generated by Syngenta and referred to as SAIL Lines (Syngenta Arabidopsis Insertion Library) (Session et al. 2002). SAIL lines are also searchable through the SIGnAl T-DNA Express (http://signal.salk.edu/cgi-bin/tdnaexpress). When choosing suitable T-DNA insertion lines preference is given to lines with a presumptive insertion site in the exon of the gene of interest. It should be noted that the insertion point provided by the web browser is approximate (with 300bp either side). Insertion into the exon of a gene has the greatest likelihood of

resulting in a knockout mutant, which is preferable for the purpose of this study since we expect the phenotype to be subtle. Due to the high level of redundancy in this gene family a knockout mutant is unlikely to be lethal. If an insertion line in the exon is not available the preference is for the insertion to be before the start codon rather than after. An insertion in the promoter region of the 5'UTR will more likely cause a knockdown rather than a knockout mutant, but is still likely to have a significant effect on the activity of the gene. In some cases T-DNA insertions in the promoter region can change the expression pattern of the downstream gene or lead to an up-regulation of the gene (Wang 2008).

5.2.5.2 Isolating homozygous mutants

The isolation of homozygous T-DNA insertion lines took significantly longer than expected. The PCR results were at time contradictory requiring additional confirmation steps to be carried out. In the case of *tcp21* a second set of primers was designed to try and alleviate the problem. However, in the end the additional time spent on this task has led to the decision to abandon the attempt to isolate homozygous *tcp21* (N643403) plants. This line is believed to carry a single forward insert, though this was not confirmed by sequencing and the exact insertion point was not determined.

Resolution of ambiguous insertion points could potentially be resolved by sequencing multiple individuals. If the exact insertion point is undetermined due to gaps in the alignment sequencing multiple individuals would allow the creation of a consensus sequence to exclude sequencing errors. The T-DNA insertion point results outlined above are consistent with the literature that T-DNA inserts as concatamers and produce deletions in the majority of cases (Wang 2008). None of the deletions seen in the TCP T-DNA insertion lines are considered large.

The RT-PCR shows no remaining expression for *tcp23,* which could indicate a null mutant, for *tcp8-1* and *tcp22* transcript levels comparable to

wild-type were detected. When interpreting the results of the RT-PCR it should be considered that even if mRNA is transcribed, the T-DNA sequence may contain stop codons, thereby resulting in termination of translation (Krysan et al. 1999). Premature termination of translation can result in a non-functional truncated protein. Transcript levels may not be representative of protein levels and can be dependent on the insertion point. Wang et al. 2008 estimated in a review that in 90% of the cases a T-DNA insertion in the coding region of a gene results in a knockout mutant, with the T-DNA insertion site upstream of the start codon this figure drops to 25% but an additional 67% of cases result in a knockdown. Even though these figures are potentially biased towards knockout and knockdown lines, stemming from published work, it is nonetheless sufficient reason to further investigate the *TCP8* and *TCP22* T-DNA insertion mutants regardless of the results of the RT-PCR.

To clean up the mutant lines each homozygous line should be backcrossed to the wild-type line a minimum of 4, and up to 10 times to eliminate any unlinked secondary insertions. The analyses in the upcoming chapters have been carried out with the homozygous un-backcrossed lines. To publish this work the results need to be confirmed with the backcrossed mutants. Alternatively a co-segregation analysis could confirm that the observed phenotype is linked to the T-DNA insertion in the TCP gene of interest.

5.2.5.3 Further work

If in future experiments an attempt to construct the triple mutants will be made the most efficient way for this to be accomplished would be by crossing specific double mutants (*tcp22tcp8-2* x *tcp8-2tcp23*; *tcp8-1tcp22* x *tcp8-1tcp23*). The different antibiotic resistance markers and the position of the TCP genes on the chromosome should be taken into account in an attempt to maximize the percentage of triple mutants. The assumption would be that the triple mutant could be identified by a visual screening due to the more pronounced phenotype in the multiple mutant. This theory is

supported by the stronger phenotype exhibited by the *tcp14tcp15* mutant and the observations of Kieffer et al. (2011) when fusing *TCP14* to the short EAR motif (*TCP14:SRDX*) to create a dominant-negative (phenotype also enhanced). A primary visual screening could be performed, followed by a secondary confirmation step using PCR screening. If this strategy is successful different triple mutant combinations could be attempted including *TCP14*, *TCP15* and *TCP21*.

5.3 Leaf size and shape analysis for *TCP8, TCP22* and *TCP23*

In the previous sections the isolation of homozygous T-DNA insertion mutant for *TCP8, TCP22* and *TCP23,* and the creation of double mutants was described. The exact T-DNA insertion points were determined, and mRNA expression levels analysed. The following chapter will outline the phenotypic characterization of the mutant alleles *tcp8-1*, *tcp22*, *tcp23* and the double mutant alleles *tcp8-1tcp22*, *tcp8-1tcp23* and *tcp22tcp23*. The phenotypic characterization will focus on the quantitative imaging analysis of leaf shape and size using LeafAnalyser. We will use the stable reference set developed from the *Arabidopsis* leaf size and shape library to quantify differences in leaf size and shape between the isolated TCP T-DNA insertion mutants. To gain understanding of the functional role of class I TCP genes we will compare a possible leaf phenotype to wild-type plants and the previously analysed closely related genes *TCP14* and *TCP15.* Previous morphometric analysis revealed that *TCP14* and *TCP15* modulate leaf shape. When combined with work carried out by Kieffer et al. 2011, it suggests that *TCP14* and *TCP15* repress cell proliferation in leaf tissue.

5.3.1 Quantitative analysis of modification to leaf shape in putative TCP mutants

The high number of samples we are analysing in this experiment allows us to draw conclusions based on the mean leaf for each line as well compare each individual leaf between the lines. A total of 1459 leaves from 167 plants were scanned and processed using LeafAnalyser to determine whether there are any differences in leaf shape and size between wild-type, *tcp8-1, tcp22, tcp23, tcp8-1tcp22, tcp8-1tcp23* and *tcp22tcp23*. Standardised PC scores were generated for each leaf by applying the eigensystem from the *Arabidopsis* reference library to the *TCP* leaf-point models. On the basis of these PC scores the mean PC values for each line are calculated and compared. Mean leaves were produced from LeafPredictor as previously described.

A Kruskal-Wallis test was used to determine whether any of the PCs are significantly different between the lines. The analysis reveals that there are significant differences in leaf size ($p<0.05$) and leaf shape ($p<0.001$) between wild-type, *tcp8-1, tcp22, tcp23, tcp8-1tcp22, tcp8-1tcp23* and *tcp22tcp23*; depicted by PC1 and PC2. The lines showed no significant differences along PC3 and PC4, revealing that there is no change in leaf curvature and leaf aspect ratio (figure 5.10).

A pairwise comparison was carried out for PC1 and PC2 to determine the differences between the lines. The Wilcoxon test reveals that there is a significant difference in PC1 between wild-type and *tcp23* ($p<0.05$); all other lines including *tcp8tcp23* and *tcp22tcp23* do not significantly differ from the wild type line. No significant difference is found between *tcp23* and any of the other TCP lines. Along PC1 *tcp23* has a shift to a higher PC1 value indicating that the line has slightly larger leaf size compared to wild-type plants.

The situation is more complex when we examine the differences along PC2. The Wilcoxon test reveals that along PC2 *tcp8-1, tcp22, tcp23, tcp8-1tcp22, tcp8-1tcp23* and *tcp22tcp23* significantly differ from the wild-type line ($p<0.05$ or $P<0.001$). There is no difference between the single mutants *tcp8-1*, *tcp22* and *tcp23*, but *tcp8-1* significantly differs from *tcp8-1tcp22* and *tcp8-1tcp23* ($p<0.05$), *tcp22* is significantly different from *tcp8-1tcp22* $p<0.001$) and *tcp8-1tcp23* ($p<0.05$), as is *tcp23* to *tcp8-1tcp22* and *tcp8-1tcp23* ($p<0.05$). The double mutants *tcp8-1tcp22, tcp8-1tcp23* and *tcp22tcp23* do not show any significant differences (figure 5.10 and table 5.3).

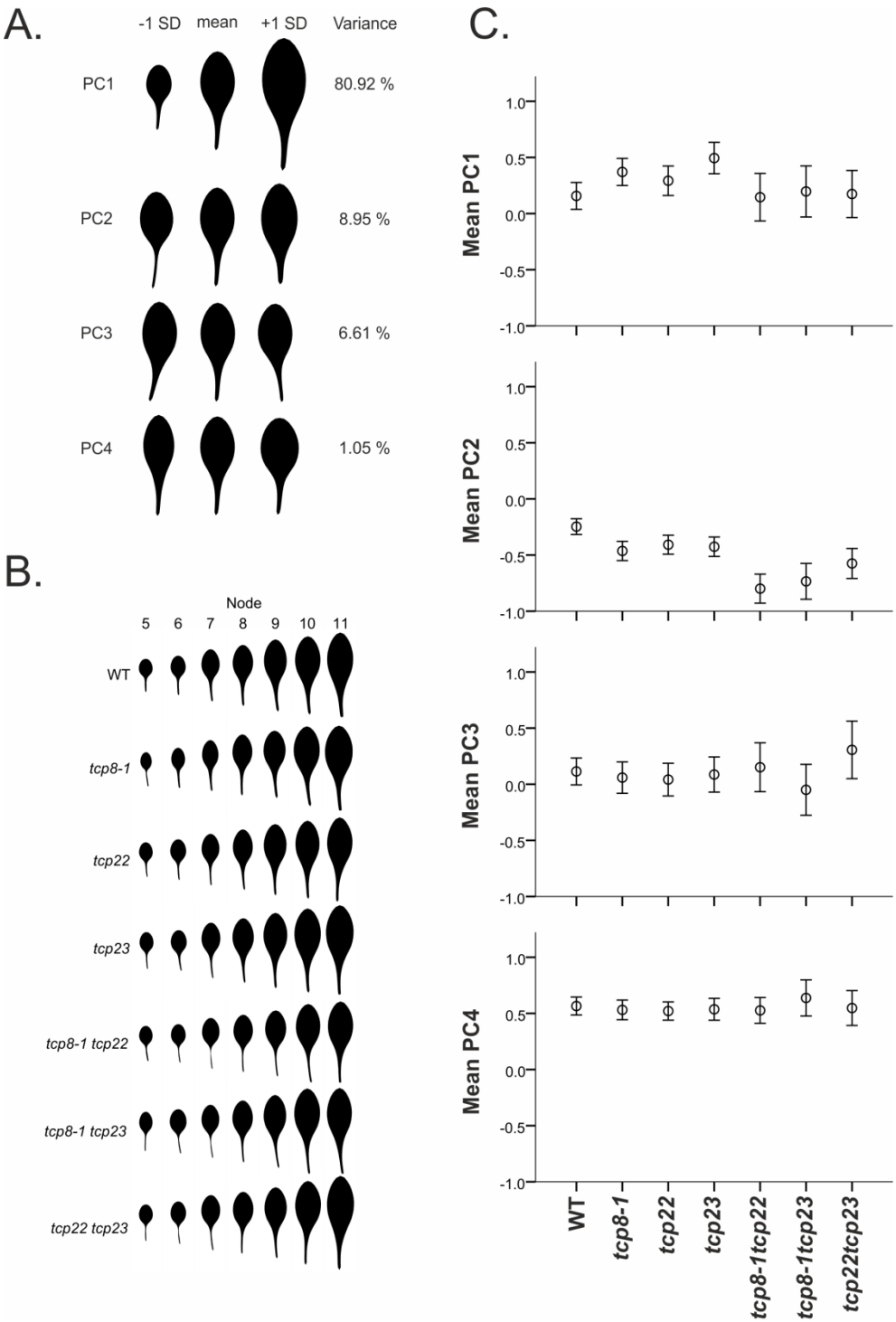

Figure 5.10: Leaf shape and size analysis for wild-type, *tcp8-1*, *tcp22*, *tcp23*, *tcp8-1tcp22*, *tcp8-1tcp23* and *tcp22tcp23* plants.

A. Leaf size and shape according to variation along the first four PCs for the *Arabidopsis* stable reference set of 1050 leaves.

B. Comparison of leaf point models for nodes 5–11 for WT, *tcp8-1*, *tcp22*, *tcp23*, *tcp8-1tcp22*, *tcp8-1tcp23* and *tcp22tcp23* plants. The mean node PC score is calculated from mean PC1, PC2, PC3 and PC4 node scores, visualising the mean size and shape of the

leaves for each line. These leaves were constructed using LeafPredictor and the eigensystem of the reference set.
C. Mean PC scores for all leaves for wild-type, *tcp8-1, tcp22, tcp23, tcp8-1tcp22, tcp8-1tcp23* and *tcp22tcp23*. Error bars represents 95% confidence intervals. Wilcoxon Rank Sum test was used to determine the differences between the lines (table 5.3).

PC2	WT	*tcp8-1*	*tcp22*	*tcp23*	*tcp8-1tcp22*	*tcp8-1tcp23*
tcp8-1	0.00105	-	-	-	-	-
tcp22	0.00590	1.00000	-	-	-	-
tcp23	0.00108	1.00000	1.00000	-	-	-
tcp8-1tcp22	2.1E-09	0.00393	0.00030	0.00115	-	-
tcp8-1tcp23	1.3E-06	0.04439	0.00590	0.01659	1.00000	-
tcp22tcp23	0.00025	0.89676	0.44153	0.89676	0.10850	0.44153

P < 0.05
P < 0.001

Table 5.3: Pairwise comparisons between wild-type, *tcp8-1, tcp22, tcp23, tcp8-1tcp22, tcp8-1tcp23* and *tcp22tcp23* using Wilcoxon rank sum test.

5.3.2 Discussion

5.3.2.1 Biological function of *TCP8*, *TCP22* and *TCP23*

It was concluded in a previous chapter that *TCP14* and *TCP15* repress cell proliferation in the leaf and thereby modulate leaf shape. To investigate the hypothesis that leaf size and shape are controlled by the interplay of several *TCP* genes we have isolated homozygous insertion mutants for the related *TCP8*, *TCP22* and *TCP23* genes and analysed their leaf size and shape. We have quantified the variation in leaf size and shape seen in these mutants and compared mean leaves between lines to describe differences between the rosettes.

Compared to the wild-type line *tcp23* has slightly larger leaves, suggesting that *TCP23* might have a negative effect on cell proliferation (or cell expansion) similar to *TCP14* and *TCP15*. However, this increase in leaf size

is not visible in the mean leaves for either *tcp8-1tcp23* or *tcp22tcp23* (or *tcp8-1tcp22*). It is however possible that there is a difference between the individual leaves that is not detected in the mean leaves. Further investigation will be necessary to make this determination. If this is not the case it is puzzling why a size effect is visible in the single mutant but actively compensated by an additional mutation in a closely related gene. This result might lead us to believe that *TCP8* and *TCP22* could work redundantly to promote cell proliferation in leaves, yet *tcp8-1tcp22* does not show a corresponding decrease in leaf size as we might expect if this was the case. A co-segregation analysis should be conducted to confirm that the observed phenotype is linked to the mutation.

The single mutant lines have a shift towards a lower PC2 value compared to the wild-type line, resulting in a leaf that is rounder, more compact and has a narrower, longer petiole. The extent of the negative shift appears to be similar for *tcp8-1*, *tcp22*, and *tcp23*. The blade defect is more pronounced for the double mutants; there is a slight difference in the mean PC2 scores of the double mutants (score is lower when *TCP8* is disrupted) but the difference is not significant. The analysis of the double mutant suggests redundant functions for *TCP8*, *TCP22* and *TCP23*, though *tcp23* showed the slight increase in leaf size in the single mutant.

5.3.2.2 Do *TCP8, TCP22* and *TCP23* act antagonistically with *TCP14* and *TCP15*?

When we compare the effects of *TCP8, TCP22* and *TCP23* on leaf shape and size to the proposed role of *TCP14* and *TCP15* an interesting pattern emerges. Initial experiments suggest that *TCP8, TCP22* and *TCP23* could act to some extend antagonistically to *TCP14* and *TCP15*. We would need to analyse double mutant combinations with *TCP14* and *TCP15* to draw more certain conclusion. Mutations in *TCP14* and *TCP15* resulted in a shift to a higher PC2 value (and lower PC4 value) yielding a leaf that is broader towards the base and has a broader and shorter petiole. This blade defect is

more pronounced in the double mutant. In contrast to *TCP14* and *TCP15*, disruption of *TCP8, TCP22* and *TCP23* does not change the leaf aspect ratio (figure 5.10).

To be able to fully interpret the results of the morphometric analysis and the biological significance of the seemingly opposite action of *TCP8, TCP22* and *TCP23* compared to *TCP14* and *TCP15* the expression patterns of *TCP8, TCP22* and *TCP23* need to be examined. More in depth phenotypic characterization of *tcp8-1, tcp22, tcp23, tcp8-1tcp22, tcp8-1tcp23* and *tcp22tcp23* may allow us to make a better assessment about the functional role of *TCP8, TCP22* and *TCP23*, and let us determine in how far the *TCP14*-like sub-clade has a redundant function in *Arabidopsis* organ development.

5.4 Phenotypic characterization of *TCP8, TCP22* and *TCP23*

We have previously conducted a morphometric analysis of the leaf shape and size of the *TCP8, TCP14, TCP15, TCP22* and *TCP23* mutants. To aid the biological interpretation of the analysis of *tcp8-1, tcp22* and *tcp23* and gain more insight in the functional role of *TCP8, TCP22* and *TCP23* we want to determine their spatial and temporal expression patterns. To conclude the results section of this manuscript additional phenotypic characterization of *TCP8, TCP22* and *TCP23* was carried out focussing on root architecture and epidermal cell organisation. During the processing of leaf material a possible reduction of root growth was observed for some of the TCP insertion mutants. A root growth assay was developed to investigate the possibility of a root growth phenotype in the TCP insertion mutants. We chose to investigate the epidermal cell organisation because it is possible for changes at the epidermal cell level to affect the final leaf shape and size.

5.4.1 *Analysing the expression patterns of* TCP8, TCP22 *and* TCP23

Kieffer et al. 2011 reported that they were unsuccessful in visualizing the expression of *TCP14* and *TCP15* by in situ hybridization. Knowing that our genes of interest are closely related and one of the possible reasons for the failure of the in situ hybridization is the low level of expression of TCP genes, it was decided to construct promoter-GUS constructs; lines expressing translational fusions under the control of the native TCP promoter (e.g *pTCP8:TCP8:GUS*), as an alternative strategy. To ensure that the full promoter region was included a large region upstream of the *TCP8*, *TCP22* and *TCP23* was selected for the promoter construct.

5.4.1.1 Construction of *pTCP8:TCP8:GUS* and *pTCP22:TCP22:GUS*

The promoter region of *TCP8* (+/- 2kb) and *TCP22* (+/- 2.5 kb) have been cloned using error-free PCR and ligated into the entry vector (pENTR™/D-TOPO®) by TOPO® cloning reaction (Appendix 4). The entry vector was sent for sequencing and revealed that the promoter region was cloned and ligated successfully into the vector (Appendix 3). The expression clone was created by the subsequent Gateway® LR recombination reaction using a destination vector (pMDC163) containing the GUS gene (Appendix 4). *E. coli* and *A. tumefaciens* transformation were completed prior to setting up the *Arabidopsis* transformation and outlined in the Material and Methods section of this thesis (Chapter 2).

Arabidopsis wild-type plants were transformed using the floral dip method of transformation by immersion of inflorescences in a suspension of *Agrobacterium* (method adapted from Clough and Bent 1998). Plants were allowed to set seed and subsequently placed on selective media (Hygromycin 25µg/ml). No positive transformants were recovered; the method developed by Harrison et al. (2006) was used to select positive transformants.

5.4.1.2 Construction of pTCP23:TCP23:GUS

The attempt to create an entry clone containing the *TCP23* promoter region was unsuccessful. The *TCP23* promoter primer sets, tested with BLAST to avoid non-specific binding, repeatedly yielded a multitude of bands. A new set of primers was designed with more stringent conditions. Efforts were made to optimize the PCR conditions to limit non-specific binding, all stock solutions were replaced in case of contamination, and a new high fidelity DNA polymerase (Phusion™, NEB) used to reduce extension time. The second primer set also yielded a multitude of bands or the reaction failed completely.

A touchdown PCR adapted from Hecker and Roux (1996) was designed to reduce non-specific binding by bracketing the annealing temperature. The primer will anneal at the highest possible temperature reducing the potential of non-specific binding. Towards the end of the programme the efficiency of the amplification should be increased due to lowering of the annealing temperature. At this point of the PCR the sequence of interest should have amplified to such a degree that it will outcompete any non-specific binding. The reaction did not yield any amplification.

The error-free PCR reaction was repeated in a 100µl reaction (10 times 10µl) in an attempt to gel purify the band presumed to correspond to the amplicon. The reaction was analysed on gel electrophoresis and showed a single band of the expected length. The TOPO® cloning reaction was carried out and positive colonies tested by colony PCR (20 colonies). Repeated colony PCR showed no successful amplification.

An improvised Hot Start & Enrichment error-free PCR method was tried, the initial amplification appeared successful but the enrichment step did not yield a higher level of amplification. The PCR product from the initial amplification step (PCR product 1) was subjected to the TOPO® cloning reaction. To verify the cloning reaction a colony PCR using one primer from the plasmid and one internal promoter primer was performed, and PCR

products visualised using gel electrophoresis. The gel did not yield any bands for the colony samples tested (15 colonies tested). To validate the result 6 colonies were used to inoculate 4ml LB cultures and plasmid DNA was extracted. Three separate restriction enzyme digestions (2 double, one single digestion) were set up and visualised using gel electrophoresis. All 6 samples showed identical restriction enzyme profiles but the resulting bands did not correspond to what we would expect if the promoter region was successfully inserted in the vector, nor did they correspond to the empty vector. In an attempt to figure out what was inserted in the vector the plasmid sample with the highest concentration was sent for sequencing; the sequencing reaction failed.

In light of the time constraints at this stage of the project and the persistent failure to sequence the *TCP23* promoter the decision was made to abandon the construction of *pTCP23:TCP23:GUS* construct in favour of focussing on the *TCP8* and *TCP22* promoter-GUS constructs.

5.4.2 Spatial and temporal patterns of cell division

In order to assess whether *TCP8, TCP22* and *TCP23* are involved in cell division it was decided to analyse and compare the spatial and temporal patterns of cell division in developing leaves by using the *cyc1At::GUS* reporter construct (Donnelly *et al.* 1999).

The homozygous T-DNA insertion lines *tcp8-1, tcp14, tcp15, tcp22* and *tcp23* were crossed to the *cyc1At::GUS* reporter line. It was not possible to screen for the presence of the GUS construct based on antibiotic resistance. The antibiotic resistance gene was likely silenced over successive generation of growth. Detection of homozygous T-DNA insertions was carried out by PCR (Appendix 2). A preliminary experiment was conducted to ascertain whether the insertion lines (*tcp8, tcp22* and *tcp23*) carried the GUS construct and to familiarize the author with the histochemical staining protocol. The original line carrying the GUS construct was used as a

positive control. For each line six plants were screened for the presence of the GUS gene (figure 5.11). The positive control plants all exhibited staining in the shoot apical meristem or developing leaf tissue, it is hard to determine exactly where the staining is, as well as the root tips (main and lateral roots). Half the *tcp23cyc1At::GUS* plants and 60% of the *tcp22cyc1At::GUS* plants displayed staining in the shoot apical meristem (or developing leaf tissue) and the roots. Initial assessment made it appear that the staining was stronger for the insertion lines compared to the control. For *tcp8cyc1At::GUS* 20% of the plants showed faint but clear staining, 20% where negative and the remaining 20% are ambiguous.

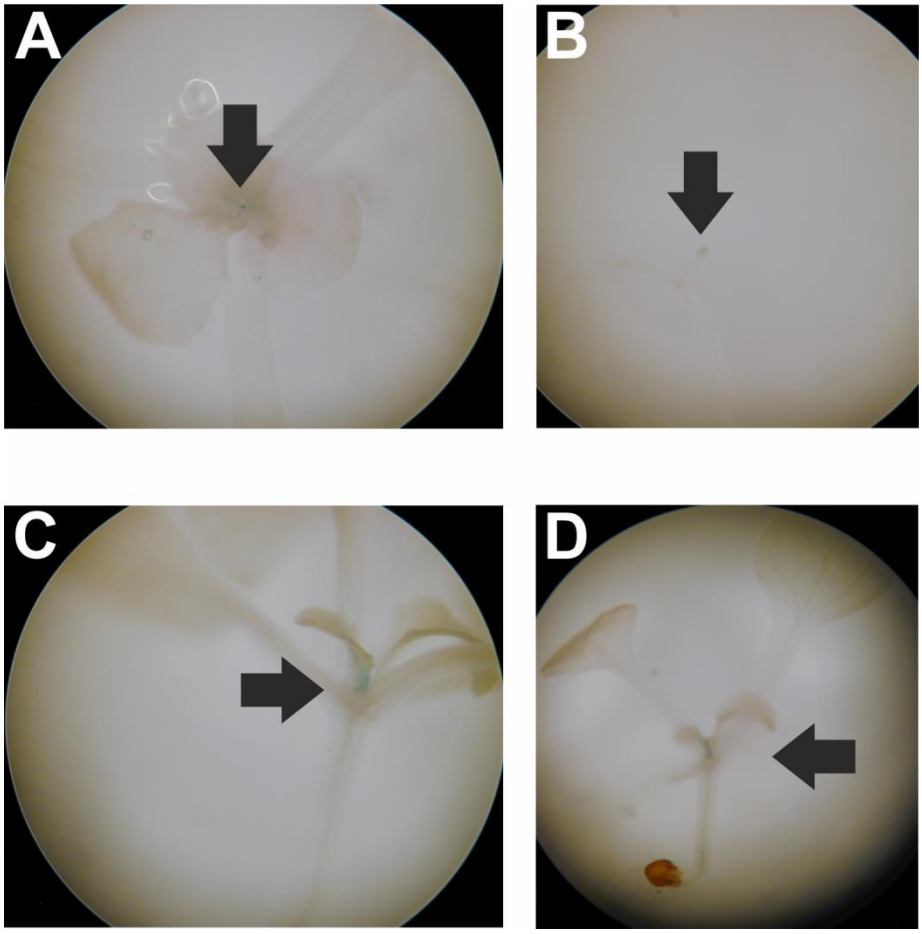

Figure 5.11: Analysing the spatial and temporal patterns of cell division in *tcp8-1*, *tcp14-4*, *tcp15-3*, *tcp22* and tcp23 lines carrying the *cyc1At::GUS* reporter line. A, B meristematic or developing leaf tissue and lateral root staining in the positive control. C, D meristematic or developing leaf tissue staining in *tcp22cyc1At::GUS* (C) and *tcp23cyc1At::GUS* (D).

The *cyc1At::GUS* reporter line was crossed to *tcp14-4* and *tcp15-3* and the homozygous insertion lines isolated but presence of the construct has as yet not been verified.

5.4.3 Epidermal cell analysis

Small changes in mature leaf size and shape may be due to quite fundamental differences in the organisation at the cellular level. Flowering plants are known to be able to compensate for certain types of cell proliferation defects by triggering excessive cell expansion. The compensation phenomenon is thought to be part of the plants ability to regulate organ size (Horiguchi and Tsukaya, 2011). The following experiment was set up to yield a detailed characterisation of cell size and shape, to correlate the findings with the observed changes in leaf size and shape.

There are multiple methods to visualise epidermal cell organisation; we tested two methods, a gel imprint method described by Horiguchi et al., 2006 and a method based on leaf bleaching (kindly provided by Dr. S. Bougourd). Though fast and technically straight forward to implement, the absence of a dyeing agent in the agarose imprinting method results in low contrast samples hampering subsequent microscope imaging (Nikon optiphot axiocam).

The second method strips the cuticle off the leaf surface and subsequently stains the exposed epidermal cell tissue with methylene blue. The protocol takes significantly longer than the first method tested (approximately 5 days) but produces epidermal cell images of good quality for subsequent downstream analysis. For each line 30 cells were measured (cells clustered together in the top quarter of the leaf blade) from 2 samples at the adaxial and abaxial side (adaxial N=60 per line, abaxial N=60 per line).

Exploration of the data revealed that the data had a non-normal distribution and was therefore analysed using non-parametric tests. For each cell the

area, perimeter and circularity was measured. The calculated value of area/perimeter was used as an indicator of the cell shape. The adaxial and abaxial cell morphology has been analysed separately.

5.4.3.1 Adaxial epidermal cell morphology

On the adaxial side of the leaf the Kruskal-Wallis revealed a significant difference between the lines for the cell area, perimeter, cell shape (area/perimeter) ($p<0.001$) and circularity ($P<0.05$) (figure 5.12 and figure 5.13). A pairwise comparison was used to determine the differences between the wild-type, *tcp14-4*, *tcp15-3*, *tcp14-4tcp15-3*, *tcp8-1*, *tcp22*, *tcp23*, *tcp8-1tcp22*, *tcp8-1tcp23*, and *tcp22tcp23* lines.

The data trend is somewhat consistent across the area, perimeter and cell shape, the *tcp14-4*, *tcp15-3* and *tcp14-4tcp15-3* lines form a separated cluster. There is a significant difference between *tcp14-4* and *tcp8-1tcp22* ($p<0.05$), as well as between *tcp14-4tcp15-3* and *tcp8-1*, *tcp22* ($p<0.05$), *tcp8-1tcp22* ($p<0.001$) and *tcp8-1tcp23* ($p<0.05$). For the cell perimeter there is a significant difference between *tcp14-4tcp15-3* and *tcp8-1* and *tcp8-1tcp22* ($p<0.05$). As on the abaxial side the differences are most pronounced when comparing the cell shape. The difference is significant between the wild-type lines and *tcp14-4*, *tcp15-3* ($p<0.05$) and *tcp14-4tcp15-3* ($p<0.001$) (table 5.4). With the exception of the difference between *tcp15-3* and *tcp8-1* the differences between *tcp14-4*, *tcp15-3* and *tcp14-4tcp15-3* and the other TCP lines are significantly. On the adaxial side the Kruskal-Wallis test showed that there was a significant difference between the lines for cell circularity, however, the pairwise comparison reveals that these differences are not significant.

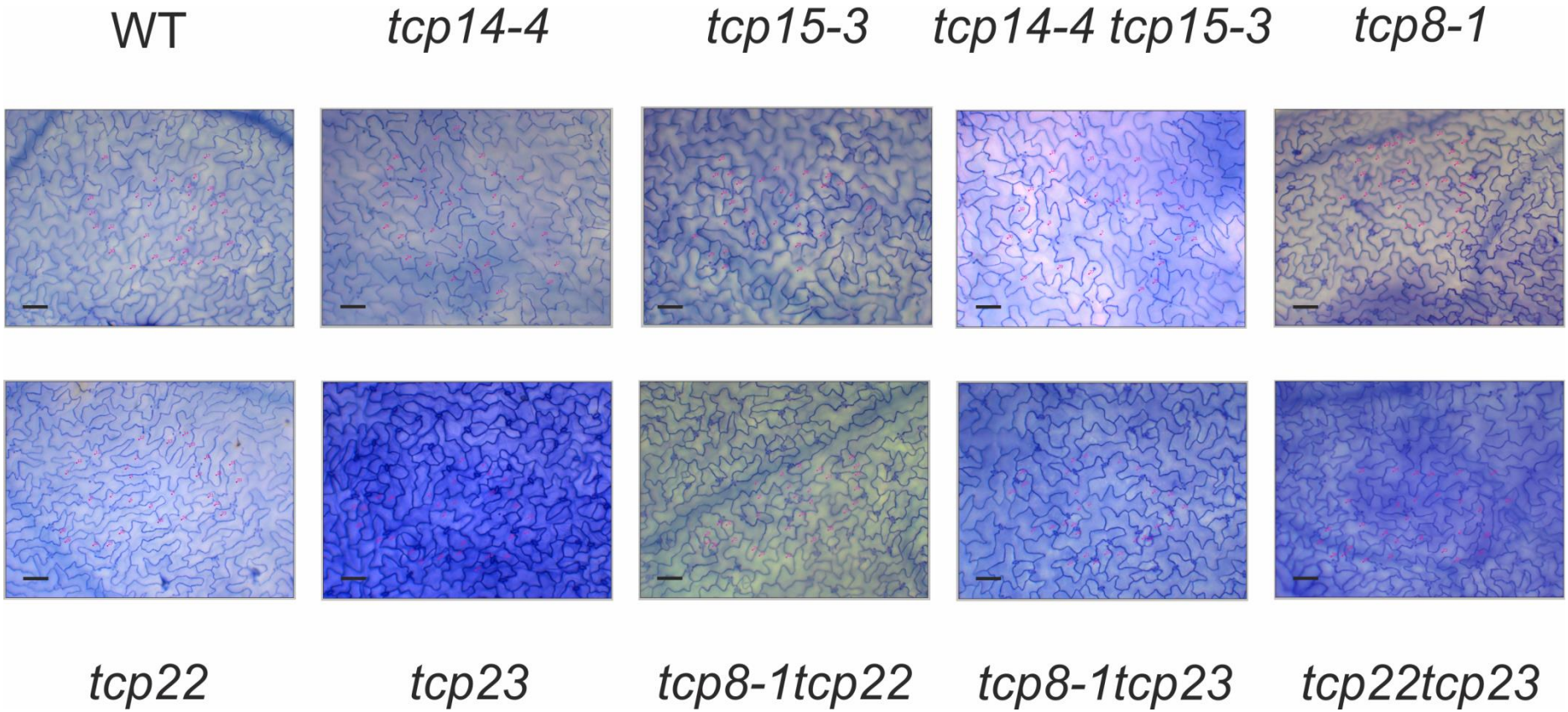

Figure 5.12: Adaxial epidermal cells for wild-type, *tcp14-4*, *tcp15-3*, *tcp14-4tcp15-3*, *tcp8-1*, *tcp22*, *tcp23*, *tcp8-1tcp22*, *tcp8-1tcp23*, and *tcp22tcp23* plants. Scale bar = 50 μm

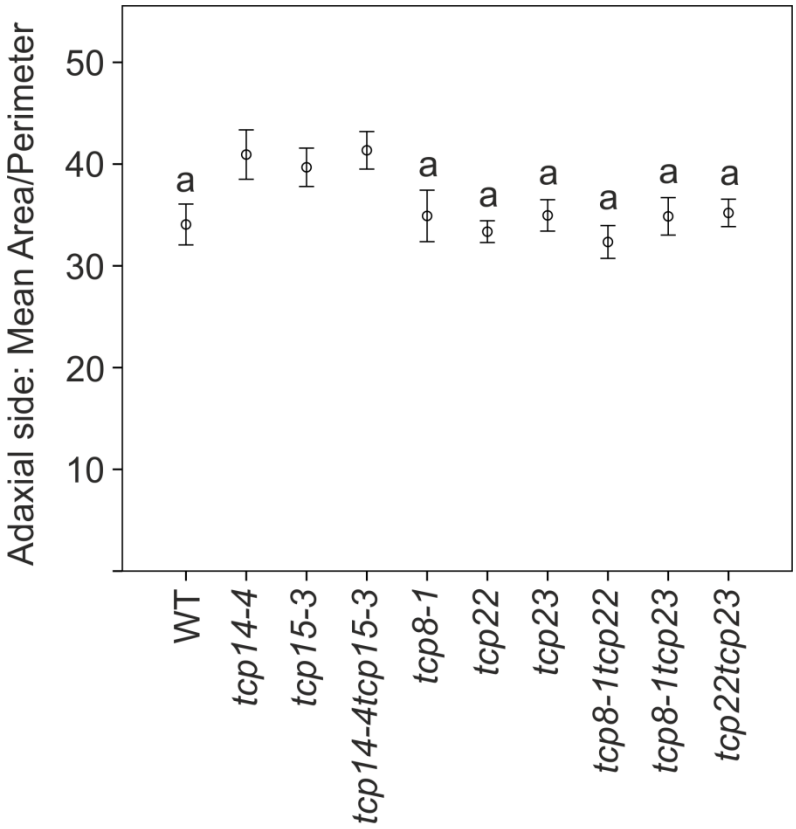

Figure 5.13: Adaxial epidermal cell analysis of wild-type, *tcp14-4*, *tcp15-3*, *tcp14-4tcp15-3*, *tcp8-1*, *tcp22*, *tcp23*, *tcp8-1tcp22*, *tcp8-1tcp23*, and *tcp22tcp23* plants. Mean area / perimeter of the adaxial epidermal leaf cells of wild-type, *tcp14-4*, *tcp15-3*, *tcp14-4tcp15-3*, *tcp8-1*, *tcp22*, *tcp23*, *tcp8-1tcp22*, *tcp8-1tcp23*, *tcp22tcp23*. Error bars represent 95% confidence intervals. The letter 'a' indicates that there is no significant difference between genotypes.

Adaxial Area/Perimeter	WT	*tcp14-4*	*tcp15-3*	*tcp14-4tcp15-3*	*tcp8-1*	*tcp22*	*tcp23*	*tcp8-1tcp22*	*tcp8-1tcp23*
tcp14-4	0.00364	-	-	-	-	-	-	-	-
tcp15-3	0.00393	1.00000	-	-	-	-	-	-	-
tcp14-4tcp15-3	5.9e-05	1.00000	1.00000	-	-	-	-	-	-
tcp8-1	1.00000	0.03997	0.17313	0.00519	-	-	-	-	-
tcp22	1.00000	3.5e-05	1.0e-05	5.6e-08	1.00000	-	-	-	-
tcp23	1.00000	0.00504	0.00393	4.1e-05	1.00000	0.63804	-	-	-
tcp8-1tcp22	1.00000	1.0e-05	4.0e-06	3.2e-08	1.00000	1.00000	0.52644	-	-
tcp8-1tcp23	1.00000	0.00973	0.01315	0.00024	1.00000	1.00000	1.00000	0.79789	-
tcp22tcp23	1.00000	0.00618	0.00395	4.1e-05	1.00000	0.58488	1.00000	0.22672	1.00000

p < 0.05
p < 0.001

Table 5.4: Adaxial epidermal cell analysis of wild-type, *tcp14-4*, *tcp15-3*, *tcp14-4tcp15-3*, *tcp8-1*, *tcp22*, *tcp23*, *tcp8-1tcp22*, *tcp8-1tcp23*, and *tcp22tcp23* plants. Pairwise comparison of the mean area / perimeter of the adaxial epidermal leaf cells of wild-type, *tcp14-4*, *tcp15-3*, *tcp14-4tcp15-3*, *tcp8-1*, *tcp22*, *tcp23*, *tcp8-1tcp22*, *tcp8-1tcp23*, *tcp22tcp23*.

5.4.3.2 Abaxial epidermal cell morphology

Kruskal-Wallis test was used to determine whether there is a significant difference between the lines based on the cell morphology parameters. On the abaxial side of the leaf there is a significant difference between the wild-type, *tcp14-4*, *tcp15-3*, *tcp14-4tcp15-3*, *tcp8-1*, *tcp22*, *tcp23*, *tcp8-1tcp22*, *tcp8-1tcp23*, and *tcp22tcp23* plant lines ($p < 0.001$). The area of the cells ($p<0.001$), perimeter ($p < 0.05$) and area/perimeter ($p<0.001$) are significantly different. There is no significant difference in the circularity of the cells on the abaxial side. A pairwise comparison was carried out to ascertain the differences between the lines. The mean area of the cells shows no significant differences between the wild-type plants and any of the mutant TCP lines. However, there is a significant difference between *tcp8-1* and *tcp14-4tcp15-3* ($p <0.001$), *tcp22tcp23* ($p <0.001$) and *tcp23* (p 0.05). For the abaxial perimeter only *tcp8-1* and *tcp14-4tcp15-3* are significantly different from each other.

The calculated value of area/perimeter was used as an indicator of the cell shape. Compared to the wild-type cells there is a significant difference in cell shape for *tcp8-1* ($p <0.001$), *tcp8-1tcp22* ($p <0.05$), and *tcp22tcp23* ($p<0.05$). Figure 5.14, figure 5.15 and table 5.5 display the full pair-wise comparison between the lines.

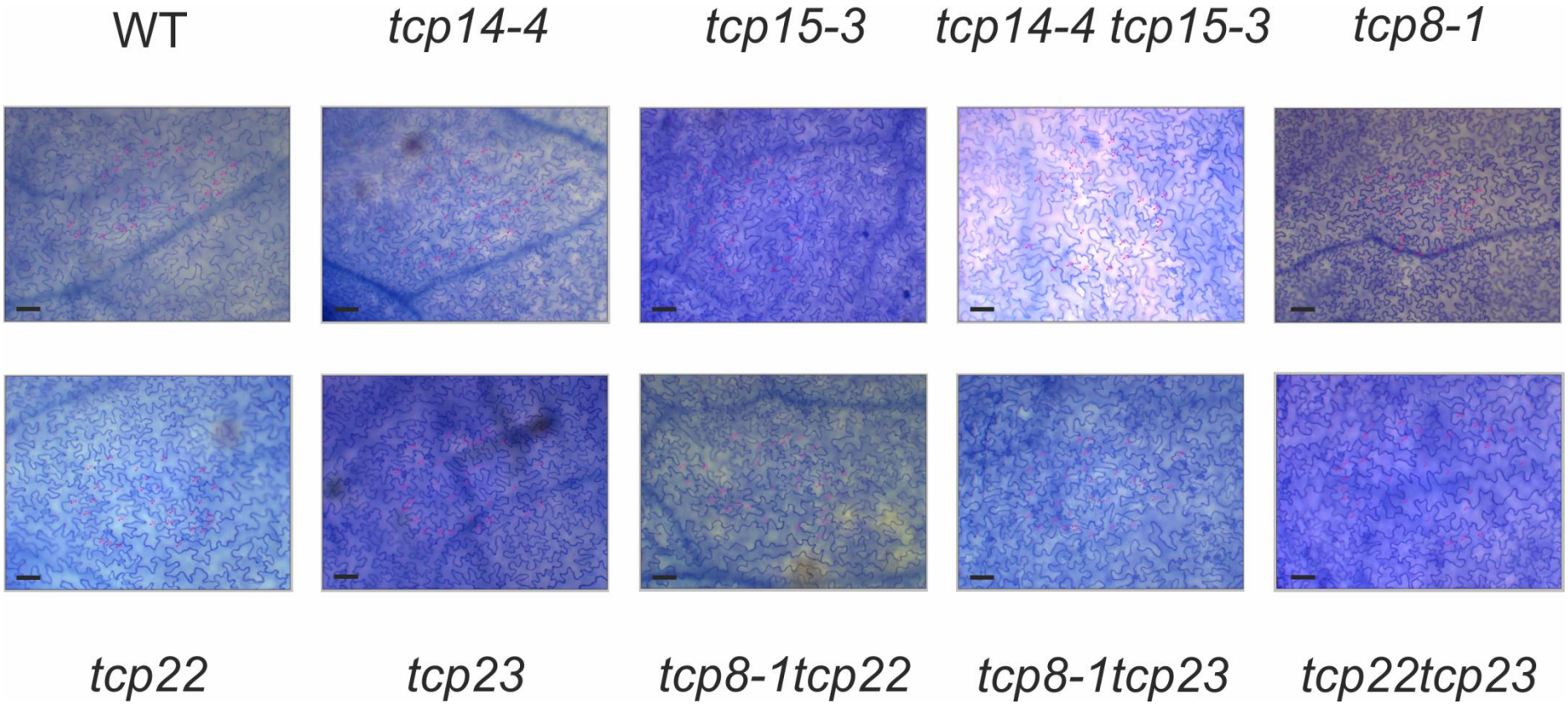

Figure 5.14: Abaxial epidermal cells for wild-type, *tcp14-4*, *tcp15-3*, *tcp14-4tcp15-3*, *tcp8-1*, *tcp22*, *tcp23*, *tcp8-1tcp22*, *tcp8-1tcp23*, and *tcp22tcp23* plants.

Scale bar = 50 μm

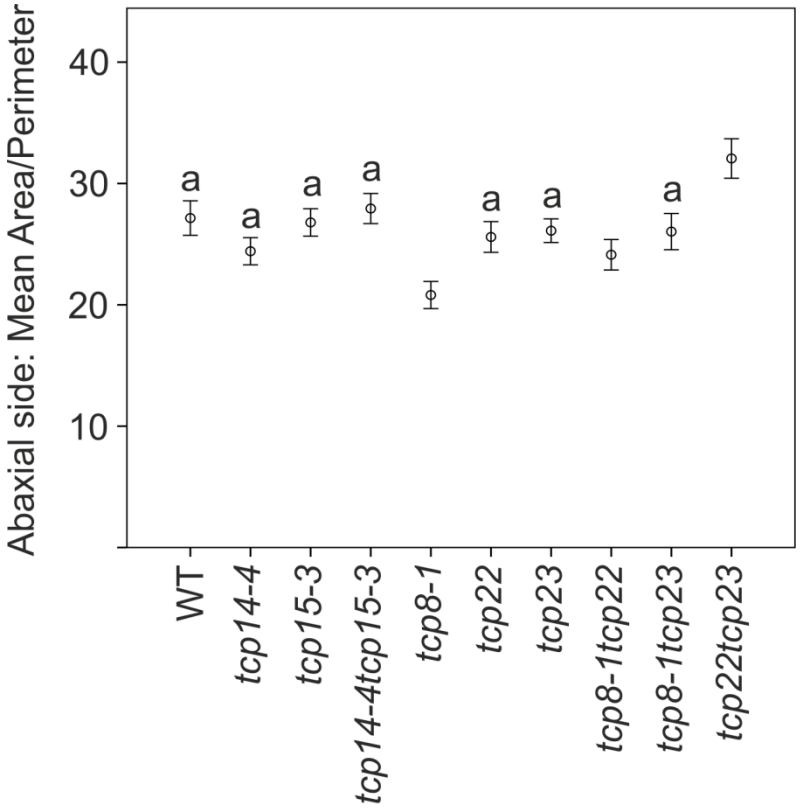

Figure 5.15: Abaxial epidermal cell analysis of wild-type, *tcp14-4*, *tcp15-3*, *tcp14-4tcp15-3*, *tcp8-1*, *tcp22*, *tcp23*, *tcp8-1tcp22*, *tcp8-1tcp23*, and *tcp22tcp23* plants. Mean area / perimeter of the abaxial epidermal leaf cells of wild-type, *tcp14-4*, *tcp15-3*, *tcp14-4tcp15-3*, *tcp8-1*, *tcp22*, *tcp23*, *tcp8-1tcp22*, *tcp8-1tcp23*, *tcp22tcp23*. Error bars represent 95% confidence intervals. The letter 'a' indicates that there is no significant difference between genotypes.

Abaxial Area/Perimeter	WT	*tcp14-4*	*tcp15-3*	*tcp14-4tcp15-3*	*tcp8-1*	*tcp22*	*tcp23*	*tcp8-1tcp22*	*tcp8-1tcp23*
tcp14-4	0.08237	-	-	-	-	-	-	-	-
tcp15-3	1.00000	0.11006	-	-	-	-	-	-	-
tcp14-4tcp15-3	1.00000	0.00406	1.00000	-	-	-	-	-	-
tcp8-1	1.1e-07	0.00230	7.3e-09	2.6e-10	-	-	-	-	-
tcp22	1.00000	1.00000	1.00000	0.22398	4.3e-05	-	-	-	-
tcp23	1.00000	0.42135	1.00000	1.00000	8.9e-08	1.00000	-	-	-
tcp8-1tcp22	0.03263	1.00000	0.01902	0.00091	0.00748	1.00000			-
tcp8-1tcp23	1.00000	1.00000	1.00000	1.00000	2.1e-05	1.00000	1.00000	0.48506	-
tcp22tcp23	0.00167	2.6e-09	0.00011	0.00767	3.4e-15	1.6e-06	2.6e-06	9.6e-10	0.00011

p < 0.05
p < 0.001

Table 5.5: Abaxial epidermal cell analysis of wild-type, *tcp14-4*, *tcp15-3*, *tcp14-4tcp15-3*, *tcp8-1*, *tcp22*, *tcp23*, *tcp8-1tcp22*, *tcp8-1tcp23*, and *tcp22tcp23* plants. Pairwise comparison of the mean area / perimeter of the abaxial epidermal leaf cells of wild-type, *tcp14-4*, *tcp15-3*, *tcp14-4tcp15-3*, *tcp8-1*, *tcp22*, *tcp23*, *tcp8-1tcp22*, *tcp8-1tcp23*, *tcp22tcp23*.

5.4.4 Preliminary root growth assays

During the processing of leaf material for RNA extraction a subjective variation in root growth was observed. Root growth of the *tcp8-1* and *tcp23* mutant lines appeared reduced. To ascertain whether these observations were localised occurrences due to varying growth conditions (e.g. edge of plate effect) or a phenotypic defect a preliminary root growth assay was set up. The preliminary experiment was statistically significant but highlighted the need for a more detailed analysis especially for *tcp8-1* and *tcp23.* Both single mutant lines and the *tcp8-1tcp23* double mutant were subjected to a more thorough analysis. 20 seedlings, divided over 2 square plates were placed horizontally in the plant growth room and photographed in regular intervals (figure 5.16).

The root length data was analysed using a one-way ANOVA and Tukey Range test (tested for normality using Shapiro-Wilk test). A significant difference in root length was detected between the lines ($p<0.001$) (figure 5.17). The mean wild-type root length is significantly longer than the *tcp8-1*, *tcp23*, and *tcp8-1tcp23* mean root length ($p<0.001$). There are no significant differences between the mutant lines.

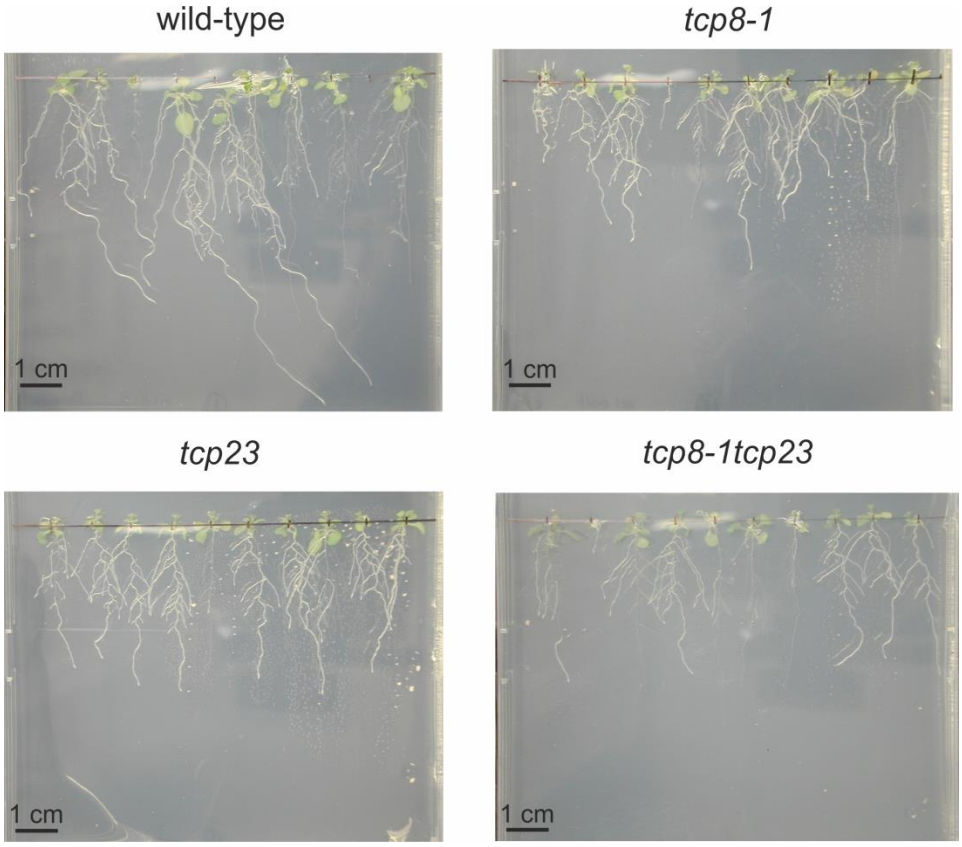

Figure 5.16: Root growth assay for wild-type, *tcp8-1*, *tcp23* and *tcp8-1tcp23.* 10 seedlings are equally spaced apart.

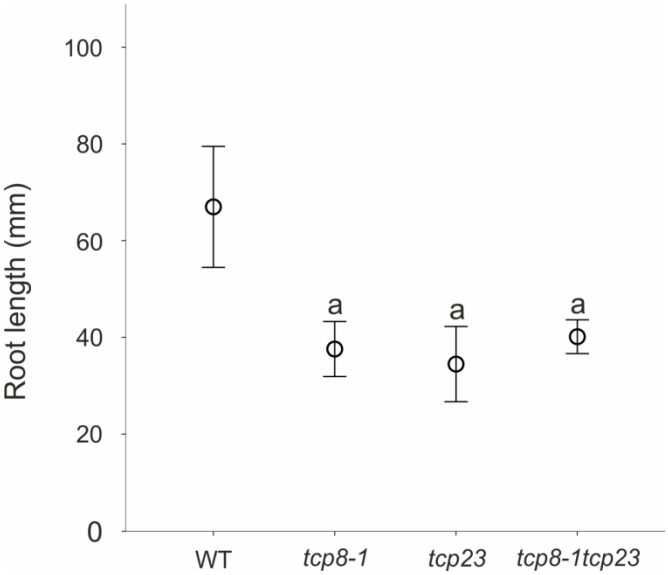

Figure 5.17: Comparison of mean root length for wild-type, *tcp8-1*, *tcp23* and *tcp8-1tcp23.* A one-way ANOVA and Tukey range test was used to determine the differences between the lines. Error bars represent 95% confidence intervals. The letter 'a' indicates that there is no significant difference between genotypes.

5.4.5 Discussion

The experiments described in this section of the thesis were for the most part conducted in the last few months of the project. Regrettably technical difficulties and other delays meant there was insufficient time to complete the experiments. For this reason we cannot draw any conclusions about the spatial and temporal expression patterns of *TCP8, TCP22* and *TCP23.* At different stages (entry clones, expression clones, *A. tumefaciens* culture) of the creation of the *pTCP8:TCP8:GUS* and *pTCP22:TCP22:GUS* constructs glycerol stocks were made and frozen at -80ºC for long term storage. The floral dip transformation of *Arabidopsis* did not yield any positive transformants. The *Agrobacterium* culture should be regrown and the floral dip repeated. If the floral dip transformation fails to yield positive transformants a second time, it will be necessary to go back one step and restart the protocol from the *Agrobacterium* transformation. If more time had been available there would have been scope to spend more time optimising the error-free PCR and research alternative cloning methods to create *pTCP23:TCP23:GUS.*

A large region, that would typically include the promoter, was selected upstream of *TCP8, TCP22* and *TCP23* to be cloned. There are a number of bioinformatics tools that can help identify motifs common in promoter sequences, but the exact promoter length can often only be determined experimentally. There are a number of ways to ascertain whether the chosen promoter region corresponds to the actual promoter. The experiment can be followed up with an in situ, if the expression patterns matches you can be confident that the full promoter was included. Multiple constructs with different promoter lengths could be compared to narrow down the promoter region. In the case of a promoter gene construct an alternative strategy would be to rescue a knockout mutant using the construct. In this particular case it is reasonable to assume that the large region we have chosen should include the promoter.

The epidermal cell analysis revealed that there are differences between the wild-type and the *TCP* insertion lines. It should be noted that this experiment should be repeated with backcrossed insertion lines. Based on the RT-PCR we are reasonable confident that *tcp23* is a knockout line. The other TCP insertion lines show a phenotype and a co-segregation analysis should be carried out to ascertain that the observed phenotype is linked to the T-DNA insertion in the TCP gene of interest. The abaxial and adaxial cell analysis shows different effects for the insertion lines; this is not necessarily a problem as different genes are involved in abaxial and adaxial specification. On the abaxial side the *tcp8-1* and *tcp22tcp23* insertion lines show the most obvious perturbations, though in opposite directions. On the adaxial side we see differences between the wild-type and *tcp14-4*, *tcp15-3* and *tcp14-4tcp15-3*. This result is consistent with observations made by Kieffer et al 2011; analysis of the leaf adaxial epidermal cell density in mature wild-type and pTCP14:TCP14:SRDX leaves revealed an excess of cell proliferation in certain areas leading to an enhancement of the shape and curling phenotype. For the analysis we used images taken in the font quarter of the leaf blade, images of the other quarters of the leaves are available and should be analysed to verify that the results are consistent across the different regions of the leaves.

Prior to a full scale histochemical staining experiment a more effective way of imaging the seedlings needs to be determined. The images displayed in this manuscript where taken in sterile dH_2O under a binocular. The tissue of the seedlings is very fragile, and therefore almost impossible to manipulate without damaging. To obtain good quality images on which it is possible to see exactly where the signal is expressed it will be necessary to embed the seedling in paraffin wax or a similar matrix and section the sample using a microtome.

In hindsight the root growth assay should have been conducted with all lines even if the preliminary analysis suggested there to only be a reduced root growth for *tcp8-1* and *tcp23*. The confirmed negative results for the other lines would have been of scientific value. Additionally, it would have been necessary to weigh the root mass of each seedling to quantitatively determine any difference in root mass between the lines. Though significant differences have been detected between the wild-type and the mutant lines it is possible that the length of the roots is negatively affected in the *tcp8-1, tcp23* and *tcp8-1tcp23* mutants but that the overall root mass is not due to formation of additional lateral roots. On the images the roots of some seedlings appear fainter (wild-type seedling 3, 8 and 10), this is not due to any difference in root growth but is determined by what depth the root is growing in the agarose (figure 5.15). To more accurately quantify the differences we can see on the images it would be necessary to measure the length of the roots, number & length of lateral roots and weigh the root mass, and potentially track the individual seedlings across time. Regrettably this analysis needs to be conducted on the seedling directly and cannot be performed retrospectively on the images.

Chapter 6.

General discussion

6.1 Quantifying leaf shape

The human eye is not made to identify subtle differences between shapes. In the past botanical experts have defined a dazzling array of individual leaf shapes found in nature. The downside of categorizing leaf shape in this fashion is that leaves are placed in absolute categories not allowing for gradual shifts from one shape to another or quantification of differences between the shapes. It is this lack of quantification that makes the application of such terms limited in developmental genetics. This work has shown that leaf size and shape, and especially the alteration of leaf size and shape, in mutants can provide us with valuable insight into the genetic basis of leaf development. Alterations in the regulatory control of early leaf development can be visualised by analysing the mature leaf.

6.1.1 The Arabidopsis *leaf shape library*

In this manuscript we employ landmark-based geometric morphometrics to analyse *Arabidopsis* leaf size and shape. Throughout this project the *Arabidopsis* leaf shape library has evolved from a library containing a wide range of *Arabidopsis* accessions and developmental mutants to a stable reference set made up of 10 *Arabidopsis* accessions with comparable flowering time. The choice to define a stable reference set for the *Arabidopsis* leaf shape library was based on the observation that adding additional leaves to the library changes the Principal Components. Though this is not unexpected since the datasets (or number of leaves) that are

included in the analysis determine the major sources of variation (Principal Components), it does make it more difficult to compare or analyse different lines over a longer period of time.

The reference data set was used to analyse all remaining lines in this study. Based on the wider set of accession lines that have been analysed it would be possible to construct a second reference set containing late-flowering accessions. This reference set could then be employed when analysing late-flowering mutants and it would be interesting to compare the principal components from the reference set to the late-flowering reference set to see what the differences are.

6.1.2 Establishing an experimental method

Leaf shape and size is modulated by both genetic and environmental factors (Nicotra et al., 2011; Yano and Terashima, 2001). In this case we are interested in the leaf shape and size changes that are caused by the specific genetic differences between the wild-type and the mutant lines. To exclude environmental effects on leaf shape the methodology used includes growing wild-type plants at the same time as the mutant lines. All lines that were to be analysed in a single experiment are grown in the same greenhouse in close proximity to each other. We do not believe it is necessary to grow the plants in the controlled environment of a growth cabinet. An additional argument against growing plants in a controlled environment is that we could miss any environmental interactions if they did occur. On the analysis side, using one eigensystem rather than a separate eigensystems for each analysis will make the analysis more robust and less influenced by potential environmental changes across the different experiments.

A consideration that has not been taken into account during the analyses presented in this thesis is the question whether all the observations for one

line can be treated as independent since some leaves come from the same individual plant and others do not. Strictly speaking the leaves from one plant are not independent observations. A related question then becomes what the biological 'n' of the experiments presented are. Below we discuss the implications of a number of different ways to address this issue.

The first way to approach this problem would be to analyse the data using the number of degrees of freedom associated with the level of the 'individual' rather than the 'leaf'. In the case of the TCP14/TCP15 analysis the biological 'n' would drop from 427 to 80. The upside of this method is that it is easy and quick, but it is a conservative approach. An alternative approach would be to use the means for each individual rather than the values for each leaf, however, this would significantly affect the power of the analysis.

A better solution would be to carry out the comparison cross the leaf node. It would be possible to use an ANOVA - General Linear Model (ANOVA / GLM) approach; in the ANOVA the factors would be 'leaf node', 'line' and the factor 'individual' nested within 'line'. We would expect that across a single node the sample distribution would be normal (confirmed by personal communication with Richard Waites and Joe Vaughan). However, when carrying out the ANOVA (using R) it would be possible to account for any deviations from normality by specifying the error. The statistical approach outlined here is more likely to pick up significant results than the approach used in this thesis. Similar to the leaf shape and size analysis the epidermal cell analysis should be considered in this light as well, since some images come from the same individual and others do not.

Tied in with this consideration it would be possible to initially only analysing one or 2 leaves per line. It would speed up the experimental procedure and allow for simultaneous leaf shape and size analysis, DNA extraction and seed collection. At a second stage you would then need to

repeat the analysis using all nodes to determine whether all the nodes follow the same trend (e.g. if a mutant line and the corresponding wild-type are significantly different at node 7, are they also significantly different at the other nodes?).

6.1.3 Procrustes superimposition

Within the field of statistical shape analysis (or Procrustes analysis) there are two common methods of performing a shape analysis, the full or partial Procrustes superimposition.

The Procrustes superimposition relies on translation, rotation and scaling, to minimize the Procrustes distance between the objects. By doing so the superimposition removes all information unrelated to shape. A partial Procrustes superimposition does not perform the scaling, thereby maintaining the size of the objects (Zelditch et al., 2012). The argument in favour of a full Procrustes superimposition is that strictly speaking the partial imposition is not a pure shape analysis because the statistical analysis is not just taking shape differences but also size differences into account. According to C.P. Klingenberg, the different methods of Procrustes fitting make little difference unless one is dealing with a data set of unusually large variation; in that case the full Procrustes fit is more suitable as it is more robust against the influence of outliers. The partial superimposition is reported to be the most widely used method (Webster and Sheets, 2010; Rohlf, 1999), especially for biological application though MorphoJ employs a full Procrustes fit (Klingenberg 2011).

The name Procrustes comes from Greek mythology; Procrustes was a bandit who strapped his victims to a bed by either stretching or truncating them. It is said that by doing so he minimised the difference between his victims and the bed. Zelditch et al., 2012 explains why the name is both apt and inapt. Procrustes superimposition minimises the differences between landmark

configurations, as did Procrustes between his victims and the bed. However, Procrustes truncated his visitor's limbs, thereby altering their shape. The superimposition method only uses those operations that do not alter shape.

The data presented in chapter 5 was analysed by the author using MorphoJ (Klingenberg 2011) (Appendix 5) to determine whether performing a Procrustes fit on the data prior to the principal component analysis would have made a difference in the conclusions we have drawn from the data as they are presented in chapter 5 and in Kieffer et al. 2011. The outcome from the principal component analysis is naturally different because the aspect of size has been removed from the analysis, therefore resulting in a different set of PCs. However, the differences identified between the wild-type and *tcp14-4*, *tcp15-3* and *tcp14-4tcp15-3* remain consistent in both superimposition methods. Based on this assessment it was decided not to alter the method of analysis half way through the project but to remain consistent in the mode of analysis to facilitate comparisons between analyses. If this project was started again it might be advisable to analyse the data using both methods, the partial superimposition would retain the size information, which can have biological relevance; the full superimposition could then be used for the shape analysis in the strictest sense of the word.

6.1.4 LeafAnalyser as a method to distinguish subtle phenotypes

The development of automated phenotyping platforms able to record growth at different scales and at high throughput (Granier et al., 2006; Walter et al., 2007) are undoubtedly better suited at large scale analysis and mutant screens, but the reality of science is also that employing those platforms is currently prohibitively expensive making it beyond the reach of less specialized research groups. Lievre et al. 2013 recently highlighted in a

review that the high throughput has on many an occasion led to a decrease in spatial and/or temporal resolution of growth analysis leading to misinterpretation of growth phenotypes. LeafAnalyser represents the best of both worlds; though we would by no means consider this method as high throughput the author has been able to analyse large amounts of leaves in a short space of time.

Though landmark-based methods and LeafAnalyser as a 2D-system in particular, have their limitations, as discussed in chapter 4, this work outlines how uniquely suited LeafAnalyser is at distinguishing the subtle changes in leaf shape and size that can characterize mutant phenotypes, especially in gene families or developmental processes with a high degree of redundancy.

The case studies of the *CUP-SHAPED COTYLEDON (CUC)* genes and *YABBY3* highlight the need for more sophisticated quantitative imaging solutions when characterizing mutant phenotypes. In both instances *cuc1/cuc2* and *yab3-2* were reported to be phenotypically normal (Aida et al., 1997; Aida et al., 1999; Goltz et al. 1999), this study has revealed that these mutants have a subtle but distinct leaf shape and size phenotype.

As is the case for most methods leaf shape analysis should be one line of evidence pursued rather than be taken as ultimate proof. The case study of *kan12* a *KANADI* mutant shows that care needs to be given when interpreting the results of leaf size and shape phenotypes. Disruption of the *KANADI* gene in either the Landsberg *erecta* (Ler-0) or Colombia (Col-0) background yields different results.

6.2 The functional role of class I TCP genes

6.2.1 TCP14 *and* TCP15 *repress cell proliferation in leaves*

One of the aims of this project was to gain a better understanding of the function of a sub-clade of class I *TCP* genes (*TCP8, TCP14, TCP15, TCP22* and *TCP23*) in leaf development. Functional characterization of class I TCP genes has been hampered by a high degree of redundancy between its family members. In collaboration with Martin Kieffer and Brendan Davies from the University of Leeds we have discovered that *TCP14* and *TCP15* modulate internode length and leaf shape in *Arabidopsis* in a partially redundant manner. We used a quantitative imaging approach to analyse the single and double T-DNA insertion mutants for *TCP14* and *TCP15*. The mutant lines produce a leaf that is broader and shorter compared to the wild-type plant. The leaves show a blade shape defect in the order wild-type > *tcp14-4* > *tcp15-3* > *tcp14-4tcp15-3*. This blade defect order mirrors the phenotypic effects discovered by Martin Kieffer in plant stature. The effect seen in the double *tcp14-4tcp15-3* mutant is enhanced in the dominant repressor lines (*pTCP14:TCP14:SRDX, pTCP15:TCP15:SRDX*), we can therefore conclude that *TCP14* and *TCP15* repress cell proliferation in leaves (Kieffer et al., 2011).

Though acting redundantly in the leaf the expression patterns of *TCP14* and *TCP15* are very distinct and dynamic. *TCP14* is expressed widely in the leaf blade while *TCP15* is predominately expressed in the margin of the leaf (Kieffer et al., 2011). Contrary to what the expression pattern might indicate the observed phenotypic effect in the leaf is stronger in the *tcp15-3* mutant compared to *tcp14-4*. As yet it is unknown what the direct (and indirect) targets of *TCP14* and *TCP15* are in the leaf, we thereby do not know the exact mechanism by which *TCP14* and *TCP15* modulate leaf shape. The results described in Kieffer et al., 2011 constitute proof that class I *TCP* genes can activate or repress transcription in a tissue dependent manner.

6.2.2 *Investigation of functional redundancy of class I* TCP *genes*

The theory has been proposed that the interplay between different TCP genes is responsible for the successful regulation of leaf development (and a range of other plant developmental processes). We expanded our investigation to the related class I TCP genes, *TCP8, TCP22* and *TCP23*. *TCP8, TCP22* and *TCP23* had hitherto not been characterised. Homozygous T-DNA insertion lines were isolated and their insertion points determined. The RT-PCR suggests that there is unlikely to be any remaining expression in the *tcp23* insertion line indicating that this line may be a null allele, though we cannot be certain based on the RT-PCR alone. Transcript levels could be detected for *tcp8-1* and *tcp22*. Evidence in the literature suggests that it is likely that protein levels in *tcp8-1* and *tcp22* are affected regardless of the observed expression levels in RT-PCR (Wang et al., 2008). Any phenotypes we observe for these lines need to be confirmed once the lines have been back-crossed and it has been established though a co-segregation analysis that the phenotype is linked to the T-DNA insertion in the TCP gene.

Compared to the wild-type line *tcp23* has slightly larger leaves, *tcp8-1* and *tcp22* did not show any change in leaf size. As discussed larger leaves in the *tcp23* mutant might indicate a cell proliferation repression activity for *TCP23* but we would expect to see a similar increase in *tcp8-1tcp23* and *tcp22tcp23* which we do not. Neither do we see a decrease in leaf size for *tcp8-1* and *tcp22* which could explain the difference between *tcp23* and the double mutant *tcp8-1tcp23* and *tcp22tcp23* if *TCP8* and *TCP22* had antagonistic functions to *TCP23*. The leaf shape analysis does not support such an antagonistic function either, the single *tcp8-1, tcp22* and *tcp23* mutants produce leaves that have rounder, more compact, spherical blades and narrower, longer petioles. The phenotypic effect seen in the single mutants is comparable and more pronounced in the double mutant

combinations. Judged purely on the leaf shape and size analysis we conclude that *TCP8, TCP22* and *TCP23* modulate leaf size and shape in a, up to this point unknown, but partially redundant manner. The shape change seen as a result of mutations in *TCP8, TCP22* and *TCP23* appears to be different, almost opposite, to the modification of leaf shape seen by the disruption of *TCP14* and *TCP15*.

Epidermal cell analysis support a separate role in leaf development for *TCP14/TCP15* compared to *TCP8, TCP22* and *TCP23.* On the abaxial side the analysis indicates that there is a difference between *TCP8, TCP22* and *TCP23*, though it is unclear how the difference relates to their biological function. Compared to wild-type cells we see a difference in shape in the *tcp8-1, tcp8-1tcp22* and *tcp22tcp23* lines, though the perturbation is not in the same direction. Adaxial epidermal cells of *tcp14-4, tcp15-4* and *tcp14-4tcp15-3* show a significant difference in cell shape compared to wild-type and the other *TCP* insertion lines. The cell shape metric mean cell area/perimeter is broadly speaking an indication of the degree of lobes the cell is exhibiting. *tcp14-4, tcp15-4* and *tcp14-4tcp15-3* are less lobed compared to the wild-type line. We do not use this metric to directly interpret a biological function, but only show when the insertion lines differ from the wild-type line.

A decrease in root growth was observed for *tcp8-1* and *tcp23*, this decrease in root length is not enhanced in the double mutant *tcp8-1tcp23* suggesting that there is no direct redundancy at play. A more thorough root growth analysis will need to be carried out to quantify the differences seen and determine whether they are statistically significant. However, these observations might indicate that the role of *TCP8* and *TCP23* is not limited to leaves.

6.2.3 New advances in the understanding of the functionality of class I TCP genes

Since the start of this project the understanding of the role of class I *TCP* genes has moved on considerably. The new developments in this field will be outlined before discussing how the results of this study fit in with the new insights in the functionality of class I *TCP* genes.

It was previously reported that class I and class II *TCP* genes bind to a partially overlapping sequence, and thereby are able to bind to similar promoter elements. Developmental processes were suggested to be regulated by the interplay of class I and class II *TCP*s, class I genes promoting and class II genes restricting cell proliferation (Li et al., 2005). In the introduction to this thesis we already indicated that this model needed to be relaxed, it is now evident that though class I and class II *TCP* genes can work antagonistically to each other (e.g. jasmonic acid metabolism, leaf development) both class I and class II *TCP* genes can function as activators and repressors of transcription (reviewed by Uberti Manassero et al., 2013; Danisman et al., 2012; Wang et al., 2013). In the case of class I TCP genes it is clear that the same gene, (e.g. *TCP14* and *TCP15*) can be an activator and a repressor depending on the tissue in which they are expressed (Kieffer et al., 2011). Recruiting co-repressors has been suggested as one by which mechanism TCP genes could accomplish context-dependent switching between activation and repression (Causier et al., 2012).

TCP15 was described to indirectly regulate *CUC* genes through binding of *IAA3/SHY2* and *SAUR65* promoters (early auxin response genes), genes that are activated by TCP3, a CIN-like class II protein (Uberti Manassero et al., 2012). *GhTCP14* (*Gossypiun hirsutum* - upland cotton) was shown to bind to the promoter of *PIN2, IAA3* and *AUX1*, and likely to have transcription activation activity (Wang et al., 2013). If it is confirmed that *TCP15* is also

a transcriptional activator of *IAA3*, likely considering the close homology with *TCP14*, this would be the first documented example of a class I (*TCP15*) and a class II (*TCP3*) *TCP* gene to regulated a specific target gene in the same direction. More investigation is needed to determine the degree of functional overlap between class I and class II TCPs, but miRNA319-targeted class II CIN-like *TCP* genes act in concert with *AS2* to repress *BP* and *KNAT2* expression. Class II TCP genes were already reported to regulate *AS1* (Koyama et al., 2007; Li et al., 2012b). We now additionally know that *STM, BP* and to some degree *AS1* are overexpressed in the class I pentuple mutant *tcp8-1tcp15-1tcp22-1tcp23-1tcp21-1* (Aguilar-Martinez et al., 2013).

Regulation of cell cycle genes is another example of overlapping function between class I and class II *TCP* genes. Class II *TCP* genes are reported to repress cell proliferation, though a direct link between class II *TCP* genes and regulation of the cell cycle has only been reported for *TCP4* (Uberti Manassero et al., 2013; Aggarwal et al., 2011). So far class I *TCP20, TCP14* and *TCP15* genes have been implicated in the regulation of cell cycle genes (Kieffer et al., 2011; Li et al., 2005; Li et al., 2012a). Aguilar-Martinez et al., 2013 reported up-regulation of *CYCA1;1* and *CYCA2;2* in the pentuple *TCP* mutant *tcp8-1tcp15-1tcp22-1tcp23-1tcp21-1* which might implicate other class I TCP genes in the regulation of cell cycle genes (Aguilar-Martinez et al., 2013). *TCP15* has specifically been implicated in the regulation of endoreduplication by directly binding to the promoters of *CYCA2;3* (type A cyclin) and *RETINOBLASTOMA-RELATED* gene (*RBR*), both of which are known negative regulators of endoreduplication (Li et al., 2012a).

TCP genes are known to form homo- and heterodimers, though class I TCPs exhibit a preference of forming protein-protein interaction with other class I members heterodimerization of TCPs can occur between class I and class II TCP genes (Aguilar-Martinez et al., 2013; Kim et al., 2014;

Danisman et al., 2013; Valsecchi et al., 2013). Class I genes had a higher number of dimerization partners per protein than class II genes (Danisman et al., 2013). A study combining bioinformatics and biochemical approaches categorize TCPs as intrinsically disordered proteins (IDP), this characteristic could help facilitate the formation of higher order complexes with several different partners (Valsecchi et al., 2013). DNA binding properties of the class I TCP proteins (except TCP16) are sensitive to redox conditions in the cell due to a redox-active Cys-20 residue, theorised to be located near the dimerization site, in the conserved TCP domain. The redox sensitivity makes class I TCP proteins potential candidates in the redox regulation of cell proliferation or plant response to oxidative stress (Viola et al., 2013).

Nuclear localisation was reported for *TCP7, TCP8, TCP14, TCP15, TCP22* (Aguilar-Martinez et al., 2013; Hammani et al., 2011; Kim et al., 2014) and *TCP23* (Balsemão-Pires et al., 2013). *TCP7, TCP14, TCP21* and *TCP23* are expressed in all major plant organs, *TCP8, TCP15* and *TCP23* expressed at low levels in siliques (Balsemão-Pires et al., 2013; Aguilar-Martinez et al., 2013), *TCP8* highly expressed in dry seed, and TCP22 expression not detected in inflorescences or mature leaves. TCP expression appears to be highest in developing tissue (Aguilar-Martinez et al., 2013).

TCP8 has been found to interact with PNM1 (PPR protein to the nucleus and mitochondria 1), a pentatricopeptide repeat (PPR) protein, presented as a potential coordinator of the expression of mitochondrial and nuclear genomes. *TCP8* and PNM1 directly interact in the plant nucleus. It is also suggested that TCP8 might bind the site II element in the promoter region of PNM1 (Hammani et al., 2011), though Giraud et al., 2010 found that *TCP8* and *TCP22* did not interact with the site II elements tested in their study (site II T and site II C; TGGGC(C/T)). *TCP2*, *TCP3*, *TCP11* and *TCP15* were shown to interact with various components of the circadian clock. It is suggested that binding of TCP proteins to the site II elements in the promoters of mitochondrial, plastid, and peroxisomal genes accomplishes

the diurnal transcription regulation of proteins involved in the energy metabolism (Giraud et al., 2010).

Early flowering in a *TCP23* knockout mutant and late flowering in the overexpression line suggest that *TCP23* may be a negative regulator of flowering time. The overexpression of *TCP23* additionally resulted in a reduced root growth phenotype and leaf morphology alterations (Balsemão-Pires et al., 2013). The comparative analysis of the functional role of *TCP7, TCP8, TCP22* and *TCP23* confirms that single *TCP* mutants have mild phenotypes, and though multiple mutants show increased defects related to number of leaves and leaf size they maintain normal morphology. The study report a reduced number of rosette leaves and shorter petiole length for *tcp15*, increased blade length, blade width, blade perimeter and blade area for *tcp23*, and *tcp8* and *tcp21* as indistinguishable from wild-type (Aguilar-Martinez et al., 2013).

Overexpression of *TCP14* under the control of a *35S* promoter led to severely altered plant development and occasionally lethality. Overexpression of *TCP14* and *TCP15* under a promoter specific to lateral organ primordia led to reduced internode length, petal growth, and fertility. Additional trichomes developed on the sepals and small dark-green leaves were formed containing higher levels of chlorophyll. Overexpression of *TCP14* and *TCP15* was also reported to promote shoot branching and delayed whole-plant, but not leaf senescence. *TCP14* and *TCP15* are found to interact with *SPINDLY* (*SPY*) to promote cytokinin responses in leaves and flowers, possibly by acting in the cytokinin pathway to promote cell proliferation at the leaf margins after activation by *SPY* (Steiner et al., 2012a). When overexpressed in tomato *Arabidopsis TCP14* and *TCP15* modulate cytokinin sensitivity (Steiner et al., 2012b).

Two recent publications link TCP transcription factors to plant defence responses to biotrophic pathogens. TCP14 was found to interact with

multiple pathogen effectors from diverse pathogen classes in yeast (Mukhtar et al., 2011), and several class I TCP genes (TCP8, TCP14, TCP15, TCP20, TCP22 and TCP23) were found to interact with *SUPPRESSOR OF rps4-RLD1* (SRFR1) a transcriptional repressor of plant defence genes. This led to the theory that SRFR1fine-tunes the Arabidopsis defence response by interacting with class I TCP proteins in the nucleus (Kim et al., 2014). Together these studies suggest that a subset of class I TCPs, are positive regulators of defence gene expression and immunity (Mukhtar *et al.*, 2011; Kim et al., 2014). It remains to be seen whether TCP genes directly or indirectly regulate plant immunity.

There is now substantial evidence that TCP transcription factors are heavily involved in the plants responses to phytohormones. We described above that class I *TCP15* and class II *TCP3* modulate early auxin response genes, and both class I and class II TCP genes have been implicated in jasmonic acid regulation (Danisman et al., 2012; Wang et al., 2013; Uberti-Manassero et al., 2012). *TCP14* is a positive regulator of seed germination, working antagonistically to *DOF6* and implicated in the regulation of a specific set of abscisic acid response genes (Tatematsu et al., 2008; Rueda-Romer et al., 2011). When we consider that gibberellin and ethylene are involved in the regulation of endoreduplication and the cell cycle, gibberellin and, jasmonic acid, salicylic acid, and cytokinin have been implicated in trichome initiation and growth the overlap between TCPs and phytohormone response becomes very substantial (Li et al., 2012a; Steiner et al., 2012a; Wang et al., 2013).

6.2.4 Final remarks and future work

Balsemão-Pires et al., 2013 reported a role for *TCP23* in the regulation of flowering time based on the observation of early flowering in the insertion mutant and late flowering in the overexpression line. During this study we did not observe this phenomenon; though flowering time was not

specifically recorded. In contrast to Balsemão-Pires we have reported reduced root growth in the null mutant; their analysis revealed no statistical difference for *tcp23* but reduced root growth in the overexpression line. An alteration in flowering time was not reported by Aguilar-Martinez et al., 2013 in either the mutant or the dominant negative form (*TCP23*-SRDX), nor did the study remark on an alteration in root length. It is worth noting at this point that all three studies were carried out with the same T-DNA insertion line (SAIL_443_F02). Analysis of the quadruple *tcp8-1tcp15-1tcp22-1tcp23-1* and the pentuple *tcp8-1tcp15-1tcp22-1tcp23-1tcp21-1* was reported to have fewer rosette leaves and bigger leaves than wild-type plants (Aguilar-Martinez et al., 2013). The bigger leaves mirror what we found for *tcp23*.

The picture that is being painted is confusing and partially contradictory. In an ideal scenario we would want to repeat the leaf size and shape analysis for *tcp23* and include the overexpression line *OxTCP23* (Balsemão-Pires et al., 2013), the dominant negative repressor *TCP23-SRDX* and the mentioned quadruple and pentuple mutants (Aguilar-Martinez et al., 2013). An extensive root growth assay (including root hair) on the TCP lines may also help clarify the situation. A comparative analysis of the abundance and localization of trichomes would be an additional experimental line yet to be explored.

Full functional redundancy within the *TCP14*-like clade would be unlikely due to evolutionary instability, it is more likely that the *TCP*s would exhibit subfunctionalization, share certain functions but be distinct in others (Danisman et al., 2013). This is in line with our analysis which suggests that *TCP8, TCP14, TCP15, TCP22* and *TCP23* may overlap in function but seem to, at least in part, work antagonistically. When taken together with the conclusion that *TCP14* and *TCP15*, and potentially the other class I *TCP* genes can repress or activate in a context-dependant manner, any phenotype, or lack thereof in a multiple mutant becomes extremely complex to

interpret. It is likely that the situation will not resolve itself until we understand the downstream targets of these genes and whether or not our TCP genes directly or indirectly bind their targets, and if they affect their targets in a monomer, homodimer or heterodimer configuration.

We have defined a number of actions we feel are necessary to further elucidate the function of class I TCP genes and investigate whether this group of TCP genes shares significant functional overlap. Additional experimental avenues to explore are the ever increasing burden of evidence that TCP genes are intricately involved in hormone response. In a search for downstream targets of class I TCP genes changes in expression have been found in cell cycle genes and boundary specific genes, hormone response genes should be added to the list of potential targets that could be investigated for *TCP8*, *TCP22* and *TCP23*.

Where little was known about class I TCP genes when this work was started the scientific community has since embraced this group of genes and though still fragmented a picture is starting to emerge. It is unclear whether a common factor will be found in the wide range of functions and developmental processes class I TCP genes have been implicated in or whether by their nature as transcription factors they will prove to simply have their metaphorical fingers in many pies.

Appendix

Appendix A1

Name	Sequence	Length	Tm ºC	Purpose
N606694_LP	TTCCGGGTCATCATCTCAAT	20	60.28	T-DNA Insertion
N606694_RP	AAGTTTTTGGTGGAACCTGAA	21	58.59	T-DNA Insertion
N645177_LP	GATGGGAAAATCAAGGTTAAAAA	23	58.48	T-DNA Insertion
N645177_RP	CAGAGGAGATAAACGGAATCG	21	58.80	T-DNA Insertion
N643403_LP	GTCGAGCAGACGTCAAACAA	20	60.03	T-DNA Insertion
N643403_LP	CCCGGAAGATAATTCCCAAC	20	60.50	T-DNA Insertion
N803036_FP	GCACGCTTCACTGTCTGAAA	20	57.3	T-DNA Insertion
N803036_RP	CCTCCTCCAGCAGAGTTCAC	20	61.4	T-DNA Insertion
N817775_FP	AAATACCCCAACGCCTTACC	20	57.3	T-DNA Insertion
N817775_RP	CGGTGAGAAAGAAGGGAAAA	20	55.2	T-DNA Insertion
N874232_FP	CTCATAGCCCCACCAGAAAA	20	57.3	T-DNA Insertion

N874232_RP	CCGAAAAGCCAACCCTAAAA	19	54.5	T-DNA Insertion RT-PCR
INS2.3_FP	GATCCGGATCATAACCATCG	20	64	T-DNA Insertion
INS2.3_RP	CTAGGAATGATGACTGGTGC	20	59.7	T-DNA Insertion
INS1.4_FP	GACGACAACCATCAACAACAACCTTC	26	63.2	T-DNA Insertion
INS1.4_RP	GTTGTTGATGATGATGTCTCTGTG	24	59.3	T-DNA Insertion
LBa1	TGGTTCACGTAGTGGGCCATCG	22	64	T-DNA Insertion
LBb1.3	ATTTTGCCGATTTCGGAAC	19	52.4	T-DNA Insertion
LB2	GCTTCCTATTATATCTTCCCAAATTACCAATACA	34	63.4	T-DNA Insertion
Jl-202	CATTTTATAATAACGCTGCGGACATCTAC	29	62.4	T-DNA Insertion
TCP8_FP1	GGTGGAGCATCAAGAGAAGC	20	63.9	RT-PCR
TCP8_RP1	CAATCAACCAAACCGCTACA	20	63.5	RT-PCR
TCP21_FP1	TTCCGGGTCATCATCTCAAT	20	64.3	RT-PCR
TCP21_RP1	GAGCAAAAGAAACCGCAAAT	20	63	RT-PCR
TCP22_FP1	TCAGCATCAGCTCCAACATC	20	64.1	RT-PCR
TCP22_RP1	ATTCAAGCATGGCAGCATTC	20	65.0	RT-PCR
TCP23_FP1	GGTTGGTCTCGGATTGAGTC	20	63.5	RT-PCR
tcp23_RT_FWD	GGAACCATACCGGCGAATATC	21	66.1	RT-PCR

tcp23_RT_REV	CGGATCTTGATCAGGAGCTTC	21	65.0	RT-PCR
TUB9_F	GTACCTTGAAGCTTGCTAATCCTA	24	61.5	RT-PCR
TUB_R	GTTCTGGACGTTCATCATCTGTTC	24	65.8	RT-PCR
TCP23_PR_FP	CACCAAAGCATGGGCTTTTTA	21	50	Cloning
TCP23_PR_RP	GTTGTTGTGGGACTCCATATT	21	50	Cloning
TCP23_PR2_FP	CACCCTCGGAACCAGCTTTGTTCGA	25	76	Cloning
TCP23_PR2_RP	AATGAGACTGAACCGGAGATTG	22	64	Cloning
TCP8_PR_FP	CACCTGGCGACTCAACAAGATCAGA	21	52	Cloning
TCP8_PR_RP	GAGATCCATTTTCCGGTGAGA	21	52	Cloning
TCP22_PR_FP	CACCACCACCAGGTAATAAGGCAT	24	57	Cloning
TCP22_PR_RP	GGAATTCTGATTCATCTTCAAATCCGT	27	55	Cloning
M13_FWD	GTAAAACGACGGCCAGT	17	59.2	pUC Sequencing Colony PCR
M13_REV	CAGGAAACAGCTATGAC	17	51.5	pUC Sequencing Colony PCR
TCP8_INT1_FP	GCTATTTCATTGCTCTTTGTC	21	58.1	pUC Sequencing Colony PCR
TCP8_INT2_RP	TGTTTACCAATTTTAGAGCACC	22	59.6	pUC Sequencing Colony PCR

TCP22_INT1_FP	CAGGTGAAACTCTATGAGC	19	54.7	pUC Sequencing Colony PCR
TCP22_INT2_RP	ATCATCATTGTTACTTTTGGAT	22	56.5	pUC Sequencing Colony PCR
TCP23_INT1_FP	CATATCTCTGACTGTTTTACTG	21	50.6	pUC Sequencing Colony PCR
TCP23_INT2_RP	TCTAACTTTGTGAGACTAAAAC	22	52.1	pUC Sequencing Colony PCR

Table A1.1: Full list of primers used during this thesis, name, sequence length, melting temperature and application provided.

Appendix A2

Appendix 2.1: T-DNA Insertion line TCP8 *(N817775)*

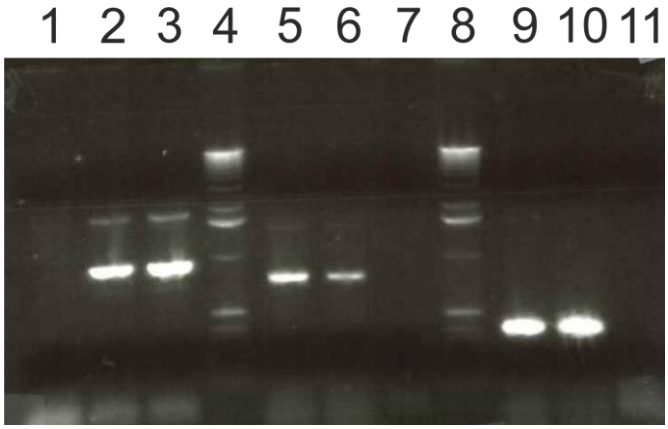

Figure A2.1: Agarose Gel to determine homozygous insertion mutants for *TCP8* (N817775).

Lane 1: Sample 1 with gene-specific primers

Lane 2: Sample 2 with gene-specific primers

Lane 3: Positive control with gene-specific primers

Lane 4: DNA ladder

Lane 5: Sample 1 with reverse gene-specific (REV) and left-border T-DNA insertion primer (LB)

Lane 6: Sample 2 with REV and LB primer

Lane 7: Negative control (H_2O) with REV and LB primer

Lane 8: DNA ladder

Lane 9: Sample 1 with forward gene-specific (FWD) and LB primer

Lane 10: Sample 2 with FWD and LB primer

Lane 11: Negative control (H_2O) with FWD and LB primer

Sample 1 is a homozygous line with a tandem T-DNA insertion in *TCP8* and sample 2 is heterozygous line with a tandem T-DNA insertion in *TCP8*. As expected, the positive (wild-type DNA) control had a band for the wild-type gene and no band was visible in the negative control(s). Expected amplification product for the wild-type gene was 974bp. Reverse gene-specific and left-border insertion primers yield an amplification band at

approximately 830bp and forward gene-specific and left-border insertion primers a product at ~400bp.

Appendix 2.2: T-DNA Insertion line TCP8 (N803036)

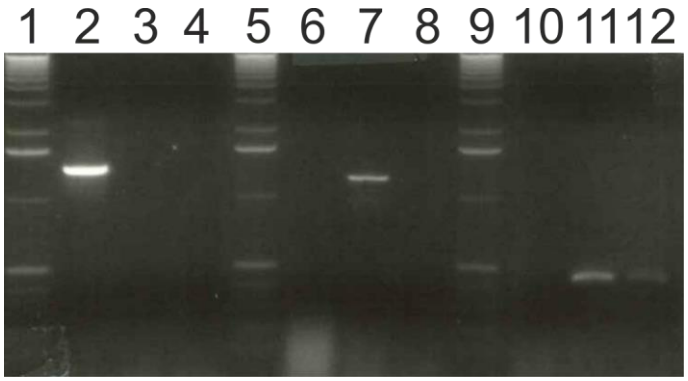

Figure A2.2: Agarose Gel to determine homozygous insertion mutants for *TCP8* (N803036).

Lane 1: DNA Ladder

Lane 2: Positive control with gene-specific primers

Lane 3: Sample 1 with gene-specific primers

Lane 4: Sample 2 with gene-specific primers

Lane 5: DNA ladder

Lane 6: Negative control (H_2O) with REV and LB primer

Lane 7: Sample 1 with reverse gene-specific (REV) and left-border T-DNA insertion primer (LB)

Lane 8: Sample 2 with REV and LB primer

Lane 9: DNA ladder

Lane 10: Sample 1 with forward gene-specific (FWD) and LB primer

Lane 11: Sample 2 with FWD and LB primer

Lane 12: Negative control (H_2O) with FWD and LB primer

Sample 1 is a homozygous line with a tandem T-DNA insertion in *TCP8.* For Sample 2 a wild-type band could not be detected, neither is there a reverse insertion, a forward insertion is present. Further investigation revealed that the line does also carry a tandem insertion in TCP8. The positive (wild-type DNA) control had a band for the wild-type gene and no

bands were visible in the negative control(s). Expected amplification product for the wild-type gene was ~1400bp. Reverse gene-specific and left-border insertion primers yield an amplification band at approximately 1250bp and forward gene-specific and left-border insertion primers a product at ~450bp.

Appendix 2.3: T-DNA Insertion line TCP22

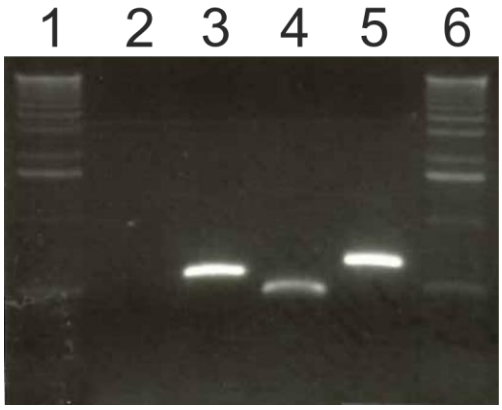

Figure A2.3: Agarose Gel to determine homozygous insertion mutants for *TCP22* (N654177).
Lane 1: DNA ladder
Lane 2: Sample 1 with gene-specific primers
Lane 3: Sample 1 with reverse gene-specific (REV) and left-border T-DNA insertion primer (LB)
Lane 4: Sample 1 with forward gene-specific (FWD) and LB primer
Lane 5: Positive control with gene-specific primers
Lane 6: DNA ladder

Sample 1 is a homozygous mutant line with a tandem T-DNA insertion in *TCP22*. The positive (wild-type DNA) control had a band for the wild-type gene, expected amplification product for the wild-type gene was 625bp. Reverse gene-specific and left-border insertion primers yield an amplification band at approximately 600bp and forward gene-specific and left-border insertion primers a product at ~500bp.

Appendix 2.4: T-DNA Insertion line TCP23

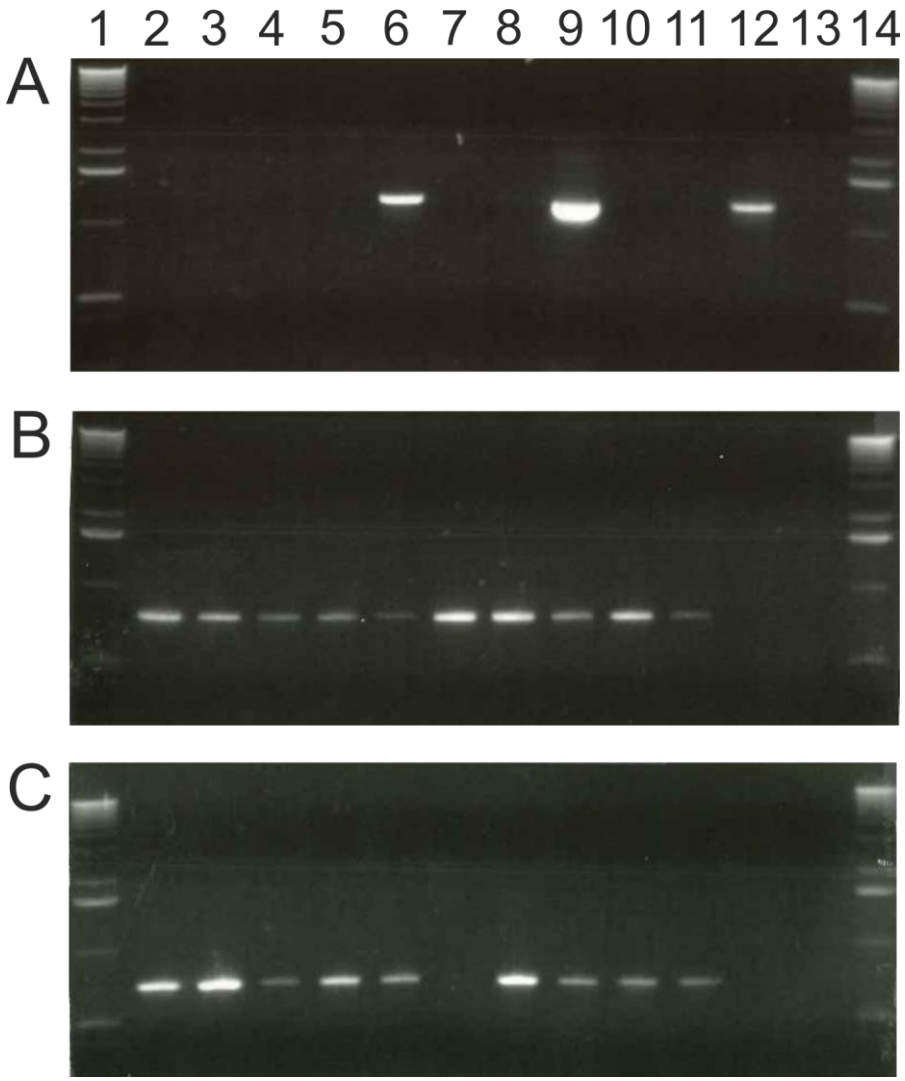

Figure A2.4: Agarose Gel to determine homozygous insertion mutants for *TCP23* (N874232). Panel A: gene-specific primers; Panel B: reverse gene-specific (REV) and left-border T-DNA insertion primer (LB); Panel C: forward gene-specific (FWD) and LB primer

Lane 1: DNA Ladder

Lane 2-11: Samples 1 to 10

Lane 12: Positive control (WT DNA)

Lane 13: Negative control (H_2O)

Lane 14: DNA ladder

Samples 1, 2, 3, 4, 6 (faint band in forward insertion band), 7, 9 and 10 are homozygous lines with a tandem T-DNA insertion line. Samples5 and 8 are

heterozygous lines. The positive control yielded a positive band for the gene-specific primers and the negative control did not yield any bands. The expected wild-type amplification product was approximately 1300bp, the insertion bands were approximately 830bp (reverse gene-specific primer) and 750bp (forward gene-specific primer).

Appendix 3

Appendix 3.1: Sequence Alignment of the pTCP8 entry vector (pENTR™/D-TOPO®).

The alignment below consists of "Plasmid", which is the entry vector to which we have added the promoter sequence. This sequence should be regarded as the expected sequence. "TCP8PR" is the sequence upstream of the ATG of the *TCP8* gene, and "8PR1VM" is the PCR product of the plasmid extraction (primer M13F used for sequencing). In a similar way the sequences generated using two internal *TCP8* promoter primers and M13R were aligned. The four sequences provided complete coverage of the inserted sequence to check for errors.

```
Plasmid         AACGACGGCCAGTCTTAAGCTCGGGCCCCAAATAATGATTTTATTTTGACTGATAGTGAC 600
TCP8PR          ------------------------------------------------------------
8PR1VM          ----------------------------------------------------GGGCCAATAT 10

Plasmid         CTGTTCGTTGCAACAAATTGATGAGCAATGCTTTTTTATAATGCCAACTTTGTACAAAAA 660
TCP8PR          ------------------------------------------------------------
8PR1VM          GGATTTTTATTTTGACTGATAGTGACCTGTTCGTTGCAACAAATTGATGAGCAATGCTTT 70

Plasmid         AGCAGGCTCCGCGGCCGCCGTACTCGAGGAAAACCTGTATTTTCAGGGCTCCTTTGGCGA 720
```

```
TCP8PR          ----------------------------------------------------------TGGCGA 6
8PR1VM          TTTATAATGCCAACTTTGTACAAAAAAGCAGGCTCCGCGGCCGCCCCCTTCACCTGGCGA 130
                                                                    ******

Plasmid         CTCAACAAGATCAGACCCTTATCTACCGCCTCACCACAGACGTTTTTAACTCCCCCGTCG 780
TCP8PR          CTCAACAAGATCAGACCCTTATCTACCGCCTCACCACAGACGTTTTTAACTCCCCCGTCG 66
8PR1VM          CTCAACAAGATCAGACCCTTATCTACCGCCTCACCACAGACGTTTTTAACTCCCCCGTCG 190
                ************************************************************

Plasmid         TTTCTTTTTTTTTCTTTTCTTATGGTTGACAAGTTAACTCACCAGTGCACCTGGAAATCC 840
TCP8PR          TTTCTTTTTTTTTCTTTTCTTATGGTTGACAAGTTAACTCACCAGTGCACCTGGAAATCC 126
8PR1VM          TTTCTTTTTTTTTCTTTTCTTATGGTTGACAAGTTAACTCACCAGTGCACCTGGAAATCC 250
                ************************************************************

Plasmid         TATATTACTTCCAGGAGATGGCTTGCCTGAGGTGGTTTAGTTCGAAGATCAGACACCTGG 900
TCP8PR          TATATTACTTCCAGGAGATGGCTTGCCTGAGGTGGTTTAGTTCGAAGATCAGACACCTGG 186
8PR1VM          TATATTACTTCCAGGAGATGGCTTGCCTGAGGTGGTTTAGTTCGAAGATCAGACACCTGG 310
                ************************************************************

Plasmid         ACTTCATTTATCTGGTGATTGTTGTAGCGACTTGTGTAATATATGGGACGAATATATTCG 960
TCP8PR          ACTTCATTTATCTGGTGATTGTTGTAGCGACTTGTGTAATATATGGGACGAATATATTCG 246
8PR1VM          ACTTCATTTATCTGGTGATTGTTGTAGCGACTTGTGTAATATATGGGACGAATATATTCG 370
                ************************************************************

Plasmid         AACCCGGACTCATCTCTGGAGTTGTACTATGATACCCACTGTTGTATTTTATGTTACTTG 1020
TCP8PR          AACCCGGACTCATCTCTGGAGTTGTACTATGATACCCACTGTTGTATTTTATGTTACTTG 306
8PR1VM          AACCCGGACTCATCTCTGGAGTTGTACTATGATACCCACTGTTGTATTTTATGTTACTTG 430
```

```
                ************************************************************

Plasmid         TAAAATGGTGCATTCCCTTCGAGTGAATGCTTCATGTAAAGTTGTTGCCATTTTCTGTAG 1080
TCP8PR          TAAAATGGTGCATTCCCTTCGAGTGAATGCTTCATGTAAAGTTGTTGCCATTTTCTGTAG 366
8PR1VM          TAAAATGGTGCATTCCCTTCGAGTGAATGCTTCATGTAAAGTTGTTGCCATTTTCTGTAG 490
                ************************************************************

Plasmid         TACTATCCCCAAGCGTCAAAATATTTGATTGCCTCAGATCTGCACTTAATTTATATGCAC 1140
TCP8PR          TACTATCCCCAAGCGTCAAAATATTTGATTGCCTCAGATCTGCACTTAATTTATATGCAC 426
8PR1VM          TACTATCCCCAAGCGTCAAAATATTTGATTGCCTCAGATCTGCACTTAATTTATATGCAC 550
                ************************************************************

Plasmid         ATTTACAGCTATTTCATTGCTCTTTGTCAAGCCTCTTGAAGGGCCTATATCAACTCAATT 1200
TCP8PR          ATTTACAGCTATTTCATTGCTCTTTGTCAAGCCTCTTGAAGGGCCTATATCAACTCAATT 486
8PR1VM          ATTTACAGCTATTTCATTGCTCTTTGTCAAGCCTCTTGAAGGGCCTATATCAACTCAATT 610
                ************************************************************

Plasmid         GTTATCAGAAAGTAAACTGGTTAGCATTGTTGTCGTTTGGTTTTAGAGGAAACTGAAACG 1260
TCP8PR          GTTATCAGAAAGTAAACTGGTTAGCATTGTTGTCGTTTGGTTTTAGAGGAAACTGAAACG 546
8PR1VM          GTTATCAGAAAGTAAACTGGTTAGCATTGTTGTCGTTTGGTTTTAGAGGAAACTGAAACG 670
                ************************************************************

Plasmid         GCTACATTAGAAATGTTTTTGGTAGGCGTGGGCAAAATACCCGAACCCGAAGAACCGAAC 1320
TCP8PR          GCTACATTAGAAATGTTTTTGGTAGGCGTGGGCAAAATACCCGAACCCGAAGAACCGAAC 606
8PR1VM          GCTACATTAGAAATGTTTTTGGTAGGCGTGGGCAAAATACCCGAACCCGAAGAACCGAAC 730
                ************************************************************
```

```
Plasmid         CGAACCTGACCCTAAAAACCCGATCTGAATTCAAACCCAAAATTTTAAAATACCTAATCA 1380
TCP8PR          CGAACCTGACCCTAAAAACCCGATCTGAATTCAAACCCAAAATTTTAAAATACCTAATCA 666
8PR1VM          CGAACCTGACCCTAAAAACCCGATCTGAATTCAAACCCAAAATTTTAAAATACCTAATCA 790
                ************************************************************

Plasmid         GATCCTAAACTACAAAACCCGAATCCGATCAAGTTTCTGAACATATCTGAAATATATATA 1440
TCP8PR          GATCCTAAACTACAAAACCCGAATCCGATCAAGTTTCTGAACATATCTGAAATATATATA 726
8PR1VM          GATCCTAAACTACAAAACCCGAATCCGATCAAGTTTCTGAACATATCTGAAATATATATA 850
                ************************************************************

Plasmid         CATAAAAATAATTTATTAGTAATAATCATATTTACAACAACTATTAAGTGCATAAAATAT 1500
TCP8PR          CATAAAAATAATTTATTAGTAATAATCATATTTACAACAACTATTAAGTGCATAAAATAT 786
8PR1VM          CATAAAAATAATTTATTAGTAATAATCATATTTACAACAACTATTAAGTGCATAAAATAT 910
                ************************************************************

Plasmid         TAGATTTTGTATATATTTTGGATATTTTACCTACTTTTCGATAGATTCGGATAGAAAATA 1560
TCP8PR          TAGATTTTGTATATATTTTGGATATTTTACCTACTTTTCGATAGATTCGGATAGAAAATA 846
8PR1VM          TAGATTTTGTATATATTTTGGATATTTTACCTACTTTTCGATAGATTCGGATAGAAAATA 970
                ************************************************************

Plasmid         CTCAAGTTTTTTGGAA--TTTTTTTTGTGTATTTTCAAGTAA-TTTAAATATATTTTGAT 1617
TCP8PR          CTCAAGTTTTTTGGAA--TTTTTTTTGTGTATTTTCAAGTAA-TTTAAATATATTTTGAT 903
8PR1VM          CTCAAGTTTTTTTGGAATTTTTTTTTGTGTATTTTCAAGTAAATTTTAATATATTTTGAT 1030
                *********** * *  ********************** *** *************

Plasmid         ACAAAATTTTGA-GTTTTGGA-TATTCCGGATGAACTCGAATCCAAACCAAAAAAACCCG 1675
TCP8PR          ACAAAATTTTGA-GTTTTGGA-TATTCCGGATGAACTCGAATCCAAACCAAAAAAACCCG 961
```

```
8PR1VM          ACAAAATTTTGAAGTTTTGGAATATTCCGGATGAACTCGAATCAA---CAAAAAAACCGG 1087
                *********** ******** ********************* *   ********** *

Plasmid         ATCTGAATCTGAAATCTTAAAATAACTGAACCGTAAACCCAAAAAGACCCAAATACCCCA 1735
TCP8PR          ATCTGAATCTGAAATCTTAAAATAACTGAACCGTAAACCCAAAAAGACCCAAATACCCCA 1021
8PR1VM          ATCTGAATCTGAA-TCCTAAAATA-CTGA-CGGTAA---CAAAGA---CCAAATACCTAA 1138
                ************* ** ******* **** * ****   **** *   *********  *

Plasmid         ACGCCTTACCATATTAAATTAGGAGGAAACCCGTTCATAAATAATTTTTCGGGTTTGGGC 1795
TCP8PR          ACGCCTTACCATATTAAATTAGGAGGAAACCCGTTCATAAATAATTTTTCGGGTTTGGGC 1081
8PR1VM          CGGCCTT--CAAGCCCGATA---------------------------------------- 1156
                  *****  **      **
```

Appendix 3.2: Sequence Alignment of the pTCP22 entry vector (pENTR™/D-TOPO®)

The alignment below consists of "Plasmid", which is the entry vector to which we have added the promoter sequence. This sequence should be regarded as the expected sequence. "TCP22PR" is the sequence upstream of the ATG of the *TCP22* gene, and "22PR1VM" is the PCR product of the plasmid extraction (primer M13F used for sequencing). In a similar way the sequences generated using two internal *TCP22* promoter primers and M13R were aligned. The four sequences provided complete coverage of the inserted sequence to check for errors.

```
22PR1VM      ------------------------------GTCAAAGATTTTATTTTGACTGATAGTGAC
```

```
Plasmid      AACGACGGCCAGTCTTAAGCTCGGGCCCCAAATAATGATTTTATTTTGACTGATAGTGAC
TCP22PR      ------------------------------------------------------------


22PR1VM      CTGTTCGTTGCAACAAATTGATGAGCAATGCTTTTTTATAATGCCAACTTTGTACAAAAA
Plasmid      CTGTTCGTTGCAACAAATTGATGAGCAATGCTTTTTTATAATGCCAACTTTGTACAAAAA
TCP22PR      ------------------------------------------------------------


22PR1VM      AGCAGGCTCCGCGGCCGCCCCCTTCACCACCACCAGGTAATAAGGCATGGGTTTAGAAGG
Plasmid      AGCAGGCTCCGCGGCCGCCCCCTT----accaccaggtaataaggcatgggtttagaagg
TCP22PR      ----------------------------accaccaggtaataaggcatgggtttagaagg
                                         ********************************


22PR1VM      AGTCATTGACTATTGACGAATCAAAAGTCTTACAAGACACAATCCGACAGAAACAAATTA
Plasmid      agtcattgactattgacgaatcaaaagtcttacaagacacaatccgacagaaacaaatta
TCP22PR      agtcattgactattgacgaatcaaaagtcttacaagacacaatccgacagaaacaaatta
             ************************************************************


22PR1VM      GAAAAAGAAGAAAAAGACAACAGAGTACGACCGTTCGATTAATATCATGCATGTACTTAT
Plasmid      gaaaaagaagaaaaagacaacagagtacgaccgttcgattaatatcatgcatgtacttat
TCP22PR      gaaaaagaagaaaaagacaacagagtacgaccgttcgattaatatcatgcatgtacttat
             ************************************************************


22PR1VM      ACAACCCTACACTTCCAGTAATTTTTGGTAACTTTACCAAGTCAAACGCAGTATAATCTC
Plasmid      acaaccctacacttccagtaatttttggtaactttaccaagtcaaacgcagtataatctc
TCP22PR      acaaccctacacttccagtaatttttggtaactttaccaagtcaaacgcagtataatctc
```

```
           ************************************************************

22PR1VM    TTATGTAACTACTTTGTGATACTTGAGGTTATGGATATTTTCGAATATGTCTATTTGAGT
Plasmid    ttatgtaactactttgtgatacttgaggttatggatattttcgaatatgtctatttgagt
TCP22PR    ttatgtaactactttgtgatacttgaggttatggatattttcgaatatgtctatttgagt
           ************************************************************

22PR1VM    TAAAATAAAGCTACGGCCTACGTCACATGTCATTTAAAAAGAAACTAGGTTGAAATTCTG
Plasmid    taaaataaagctacggcctacgtcacatgtcatttaaaaagaaactaggttgaaattctg
TCP22PR    taaaataaagctacggcctacgtcacatgtcatttaaaaagaaactaggttgaaattctg
           ************************************************************

22PR1VM    TGCTATACTAAACTAAAAGATGATACAAGAATCAATTACTTTTATAAGCAAATTGAAAAT
Plasmid    tgctatactaaactaaaagatgatacaagaatcaattacttttataagcaaattgaaaat
TCP22PR    tgctatactaaactaaaagatgatacaagaatcaattacttttataagcaaattgaaaat
           ************************************************************

22PR1VM    CTCAAAATACAAGATTTCATATACCATTTTAAGTGCATATAGGTAGACTAATAGAAAAGC
Plasmid    ctcaaaatacaagatttcatataccattttaagtgcatataggtagactaatagaaaagc
TCP22PR    ctcaaaatacaagatttcatataccattttaagtgcatataggtagactaatagaaaagc
           ************************************************************

22PR1VM    AGGTGAAACTCTATGAGCCTATAATATATAAACTTTGTGATTCTTTATCCACAAAATATT
Plasmid    aggtgaaactctatgagcctataatatataaactttgtgattctttatccacaaaatatt
TCP22PR    aggtgaaactctatgagcctataatatataaactttgtgattctttatccacaaaatatt
           ************************************************************
```

```
22PR1VM      AATTCCATAGGCCATAGACACTTTAGATAGTGTGATACAAAATGAGCAAACCCTAAATCC
Plasmid      aattccataggccatagacactttagatagtgtgatacaaaatgagcaaaccctaaatcc
TCP22PR      aattccataggccatagacactttagatagtgtgatacaaaatgagcaaaccctaaatcc
             ************************************************************

22PR1VM      TATTGATTTAAGGTTTCTGATCGTACAACTTCGGTCAAGTTCATAGAAAAACTAGGGAAA
Plasmid      tattgatttaaggtttctgatcgtacaacttcggtcaagttcatagaaaaactagggaaa
TCP22PR      tattgatttaaggtttctgatcgtacaacttcggtcaagttcatagaaaaactagggaaa
             ************************************************************

22PR1VM      AGATTCGTAAACAATAATATTTTTCTCTGAAAATCATGATCAAATTCTAAAAAAGAGAGA
Plasmid      agattcgtaaacaataatatttttctctgaaaatcatgatcaaattctaaaaaagagaga
TCP22PR      agattcgtaaacaataatatttttctctgaaaatcatgatcaaattctaaaaaagagaga
             ************************************************************

22PR1VM      GTATTGGATCGCACTTTGTATACTTTAGGCTTGACAGGGTCAACGAGTTGCTTTTATGTC
Plasmid      gtattggatcgcactttgtatactttaggcttgacagggtcaacgagttgcttttatgtc
TCP22PR      gtattggatcgcactttgtatactttaggcttgacagggtcaacgagttgcttttatgtc
             ************************************************************

22PR1VM      CTTGTTTTATTCCAGATTTTCGGCCATTTACTTTTTTTTTCTTTTCTTTAAATTCTTTTG
Plasmid      cttgttttattccagattttcggccatttacttttttttctttt-ctttaaattcttttg
TCP22PR      cttgttttattccagattttcggccatttacttttttttctttt-ctttaaattcttttg
             ************************************  *** ***************

22PR1VM      GTGGGAAAAACTTTTTTTCTTTTACTGGTAAAGTAAGAACTGTTTTATCTATATACATTA
Plasmid      gtgg-gaaaaacttttttctttttactggtaaagtaagaactgttttatctatatacatta
```

```
TCP22PR      gtgg-gaaaaactttttctttactggtaaagtaagaactgttttatctatatacatta
             ****  ****  ************************************************

22PR1VM      TCATGGACTTAAAACTTTGAAAGCTGAAATCTAAAATTAGTGATAAAGTTTGGAACGAAA
Plasmid      tcatggacttaaaacttgaaagctgaaatctaaaaattagtgataaagtttggacgaaaa
TCP22PR      tcatggacttaaaacttgaaagctgaaatctaaaaattagtgataaagtttggacgaaaa
             *****************  **     **    **********************   ***

22PR1VM      AATAGCAGTTAACTAAAATGATTTGTTTGAGACAAACTAATATAATAAT----C-AGATC
Plasmid      attagcagttaactaaaatgatttgttttgagaccaaaactaataataataatcaagatc
TCP22PR      attagcagttaactaaaatgatttgttttgagaccaaaactaataataataatcaagatc
             * ***************************       *  * **  *  *     * *****

22PR1VM      TAGCCTTTTTTTTTCATGTGGATAGAATAATTAAAAGGAAGCCAAACCTG----------
Plasmid      tagctttttttcatgtgggaataagaataataaaaaggaggcaaaacgggttgttgagga
TCP22PR      tagctttttttcatgtgggaataagaataataaaaaggaggcaaaacgggttgttgagga
             **** ******  *   *     ******** ******* ** ****  *
```

Appendix A4

pENTR™/D-TOPO®

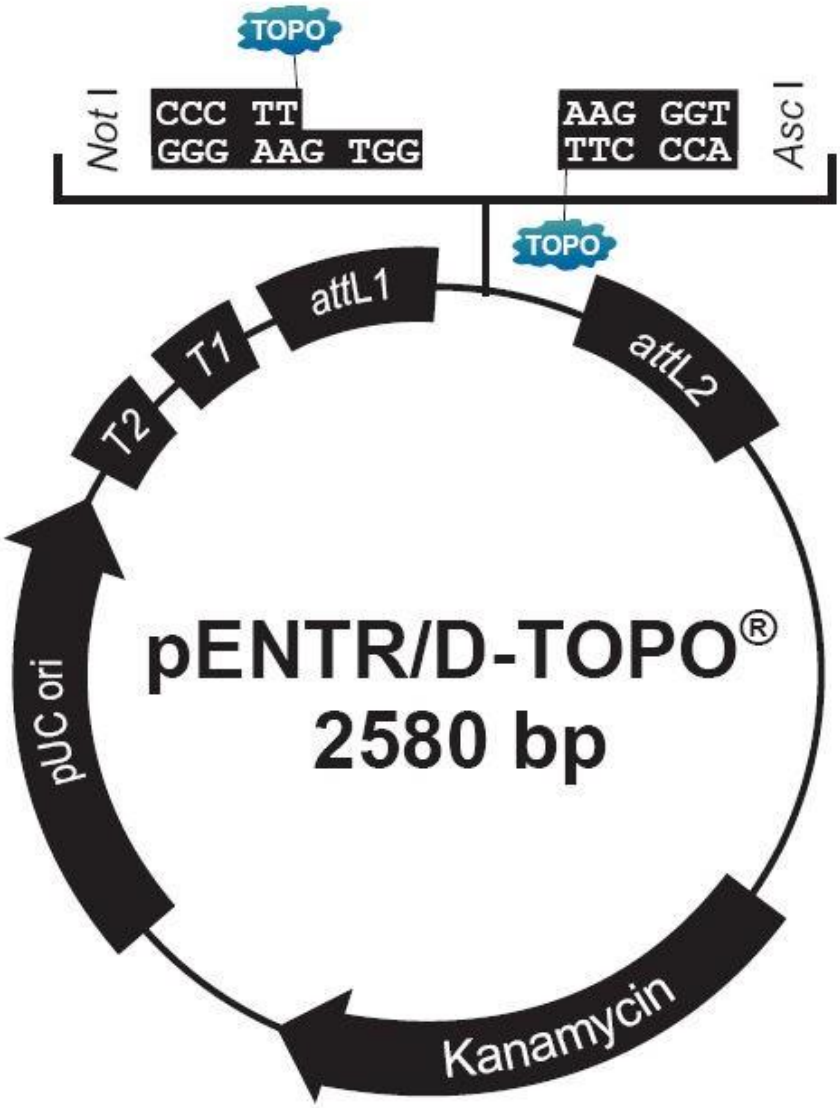

Figure A4.1: Graphical representation of the pENTR/D-TOPO® vector.

pMDC163

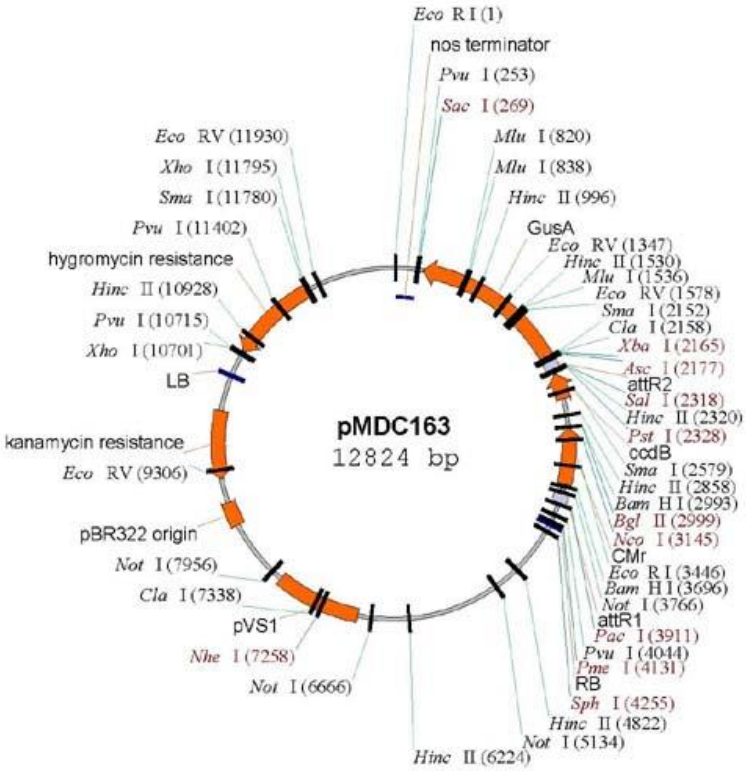

Figure A4.2: Graphical representation of the pMDC163 vector.

Appendix A5

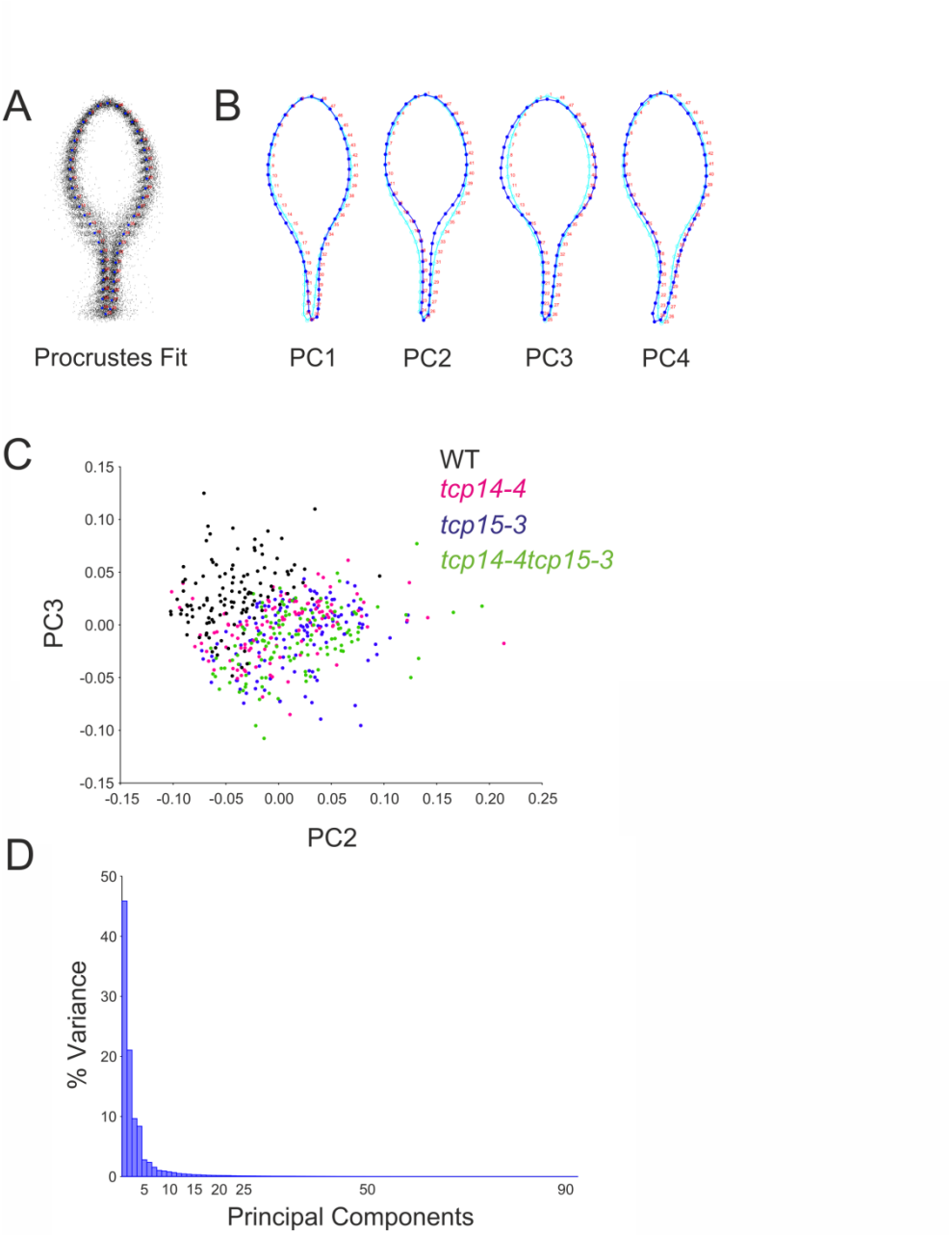

Figure A5.1: Leaf shape analysis for wild-type (WT), *tcp14-4*, *tcp15-3* and *tcp14-4tcp15-3* plants using MorphoJ. Panel A: Procrustes fit for wild-type (WT), *tcp14-4*, *tcp15-3* and *tcp14-4tcp15-3* leaves (N=427). Panel B: Graphical representation of Principal Components 1 through 4. Panel C: Scatterplot for Principal component 2 versus Principal component 3, each point represents a leaf of wild-type (black), *tcp14-4* (pink), *tcp15-3* (blue), or *tcp14-4tcp15-3* (green). Panel D: Graphical output of the percentage of variance per Principal Component.

References

Adams D, Rohlf F, Slice D. (2004) Geometric morphometrics: ten years of progress following the 'revolution'. *Ital. J. Zool.* **71**: 5-16

Aggarwal P, Das Gupta M, Joseph AP, Chatterjee N, Srinivasan N, Nath U. (2010) Identification of specific DNA binding residues in the TCP family of transcription factors in Arabidopsis. *Plant Cell.* **22(4)**: 1174-1189

Aguilar-Martínez J, Sinha N. (2013) Analysis of the role of Arabidopsis class I TCP genes AtTCP7, AtTCP8, AtTCP22, and AtTCP23 in leaf development. *Front. Plant Sci.* **4**: Article 406

Aida M, Ishida T, Fukaki H, Fujisawa H, Tasaka M. (1997) Genes Involved in Organ Separation in Arabidopsis: An Analysis of the cup-shaped cotyledon Mutant. *Plant Cell*. **9**: 841-857

Aida M, Ishida T, Tasaka, M. (1999) Shoot apical meristem and cotyledon formation during Arabidopsis embryogenesis: interaction among the CUP-SHAPED COTYLEDON and SHOOT MERISTEMLESS genes. *Dev*. **126**: 1563-1570

Aida M, Tasaka M. (2006) Genetic control of shoot organ boundaries. *Current Opinion in Plant Biology*. **9**:72-77

Alonso JM, Stepanova AN, Leisse TJ, Kim CJ, Chen HM, Shinn P, Stevenson DK, Zimmerman J, Barajas P, Cheuk R, Gadrinab C, Heller C, Jeske A, Koesema E, Meyers CC, Parker H, Prednis L, Ansari Y, Choy N, Deen H, Geralt M, Hazari N, Hom E, Karnes M, Mulholland C, Ndubaku R, Schmidt I, Guzman P, Aguilar-Henonin L, Schmid M, Weigel D, Carter D, Marchand T, Risseeuw E, Brogden D, Zeko A, Crosby W, Berry C, Ecker JR. (2003) Genome-wide insertional mutagenesis of Arabidopsis thaliana. *Science*. **301**: 653-657

Arazi T, Talmor-Neiman M, Stav R, Riese M, Huijser P, Baulcombe DC. (2005) Cloning and characterization of micro-RNAs from moss. *Plant J.* **43**: 837–848

Baba K, Nakano T, Yamagishi K, Yoshida S. (2001) Involvement of a nuclear-encoded basic helix-loop-helix protein in transcription of the light-responsive promoter of PSBD. *Plant Physiol.* **125(2):** 595-603

Backhaus A, Kuwabara A, Bauch M, Monk N, Sanguinetti G, Fleming A. (2010) LEAFPROCESSOR: a new leaf phenotyping tool using contour bending energy and shape cluster analysis. *New Phytologist.* **187**: 251–261

Balsemão-Pires E, Andrade L, Sachetto-Martins G. (2013) Functional study of TCP23 in Arabidopsis thaliana during plant development. *Plant Physiology and Biochemistry.* **67**: 120-125

Barkoulas M, Galinha C, Grigg SP, Tsiantis M. (2007) From genes to shape: regulatory interactions in leaf development. *Curr Biol*. **10**: 660-666

Bennett T, Sieberer T, Willett B, Booker J, Luschnig C, Leyser O. (2006) The Arabidopsis *MAX* pathway controls shoot branching by regulating auxin transport. *Current Biology.* **16**: 553–563

Besnard F, Refahi Y, Morin V, Marteaux B, Brunoud G, Chambrier P, Rozier F, Mirabet V, Legrand J, Lainé S, Thévenon E, Farcot E, Cellier C, Das P, Bishopp A, Dumas R, Parcy F, Helariutta Y, Boudaoud A, Godin C, Traas J, Guédon Y, Vernoux T. (2014) Cytokinin signalling inhibitory fields provide robustness to phyllotaxis. *Nature.* **16;505(7483)**: 417-421

Besnard F, Vernoux T, Hamant O. (2011) Organogenesis from stem cells in planta: multiple feedback loops integrating molecular and mechanical signals. *Cellular and Molecular Life Sciences.* **68**: 2885–2906

Bilsborough G, Runions A, Barkoulas M, Jenkins H, Hasson A, Galinha C, Laufs P, Hay A, Prusinkiewicz P, Tsiantis M. (2011) Model for the regulation of *Arabidopsis thaliana* leaf margin development. *PNAS* **108(8):** 3424–3429

Bowman J, ed (1993) Arabidopsis: An Atlas of Morphology and Development. New York: Springer-Verlag

Bowman JL and Smyth DR. (1999) CRABS CLAW, a gene that regulates carpel and nectary development in Arabidopsis, encodes a novel protein with zinc finger and helix-loop-helix Domains. *Development.* **126:** 2387-2396

Braybrook SA and Kuhlemeier C. (2010) How a plant builds leaves. The *Plant Cell.* **22**: 1006-1018

Bylesjö M, Segura V, Soolanayakanahally RY, Rae A, Trygg J, Gustafsson P, Jansson S, Street NR. (2008) LAMINA: a tool for rapid quantification of leaf size and shape parameters. *BMC Plant Biology.* **8**:82

Byrne ME. (2012) Making leaves. *Curr Biol.* **15**:24–30

Causier, B., Ashworth, M., Guo, W. and Davies, B. (2012) The TOPLESS interactome: a framework for gene repression in Arabidopsis. *Plant Physiol.* **158**, 423-438.

Chitwood D, Ranjan A, Martinez C, Headland L, Thiem T, Kumar R, Covington M, Hatcher T, Naylor D, Zimmerman S, Downs N, Raymundo N, Buckler E, Maloof J, Aradhya M, Prins B, Li L, Myles S, and Sinha N. (2014) A Modern Ampelography: A Genetic Basis for Leaf Shape and Venation Patterning in Grape. *Plant Physiology.* **164(1):** 259-272

Chitwood D, Kumar R, Headland LR, Ranjan A, Covington MF, Ichihashi Y, Fulop D, Jiménez-Gómez JM, Peng J, Maloof J, Sinha NR. (2013) A quantitative genetic basis for leaf morphology in a set of precisely defined tomato introgression lines. *Plant Cell.* **25(7):** 2465-81

Clough SJ and Bent AF. (1998) Floral dip: a simplified method for Agrobacterium-mediated transformation of Arabidopsis thaliana. *Plant J.* **16**: 735-743.

Crawford BC, Nath U, Carpenter R, Coen ES. (2004) CINCINNATA controls both cell differentiation and growth in petal lobes and leaves of Antirrhinum. *Plant Physiol*. **135**: 244–253

Crawford S, Shinohara N, Sieberer T, Williamson L, George G, Hepworth J, Mueller D, Domagalska MA, Leyser O. (2010) Strigolactones enhance competition between shoot branches by dampening auxin transport. *Development.* **137**: 2905–2913

Cubas P, Lauter N, Doebley J, Coen E. (1999) The TCP domain: a motif found in proteins regulating plant growth and development. *Plant J.* **18**: 215–222

Cubas P. (2002) Role of TCP genes in the evolution of key morphological characters in angiosperms. *In Developmental Genetics and Plant Evolution* (Cronk, Q. et al., eds), pp. 247–266, Taylor & Francis

Curtis MD, Grossniklaus U. (2003) A gateway cloning vector set for high-throughput functional analysis of genes in planta. *Plant Physiol*. **133(2)**:462-469

Danisman, S., van der Wal, F., Dhondt, S., Waites, R., de Folter, S., Bimbo, A., van Dijk, A.D., Muino, J.M., Cutri, L., Dornelas, M.C., Angenent, G.C. and Immink, R.G. (2012) Arabidopsis class I and class II TCP transcription factors regulate jasmonic acid metabolism and leaf development antagonistically. *Plant Physiol.* **159**: 1511-1523.

Danisman, S., van Dijk, A.D., Bimbo, A., van der Wal, F., Hennig, L., de Folter, S., Angenent, G.C. and Immink, R.G. (2013) Analysis of functional redundancies within the *Arabidopsis* TCP transcription factor family. *J. Exp. Bot.* **64**: 5673-5685.

Doebley J, Stec A, Hubbard L. (1997) The evolution of apical dominance in maize. *Nature.* **386**: 485–488

Domozych D. (2012) The quest for four-dimensional imaging in plant cell biology: it's just a matter of time. *Ann Bot.* **110(2):** 461–474

Donnelly PM, Bonetta D, Tsukaya H, Dengler RE, Dengler NG. (1999) Cell cycling and cell enlargement in developing leaves of Arabidopsis. *Dev.Biol.* **215**: 407–419.

Durbak A, Yao H, McSteen P. (2012) Hormone signaling in plant development. *Current Opinion in Plant Biology.* **15**: 92–96

Eshed Y, Baum SF, Perea JV, and Bowman JL. (2001) Establishment of polarity in lateral organs of plants. *Current Biology.* **11**:1251–1260

Eshed Y, Izhaki A, Baum SF, Floyd SF, Bowman JL. (2004) Asymmetric leaf development and blade expansion in Arabidopsis are mediated by KANADI and YABBY activities. *Dev.* **131(12)**: 2997-3006

Filiault DL, Maloof JN. (2012) A genome-wide association study identifies variants underlying the Arabidopsis thaliana shade avoidance response. *PLoS Genet.* **8(3): e1002589**

Fleming AJ. (2005) Formation of primordia and phyllotaxy. *Current Opinion in Plant Biology.* **8**: 53-58

Floyd SK and Bowman JL. (2007) The ancestral developmental tool kit of land plants. *Int. J. Plant Sci.* **168**: 1–35

Giraud E, Ng S, Carrie C, Duncan O, Low J, Lee C, Van Aken O, Millar A, Murcha M, Whelan J. (2010). TCP transcription factors link the regulation of genes encoding mitochondrial proteins with the circadian clock in Arabidopsis thaliana. *PlantCell.* **22**: 3921–3934

Gnan S, Priest A, Kover PX. (2014) The Genetic Basis of Natural Variation in Seed Size and Seed Number and Their Trade-Off Using *Arabidopsis thaliana* MAGIC Lines. *Genetics.* **198(4):**1751-8

Golz JR and Hudson A. (1999) Plant development: YABBYs claw to the fore. *Current Biology.* **9**: R861-R863

Granier C, Aguirrezabal L, Chenu K, Cookson S, Dauzat M, Hamard P, Thioux J, Rolland G, Bouchier-Combaud S, Lebaudy A, Muller B, Thierry Simonneau, François Tardieu. (2006) PHENOPSIS, an automated platform for reproducible phenotyping of plant responses to soil water deficit in Arabidopsis thaliana permitted the identification of an

accession with low sensitivity to soil water deficit. *New Phytologist.* **169**: 623–635

Grennan A, (2006) Regulation of Starch Metabolism in Arabidopsis Leaves. *Plant Physiol.* **142(4):** 1343–1345

Hamant O, Pautot V. (2010) Plant development: A TALE story. *C. R. Biologies.* **333:** 371–381

Hammani K, Gobert A, Hleibieh K, Choulier L, Small I, Giege P. (2011) An Arabidopsis Dual-Localized Pentatricopeptide Repeat Protein Interacts with Nuclear Proteins Involved in Gene Expression Regulation. *The Plant Cell*. **23**: 730–740

Harrison S, Mott E, Parsley K, Aspinall S, Gray J, Cottage A. (2006) A rapid and robust method of identifying transformed Arabidopsis thaliana seedlings following floral dip transformation. *Plant Methods*. **2**:19

Hay A, and Tsiantis M. (2010) KNOX genes: versatile regulators of plant development and diversity. *Dev.* **137**: 3153-3165

Hecker K, Roux K. (1996) High and low annealing temperatures increase both specificity and yield in touchdown and stepdown PCR. *Biotechniques*. **20(3)**:478-85.

Hepworth SR, Zhang Y, McKim S, Li X, Haughn GW. (2005) BLADE-ON-PETIOLE–Dependent Signaling Controls Leaf and Floral Patterning in Arabidopsis. *The Plant Cell.* **17**: 1434–1448

Hibara K, Karim MR, Takada S, Taoka K, Furutani M, Aida M, Tasaka M. (2006) Arabidopsis CUP-SHAPED COTYLEDON3 Regulates Postembryonic Shoot Meristem and Organ Boundary Formation. *Plant Cell.* **18**: 2946-2957

Hiratsu K, Matsui K, Koyama T and Ohme-Takagi M. (2003) Dominant repression of target genes by chimeric repressors that include the EAR motif, a repression domain, in Arabidopsis. *Plant J. 34:* 733–739

Höfgen R, Willmitzer L (1988) Storage of competent cells for Agrobacterium transformation. *Nucleic Acids Res*. **16**: 9877

Horiguchi G, Ferjani A, Fujikura U, Tsukaya H. (2006) Coordination of cell proliferation and cell expansion in the control of leaf size in Arabidopsis thaliana. *J Plant Res*. **119(1)**: 37-42

Horiguchi G. and Tsukaya H. (2011) Organ size regulation in plants: insights from compensation. *Front. Plant Sci.* **2:24**

Howarth DG, and Donoghue MJ. (2006) Phylogenetic analysis of the 'ECE' (CYC/TB1) clade reveals duplications predating the core eudicots. *Proc. Natl. Acad. Sci. U. S. A.* **103**: 9101–9106

Katsir L, Davies KA, Bergmann DC, Laux T. (2011) Peptide signaling in plant development. *Curr Biol.* **21**: R356–364

Kendall DG. (1977) The diffusion of shape. *Advances in Applied Probability*. **9**:428–430

Kerstetter RA, Bollman K, Taylor RA, Bomblies K, Poethig RS. (2001) KANADI regulates organ polarity in Arabidopsis. *Nature*. **411(6838)**:706-9

Kieffer M, Master V, Waites R, Davies B. (2011) *TCP14* and *TCP15* affect internode length and leaf shape in Arabidopsis. *Plant J.* **68**: 147–158

Kim GT, Tsukaya H, Uchimiya H. (1998) The CURLY LEAF gene controls both division and elongation of cells during the expansion of the leaf blade in Arabidopsis thaliana. *Planta.* **206(2)**:175-83

Kim S, Son G, Bhattacharjee S, Kim H, 3, Nam J, Nguyen P, Hong J, Gassmann W. (2014) The Arabidopsis Immune Adaptor SRFR1 Interacts with TCP Transcription Factors that Redundantly Contribute to Effector-Triggered Immunity. *Plant J.* 2014 [Epub ahead of print]

Klingenberg CP, McIntyre GS. (1998) Geometric Morphometric of Developmental Instability: Analyzing Patterns of Fluctuating Asymmetry with Procrustes Methods. *Evolution*. **52(5)**:1363-1375

Klingenberg CP and Zaklan SD. (2000) Morphological integration between developmental compartments in the *Drosophila* wing. *Evolution* **54:**1273–1285

Klingenberg CP. (2008) Analysis of Organismal Form - An introduction to morphometrics, delivered as a Web-based course, course material.

Klingenberg CP. (2011) MorphoJ: an integrated software package for geometric morphometrics. *Mol Ecol Resour.* **11**: 353–357

Kosugi S, Ohashi Y. (2002) DNA binding and dimerization specificity and potential targets for the TCP protein family. *Plant J.* **30**: 337-348

Kosugi S, Suzuka I, Ohashi Y. (1995) Two of three promoter elements identified in a rice gene for proliferating cell nuclear antigen are essential for meristematic tissue-specific expression. *Plant J.* **7(6)**: 877-886

Kosugi S. and Ohashi Y. (1997) PCF1 and PCF2 specifically bind to cis elements in the rice PROLIFERATING CELL NUCLEAR ANTIGEN gene. *Plant Cell.* **9**: 1607–1619

Kover PX, Valdar W, Trakalo J, Scarcelli N, Ehrenreich IM, Purugganan M, Durrant C, Mott R. (2009) A Multiparent Advanced Generation Inter-Cross to Fine-Map Quantitative Traits in *Arabidopsis thaliana*. *PLoS Genet.* **5(7):** e1000551

Koyama T, Furutani M, Tasaka M, Ohme-Takagi M. (2007) TCP transcription factors control the morphology of shoot lateral organs via negative regulation of the expression of boundary-specific genes in Arabidopsis. *Plant Cell.* **19**: 473–484

Koyama T, Sato F and Ohme-Takagi M. (2010a) A role of TCP1 in the longitudinal elongation of leaves in Arabidopsis. *Biosci. Biotechnol. Biochem.* **74:** 2145–2147

Koyama T, Mitsuda N, Seki M, Shinozaki K, Ohme-Takagi M. (2010b) TCP transcription factors regulate the activities of ASYMMETRIC LEAVES1 and miR164, as well as the auxin response, during differentiation of leaves in Arabidopsis. *Plant Cell*. **22:** 3574 – 3588

Krysan P, Young J, Sussman M. (1999) T-DNA as an Insertional Mutagen in Arabidopsis. *The Plant Cell*. **11**: 2283–2290

Langlade NB, Feng X, Dransfield T, Copsey L, Hanna AI, Thebaud C, Bangham A, Hudson A, Coen E. (2005) Evolution through genetically controlled allometry space. *Proc. Natl. Acad. Sci. USA.* **102:** 10221–10226

Laufs P, Peaucelle A, Morin H, Traas J. (2004) MicroRNA regulation of the CUC genes is required for boundary size control in Arabidopsis meristems. *Dev.* **131**: 4311-4322

Lee JY, Baum SF, Alvarez J, Patel A, Chitwood DH, Bowman JL. (2005) Activation of CRABS CLAW in the Nectaries and Carpels of Arabidopsis. *Plant Cell.* **17(1)**:25-36

Li C, Potuschak T, Colón-Carmona A, Gutiérrez RA, Doerner P. (2005) Arabidopsis TCP20 links regulation of growth and cell division control pathways. *Proc. Natl. Acad. Sci. U. S. A.* **102**: 12978–12983

Li Z, Li B, Dong A. (2012a) The Arabidopsis transcriptionfactor AtTCP15 regulates endoreduplication by modulating expression of key cellcycle genes. *Mol Plant.* **5**: 270–280

Li Z, Li B, Shen W, Huang H, Dong A. (2012b) TCP transcription factors interact with AS2 in the repression of class I KNOX genes in Arabidopsis thaliana. *Plant J.* **71**: 99–107

Lièvre M, Wuyts N, Cookson S, Bresson J, Dapp M, Vasseur F, Massonnet C, Tisné S, Bettembourg M, Balsera C, Bédiée A, Bouvery F, Dauzat M, Rolland G,Vile D, Granier C. (2013) Phenotyping the kinematics of leaf development in flowering plants: recommendations and pitfalls. *Dev Biol.* **2**:809–821

Liu F, van der Lijn F, Schurmann C, Zhu G, Chakravarty M, Hysi P, Wollstein A, Lao O, de Bruijne M, Ikram M, van der Lugt A, Rivadeneira F, Uitterlinden A, Hofman A, Niessen W, Homuth G, de Zubicaray G, McMahon K, Thompson P, Daboul A, Puls R, Hegenscheid K, Bevan L, Zdenka Pausova, Medland S, Montgomery G, Wright M, Wicking C, Boehringer S, Spector T, Paus T, Martin N, Biffar R, Kayser M. (2012) A Genome-Wide Association Study Identifies Five Loci Influencing Facial Morphology in Europeans. *PLoS Genet.* **8(9):** e1002932

Lukens L, Doebley J. (2001) Molecular evolution of the teosinte branched gene among maize and related grasses. *Mol Biol Evol.* **18(4)**: 627-638

Luo D, Carpenter R, Vincent C, Copsey L, Coen E. (1996) Origin of floral asymmetry in Antirrhinum. *Nature.* **383**: 794–799

Macleod N. (2013) Landmarks and Semilandmarks: Differences without Meaning and Meaning without Difference. *The Palaeontological Association, the Palaeontology Newsletter*. **82**: 32-43

Maloof JN, Nozue K, Mumbach MR, Palmer CM. (2013) LeafJ: An ImageJ Plugin for Semi-automated Leaf Shape Measurement. *J. Vis. Exp.* **71**: 50028

Mankin H, Jupiter J, Trahan C. (2011) Hand and foot abnormalities associated with genetic diseases. *Hand (N Y)* **6(1):** 18–26

Martín-Trillo M, Cubas P. (2010) TCP genes: a family snapshot ten years later. *Trends Plant Sci.* **15(1)**: 31-39

McElver J, Tzafrir I, Aux G, Rogers R, Ashby C, Smith K, Thomas C, Schetter A, Zhou Q, Cushman M A, Tossberg J, Nickle T, Levin J Z, Law M, Meinke D, Patton D. (2001) Insertional mutagenesis of genes required for seed development in Arabidopsis thaliana. *Genetics*. **12**: 159(4)

McSteen P, Leyser O. (2005) Shoot branching. *Annual Review of Plant Biology*. **56**: 353–374

Montagutelli X. (2000) Effect of the Genetic Background on the Phenotype of Mouse Mutations. *JASN.* **11(2):** S101-S105
Moon J and Hake S. (2011) How a leaf gets its shape. *Curr Biol.* **14**:24–30

Mukhtar MS, Carvunis AR, Dreze M, Epple P, Steinbrenner J, Moore J, Tasan M, Galli M, Hao T, Nishimura MT, Pevzner SJ, Donovan SE, Ghamsari L, Santhanam B, Romero V, Poulin MM, Gebreab F, Gutierrez BJ, Tam S, Monachello D, Boxem M, Harbort CJ, McDonald N, Gai L, Chen H, He Y, Vandenhaute J, Roth FP, Hill DE, Ecker JR, Vidal M, Beynon J, Braun P Dangl JL. (2011) Independently evolved virulence effectors converge onto hubs in a plant immune system network. *Science*. **333**: 596-601

Nakata M, Matsumoto N, Tsugeki R, Rikirsch E, Laux T, Okada K. (2012a) Roles of the middle domain-specific WUSCHEL-RELATED HOMEOBOX genes in early development of leaves in Arabidopsis. *Plant Cell.* **24**: 519–535

Nakata M, Okada K. (2012b) The three-domain model - A new model for the early development of leaves in Arabidopsis thaliana. *Plant Signaling & Behavior.* **7(11)**:1–5

Nath U, Crawford C, Carpenter R, Coen E. (2003) Genetic control of surface curvature. *SCIENCE.* **299**: 1404-1407

Navaud O, Dabos P, Carnus E, Tremousaygue D, Hervé C. (2007) TCP transcription factors predate the emergence of land plants. *J. Mol. Evol.* **65**: 23–33

Nicotra AB, Leigh A, Boyce CK, Jones CS, Niklas KJ, Royer DL, Tsukaya H. (2011) The evolution and functional significance of leaf shape in the angiosperms. *Funct. Plant Biol.* **38:** 535–552

Nikovics K, Blein T, Peaucelle A, Ishida T, Morin H, Aida M, Laufs P. (2006) The balance between the MIR164A and CUC2 genes controls leaf margins serration in Arabidopsis. *Plant Cell*. **18**: 2929-2945

Okada K, Ueda J, Komaki MK, Bell CJ, Shimura Y. (1991) Requirement of the Auxin Polar Transport System in Early Stages of Arabidopsis Floral Bud Formation. *Plant Cell.* **3(7)**:677-684

Pajor R, Fleming A, Osborne CP, Rolfe SA, Sturrock CJ, Mooney SJ. (2013) Seeing space: visualization and quantification of plant leaf structure using X-ray micro-computed tomography. *J. Exp. Bot.* **64(2):** 385-390

Palatnik JF, Allen E, Wu X, Schommer C, Schwab R, Carrington JC, Weigel D. (2003) Control of leaf morphogenesis by microRNAs. *Nature.* **425**: 257–263

Pérez-Pérez JM, Ponce MR, Micol JL. (2002) The UCU1 Arabidopsis Gene Encodes a SHAGGY/GSK3-like Kinase Required for Cell Expansion along the Proximodistal Axis. *Dev.* **242**:161–173

Ramirez J, Bolduc N, Lisch D, Hake S. (2009) Distal Expression of knotted1 in Maize Leaves Leads to Reestablishment of Proximal/Distal Patterning and Leaf Dissection. *Plant Physiology.* **151:**1878–1888

Rédei JP. (1992) A note on Columbia wild type and Landsberg erecta. In Methods in Arabidopsis Research, C. Koncz, N.-H. Chua, and J. Schell, eds (Singapore: World Scientific), p.3

Reinhardt D, Frenz M, Mandel T, Kuhlemeier C. (2005) Microsurgical and laser ablation analysis of leaf positioning and dorsoventral patterning in tomato. *Dev.* **132**: 15–26

Riechmann JL, Heard J, Martin G, Reuber L, Jiang C, Keddie J, Adam L, Pineda O, Ratcliffe OJ, Samaha RR, Creelman R, Pilgrim M, Broun P, Zhang JZ, Ghandehari D, Sherman BK, Yu G. (2000) Arabidopsis transcription factors: genome-wide comparative analysis among eukaryotes. *Science.* **290**: 2105–2110

Rohlf F. (1999) Shape Statistics: Procrustes Superimposition and Tangent Spaces. *Journal of classification*. **16**:197-223

Rueda-Romero P, Barrero-Sicilia C, Gómez-Cadenas A, Carbonero P, Oñate-Sánchez L. (2012). Arabidopsis thaliana DOF6 negatively affects germination in non-after-ripened seeds and interacts with TCP14. *J. Exp.Bot.* **63**: 1937–1949

Sambrook J, Russell DW. (2001) Molecular cloning: a laboratory manual. Cold Spring Harbor Laboratory Press, Cold Spring Harbour, New York

Sarojam R, Sappl PG, Goldshmidt A, Efroni I, Floyd SK, Eshed Y, Bowman J. (2010) Differentiating Arabidopsis shoots from leaves by combined YABBY activities. *Plant Cell.* **22**: 2113–2130

Schofield A. (2008) LeafPredictor Version 0.7 User Manual http://fire-salamander.co.uk/leafpredictor/

Sessions A, Burke E, Presting G, Aux G, McElver J, Patton D, Dietrich B, Ho P, Bacwaden J, Ko C, Clarke JD, Cotton D, Bullis D, Snell J, Miguel T, Hutchison D, Kimmerly B, Mitzel T, Katagiri F, Glazebrook J, Law M, Goff SA. (2002) A high-throughput Arabidopsis reverse genetics system. *Plant Cell.* **14**: 2985-94

Shlens J. (2005) A Tutorial on Principal Component Analysis –

Version 2
http://citeseerx.ist.psu.edu/viewdoc/summary?doi=10.1.1.115.3503

Smith LI. (2002) A tutorial on Principal Component Analysis. http://www.cs.otago.ac.nz/cosc453/student_tutorials/principal_components.pdf

Stahle M, Janine Kuehlich J, Staron L, von Arnim A, and Golz J. (2009) YABBYs and the Transcriptional Corepressors LEUNIG and LEUNIG_HOMOLOG Maintain Leaf Polarity and Meristem Activity in Arabidopsis. *The Plant Cell.* **21(10):** 3105-3118

Steiner E, Efroni I, Gopalraj M, Saathoff K, Tseng TS, Kieffer M, Eshed Y, Olszewski N, Weiss D. (2012a) The Arabidopsis O-linked N-acetylglucosamine transferase SPINDLY interacts with class I TCPs to facilitate cytokinin responses in leaves and flowers. *The Plant Cell.* **24**: 96–108

Steiner E, Yanai O, Efroni I, Naomi Ori N, Eshed Y, Weiss D. (2012b) Class I TCPs modulate cytokinin-induced branching and meristematic activity in tomato. *Plant Signaling & Behavior.* **7(7)**: 807–810

Stirnberg P, van De Sande K, Leyser O. (2002) *MAX1* and *MAX2* control shoot lateral branching in Arabidopsis. *Development.* **129**: 1131–1141

Takada S, Hibara K, Ishida T, Tasaka M. (2001) The CUP-SHAPED COTYLEDON1 gene of Arabidopsis regulates shoot apical meristem formation. *Dev.* **128**: 1127-1135

Takeda S, Hanano K, Kariya A, Shimizu S, Zhao L, Matsui M, Tasaka M, Aida M. (2011) CUP-SHAPED COTYLEDON1 transcription factor activates the expression of LSH4 and LSH3, two members of the ALOG gene family, in shoot organ boundary cells. *Plant J.* **66(6):**1066-77

Tanksley S. (2004) The Genetic, Developmental, and Molecular Bases of Fruit Size and Shape Variation in Tomato. *The Plant Cell*. **16(1):** S181-S189

Tatematsu K, Nakabayashi K, Kamiya Y, Nambara E. (2008) Transcription factor AtTCP14 regulates embryonic growth potential during seed germination in Arabidopsis thaliana. *Plant J.* **53**: 42 – 52

Thompson DW. (1917) On Growth and Form. Cambridge University Press. Chapter XVII, Volume II, p.1062

Torii K, Mitsukawa N, Oosumi T, Matsuura Y, Yokoyama R, Whittier RF, Komeda Y. (1996) The Arabidopsis ERECTA Gene Encodes a

Putative Receptor Protein Kinase with Extracellular Leucine-Rich Repeats. *The Plant Cell.* **8**:735-746

Uberti-Manassero N, Lucero L, Viola I, Vegetti A, Gonzalez D. (2012) The class I protein AtTCP15 modulates plant development through a pathway that overlaps with the one affected by CIN-like TCP proteins. *J Exp Bot*. **63**: 809 – 23

Uberti-Manassero N, Viola I, Welchen E, Gonzalez D. (2013) TCP transcription factors: architectures of plant form. *Biomolecular Concepts*. **4**:111 – 127

Valsecchi I, Guittard-Crilat E, Maldiney R, Habricot Y, Lignon S, Lebrun R, Miginiac E, Ruelland E, Jeannettea E, Lebreton S. (2013) The intrinsically disordered C-terminal region of Arabidopsis thaliana TCP8 transcription factor acts both as a transactivation and self-assembly domain. *Mol.BioSyst.* **9**: 2282–2295

Viola I, Güttlein LN, Gonzalez D. (2013) Redox Modulation of Plant Developmental Regulators from the Class I TCP Transcription Factor Family. *Plant Physiology.* **162**: 1434–1447

Vroemen CW, Mordhorst AP, Albrecht C, Kwaaitaal M, de Vries SC. (2003). The CUP-SHAPED COTYLEDON3 gene is required for boundary and shoot meristem formation in Arabidopsis. *Plant Cell*. **15**: 1563-1577

Wagner R, and Pfannschmidt T. (2006) Eukaryotic transcription factors in plastids: bioinformatic assessment and implications for the evolution of gene expression machineries in plants. *Gene*. **381**: 62–70

Waites R, Selvadurai HRN, Oliver IR, Hudson A. (1998) The PHANTASTICA gene encodes a MYB transcription factor involved in growth and dorsoventrality of lateral organs in Antirrhinum. *Cell*. **93**: 779-789

Walter A, Scharr H, Gilmer F, Zierer R, Nagel K, Ernst M, Wiese A,Virnich O, Christ M, Uhlig B, Jünger S, Schurr U. (2007) Dynamics of seedling growth acclimation towards altered light conditions can be quantified via GROWSCREEN: a setup and procedure designed for rapid optical phenotyping of different plant species. *New Phytologist*. **174**: 447–455

Wang M, Zhao P, Cheng H, Han L, Wu X, Gao P, Wang H, Yang C, Zhong N, Zuo J, Xia G. (2013) The Cotton Transcription Factor TCP14 Functions in Auxin-Mediated Epidermal Cell Differentiation and Elongation. *Plant Physiology.* **162**: 1669–1680

Wang W, Xu B, Wang H, Li J, Huang H, Xu L. (2011) YUCCA Genes Are Expressed in Response to Leaf Adaxial-Abaxial Juxtaposition and Are Required for Leaf Margin Development. *Plant Physiology.* **157**: 1805–1819

Wang Y. (2008) How effective is T-DNA insertional mutagenesis in Arabidopsis? *J Biochem Tech*. **1(1)**:11-20

Webster M, and Sheets H. (2010) A practical introduction to landmark-based geometric morphometrics. *Quantitative Methods in Paleobiology*. **16**:163-188

Weight C, Parnham D, Waites R. (2008) LeafAnalyser: a computational method for rapid and large-scale analyses of leaf shape variation. *Plant J*. **53**: 578–586

Weir I, Lu JP, Cook H, Causier B, Schwarz-Sommer Z, Davies B. (2004) CUPULIFORMIS establishes lateral organ boundaries in Antirrhinum. *Dev*. **131**: 915-922

Winter D, Vinegar B, Nahal H, Ammar R, Wilson GV, Provart NJ. (2007) An "Electronic Fluorescent Pictograph" browser for exploring and analyzing large-scale biological data sets. *PLoS One*. **2(8)**:e718

Wuyts N, Palauqui JC, Conejero G, Verdeil JL, Granier C, Massonnet C. (2010) High-contrast three-dimensional imaging of the Arabidopsis leaf enables the analysis of cell dimensions in the epidermis and mesophyll. *Plant Methods.* **6:17**

Yadav RK, Perales M, Gruel J, Girke T, Jönsson H, Reddy GV. (2011) WUSCHEL protein movement mediates stem cell homeostasis in the Arabidopsis shoot apex. *Genes Dev.* **25(19):**2025-2030

Yamaguchi T, Nukazuka A, Tsukaya H. (2012) Leaf adaxial–abaxial polarity specification and lamina outgrowth: evolution and development. *Plant Cell Physiol.* **53(7)**: 1180–1194

Yano S, Terashima I. (2001) Separate localization of light signal perception for sun or shade type chloroplast and palisade tissue differentiation in *Chenopodium album. Plant Cell Physiol.* **42:** 1303–1310

Yeats T and Rose J. (2013) The Formation and Function of Plant Cuticles. *Plant Physiol.* **163(1):** 5–20

Zelditch M, Swiderski D, Sheets H, Fink W. (2004) Geometric Morphometrics for Biologists, A Primer. Elsevier Academic Press, ISBN: 978-0-12-778460-1